The Preparation and Characterization of a Heparin-Derived Oligosaccharide that Binds to Herpes Simplex Virus Type 1 Glycoprotein D

Ronald Jarrod Copeland

A dissertation submitted to the faculty of the University of North Carolina at Chapel Hill in partial fulfillment of the requirements for the degree of Doctor of Philosophy in the School of Pharmacy (Medicinal Chemistry and Natural Products).

Chapel Hill
2006

Approved by:

Thesis Advisor: Jian Liu, Ph.D.

Reader: Kenneth Bastow, Ph.D.

Reader: Michael Jarstfer, Ph.D.

Reader: Scott Singleton, Ph.D.

Reader: Gary Glish, Ph.D.

ABSTRACT
Ronald Jarrod Copeland: The Preparation and Characterization of a Heparin-Derived Oligosaccharide that Binds to Herpes Simplex Virus Type 1 Glycoprotein D
(Under the direction of Jian Liu, Ph.D.)

Heparan sulfate (HS) is a structurally diverse and highly sulfated polysaccharide that has been found to exist on the surface of mammalian cells in substantial quantities. Unique saccharide sequences of HS have been shown to bind specifically to a number of biologically relevant proteins, thus allowing HS to play a role in numerous biological processes including regulation of blood coagulation, inflammation, cancer cell growth and viral infections. Understanding the structure-function relationship of HS will aid in the development of novel anti-viral and/or anti-cancer therapeutics. Previous studies have shown that 3-*O*-sulfotransferase isoform 3 (3-OST-3) generates 3-*O*-sulfated HS that can bind to glycoprotein D (gD) and facilitate HSV viral entry into target cells, thus implicating 3-*O*-sulfated HS as a HSV entry receptor. The goal of this work is to provide additional structural information concerning HS ability to assist in the HSV viral infection mechanism, while providing evidence to suggest that HSV infections may be inhibited by disrupting the interactions with its polysaccharide based cellular receptors. The use of 3-*O*-sulfated heparin (HP) oligosaccharides, along with high expression levels of gD purified from *E. coli*., allowed for the investigation of the gD binding of various sized HP oligosaccharides. Results obtained from immunoprecipitation and affinity co-electrophoresis experiments suggested that the 3-*O*-sulfated HP octasaccharide was of the minimal required length for gD binding with a K_d value of 19 μM. Structural characterization using chemical and enzymatic

approaches suggested the gD binding 3-*O*-sulfated HP octasaccharide had a structure of ΔUA2S-GlcNS6S-IdoUA2S-GlcNS6S-IdoUA2S-GlcNS6S3S-IdoUA2S-GlcNS6S (3-*O*-sulfation site is underlined). Coupling a sulfo donor regeneration system with 3-OST-3 modification, sufficient amounts of the gD binding 3-*O*-sulfated HP octasaccharide was generated for cell based viral entry assays. The characterization of a novel gD binding octasaccharide as described herein, provides additional structural information concerning HS/HP ability to assist in the HSV viral entry mechanism. Specifically, it allows for further investigations to be conducted as the characterized 3-*O*-sulfated gD binding HP octasaccharide may serve as a good lead compound for the inhibition of HSV infections. The further development of this project could uncover a new way to treat diseases related to HSV infections.

To my parents, Richard M. Copeland Sr. and Barbara H. Copeland, whose love, support, and guidance have been with me throughout my educational endeavors. If it had not been for them, the completion of this thesis would not have been possible.

To the memory of my paternal grandparents, the late Johnnie C. Copeland and the late Pattie K. Copeland, whose memory has provided constant inspiration as I pursued my educational goals.

To the memory of my maternal grandfather, the late George L. Hicks and to my maternal grandmother Annie P. Hicks, who both have greatly affected my life. Their spiritual wisdom and teachings will stay with me for all of my days.

ACKNOWLEDGMENTS

I wish to express my sincerest gratitude to my advisor, Dr. Jian Liu, who has contributed the most in my development as a scientist. Dr. Liu has provided an excellent training environment in which I have learned a great deal during the conduction of my graduate studies. He has gone above and beyond the call of duty in providing support and advice as it pertained to my career interests and career development. I will always be grateful for the countless hours that he has so graciously spent with me during my graduate education.

I would also like to thank Dr. Robert Linhardt for providing the purified heparin oligosaccharide substrates, Dr. Deepak Shukla for conducting gD functional assays as well as cell-based inhibition experiments, and Dr. Arlene Bridges for assistance with mass spectrometric experiments and analysis. I would also like to thanks the members of my student advisory committee, Drs. Ken Bastow, Michael Jarstfer, Scott Singleton, and Gary Glish for the assistance and comments about my research project during the conduction of my graduate studies. Finally, I would like to thank my lab mates (former and current) Dr. Suzanne Edavettal, Dr. Michael Duncan, Dr. Jinghua Chen, Dr. Ding Xu, Danyin Song, Tanya Scarlett, Miao Chen, Courtney Jones, Heather Bethea, and Renpeng Liu for their support and assistance.

TABLE OF CONTENTS

Page

LIST OF FIGURES

Figure # Page

LIST OF TABLES

ABBREVIATIONS

ECM	Extracellular matrix
GAG	Glycosaminoglycans
UA	Uronic acid
GlcUA	Glucuronic acid
IdoUA	Iduronic acid
GalNAc	*N*-acetylgatactosamine
GlcNAc	*N*-acetylglucosamine
GlcN	Glucosamine
HexA	Hexuronic acid
GlcUA2S	2-*O*-sulfated glucuronic acid
IdoUA2S	2-*O*-sulfated iduronic acid
DS	Dermatan sulfate
HP	Heparin
HS	Heparan sulfate
HA	Hyaluronic acid
KS	Keratan sulfate
CS	Chondroitin sulfate
HSPG	Heparan sulfate proteoglycan
CSPG	Chondroitin sulfate proteoglycan
GPI	Glycosylphosphatidylinositol
Xyl	Xylose

Gal	Galactose
XylT	Xylosyltransferase
GalT-I	Galactoslytransferase I
GalT-II	Galactoslytransferase II
GlcUAT-I	Glucuronyltransferase I
UDP	Uridine diphosphate
EXT	Exostosin gene family
GlcNAcT-I	*N*-acetyl-glucosaminyltransferase I
GlcNAcT-II	*N*-acetyl-glucosaminyltranferase II
GlcUAT-II	Glucuronyltransferase II
3-OST	3-*O*-sulfotransferase
2-OST	2-*O*-sulfotransferase
6-OST	6-*O*-sulfotransferase
NDST	*N*-deacetylase *N*-sulfotransferase
C5-Epi	C_5 epimerase
PAPS	3′-phosphoadensine 5′-phosphosulfate
PAP	3′-phosphoadensine 5′-phosphate
PNPS	*p*-nitrophenyl sulfate
PNP	*p*-nitrophenol
NA	*N*-acetylated domain
NS	*N*-sulfated domain
NST	*N*-sulfotransferase
PSB	Phosphate binding loop

EST	Estrogen sulfotransferase
FGF	Fibroblast growth factor
AT	Antithrombin
gD	HSV-1 glycoprotein D
gB	HSV-1 glycoprotein B
gC	HSV-1 glycoprotein C
HSV-1	Herpes simplex virus type 1
HPLC	High performance liquid chromatography
DEAE-NPR	Diethylaminoethyl (non-porous) chromatography
PAMN	Polyamine chromatography
MALDI-MS	Matrix-assisted laser desorption/ionization mass spectrometry
nESI-MS	Nanoelectrospray ionization mass spectrometry
SPR	Surface plasmon resonance
ACE	Affinity co-electrophoresis
HVEM	Herpesvirus entry mediator
CHO	chinese hamster ovary cells
2ase	$\Delta^{4,5}$ glycuronate-2-sulfatase
2-AB	2-aminobenzamide
AST-IV	aryl sulfotransferase-IV
CHAP	Chaperone proteins (GroEL and GroES)
IPTG	Isopropyl-β-D-thiogalactopyranoside

CHAPTER I

INTRODUCTION

Section I: Glycosaminoglycans

The cell surface as well as the extracellular matrix (ECM) is comprised of abundant quantities of complex, unbranched, and heterogeneous polysaccharides. These macromolecules are known as glycosaminoglycans (GAGs). The abundant presence of these GAGs on the cell surface and in the ECM allows for a large number of proteins such as cytokines, chemokines, and growth factors to bind to GAGs and participate in a wide array of biological events. These events have been found to range from participating in the inflammatory response and embryonic development to cell adhesion, motility and morphogenesis (1-9). These polysaccharides are comprised of repeating disaccharide sugar units and carry negative charges. The disaccharide units contain a glucosamine residue, which is either *N*-acetylgalactosamine (GalNAc) or *N*-acetylglucosamine (GlcNAc), and an uronic acid residue, which is either iduronic acid (IdoUA) or glucuronic acid (GlcUA). These GAGs are predominately presented on the cell surface attached to various core proteins in the form of proteoglycans.

Glycosaminoglycans can be classified into four distinct classes; each class carries different repeating disaccharide units with various sulfations. The classes include chondroitin sulfate, hyaluronic acid, keratan sulfate and heparan sulfate/heparin (figure 1).

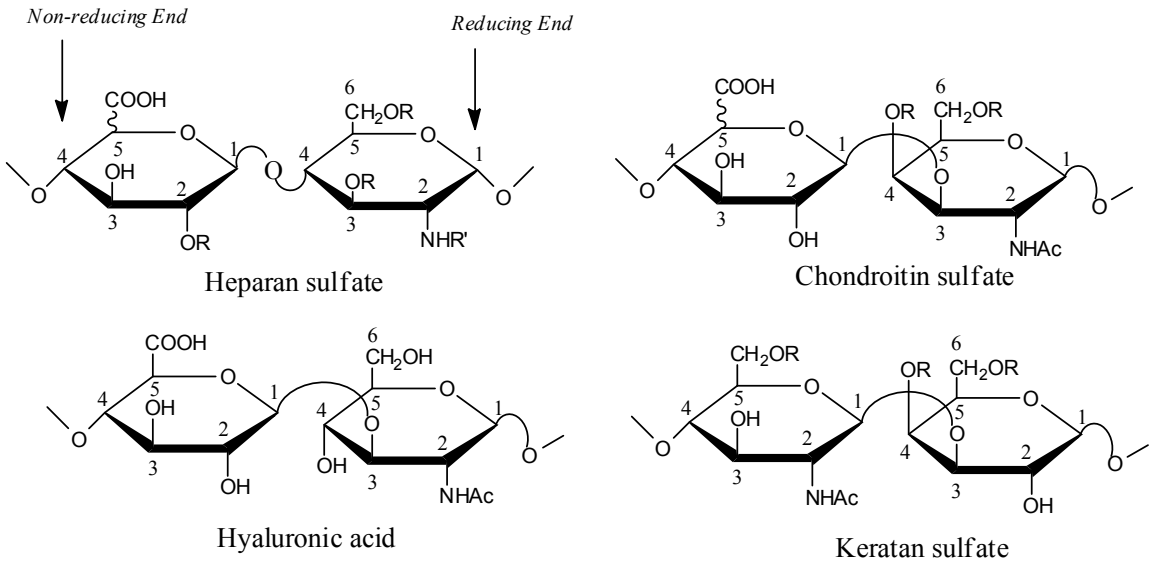

Figure 1. **Structures of disaccharide repeating units of glycosaminoglycans**. R represents H or sulfate, and R' represents acetyl, sulfate, or H. Non-reducing and reducing ends are labeled.

Hyaluronic acid

Hyaluronic acid (HA), also known as hyaluronan or hyaluronate, is very unique among GAGs in that it does not contain any sulfate groups, is not epimerized, is not covalently attached to proteins as a proteoglycan, and is not synthesized in the Golgi. HA is synthesized directly into the extracellular space as a copolymer of glucuronic acid (GlcUA) and glucosamine (GlcN) residues via a β1→3 linkage with a average approximate molecular weight (M_r) of 10^5-10^7 Da (10). HA is mostly found in the extracellular matrix (ECM) of connective tissues such as the umbilical cord, synovial fluid and the skin (10). Initially, HA was believed to only have a shock-absorbing role in the body, however a number of studies have been reported that suggest that HA plays a role in mediating various physiological functions, which include its roles in morphogenesis, regeneration, wound healing, and tumor invasion (11, 12).

Keratan sulfate

Keratan sulfate (KS), is synthesized as a copolymer of repeating disaccharide units of galactose (Gal) and *N*-acetylglucosamine (GlcNAc) residues via a β1→4 linkage, with variable carbohydrate lengths and degrees of sulfation. KS has been shown to have on average 0.9 to 1.8 sulfates per disaccharide unit and a relative molecular weight between 4×10^3 to 2×10^4 Da (13-15). KS is biosynthesized in the Golgi in proteoglycan form and localized in cornea, bone, and cartilage (16). An article by Funderburgh summarizes the biosynthesis and biological functions of KS. These biological functions includes its roles in embryonic development, wound healing and cornea hydration (16).

Chondroitin sulfate

Chondroitin sulfate (CS), is synthesized as a copolymer of repeating disaccharide units of glucuronic (GlcUA) or iduronic acid (IdoUA) residues and *N*-acetylated galactosamine (GalNAc) with various sulfation. CS can be further classified as either chondroitin sulfate A (CS-A), chondroitin sulfate B (CS-B) and chondroitin sulfate C (CS-C). CS-A contains a galactosamine 4-*O*-sulfate; CS-B, also known as dermatan sulfate (DS), contains higher degree of epimerization (i.e. more IdoUA residues); and CS-C, contains galactosamine 6-*O*-sulfate. Chondroitin sulfate proteoglycans (CSPGs) have been found to be the most abundant proteoglycan in the ECM of the central nervous system (CNS) (17). Within the CNS, CSPGs primarily acts as barrier molecules that affect axon growth, cell migration and plasticity (18).

Heparin/Heparan sulfate

Heparin (HP) and heparan sulfate (HS) are also included in this unique class of macromolecules called glycosaminoglycans. This subclass however is the major focus of this thesis and its structure, biosynthesis, and biological functions are elaborated on in greater detail in the following sections.

Section II: Heparin/Heparan Sulfate: Structure and Biosynthesis

Structure of Heparin vs. Heparan sulfate

Heparan sulfate (HS) is a structurally diverse, complex, biopolymer that is initially synthesized in the Golgi with alternating disaccharide units of hexuronic acid (HexA) and *N*-acetyl glucosamine (GlcNAc) residues attached via β1→4 linkage. The HexA residue can be either a GlcUA or an IdoUA acid residue depending upon its variable degree of epimerization at the C_5 position, by C_5 epimerase. Heparin (HP), commonly used clinically as an anticoagulant drug, is a copolymer of alternating HexA (mostly IdoUA) and GlcNAc residues (figure 2).

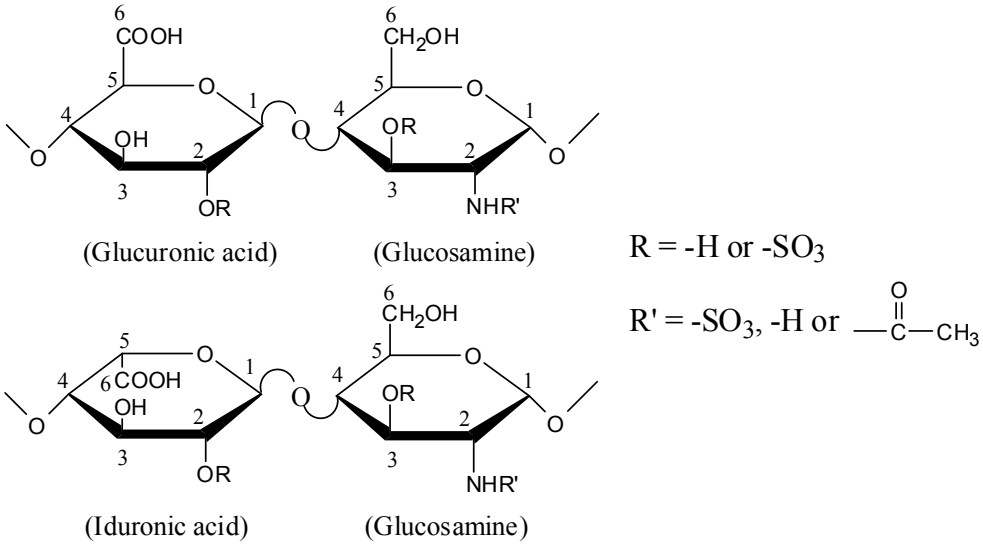

Figure 2: Disaccharide repeating units of heparin and heparan sulfate (3). Sulfation (R = $-SO_3$) at carbon 6 (known as 6-*O*-sulfo glucosamine) of glucosamine is common. Sulfation at carbon 2 of iduronic acid (known as 2-*O*-sulfo iduronic acid) is common. Sulfation at carbon 3 of glucosamine (known as 3-*O*-sulfo glucosamine) is rare. Both *N*-acetyl (R' = acetyl, GlcNAc) and *N*-sulfo glucosamine (R' = $-SO_3$, GlcNS) are common. *N*-unsubstituted glucosamine (R' = -H, $GlcNH_2$) is a low abundance component.

NMR and molecular modeling studies have provided evidence that HP and HS display a helical-type structure with the various sulfate and carboxylic groups projected in an outward fashion (19). The basis of the well documented conformational flexibility of IdoUA

residues suggest that these residues have the ability to oscillate between chair and skew boat conformations (20). This feature may manifest itself in the ability of HS and HP to display its sulfate and carboxylic groups in a flexible nature that can conform to various proteins to allow binding and modulation of protein activities.

HP is structurally similar to HS. HS is ubiquitously expressed and is a common product of all mammalian cells, while HP is generally considered to be an exclusive product of mast cells. Mast cells are cells of the connective tissue that contains granules rich in heparin that play a role in wound healing and defense against pathogens. The only noticeable difference between HS and HP is in their respective degree of modification, specifically sulfation at the *N*-, 2-, 6-, and 3-*O* positions and the epimerization patterns at C_5 position of the glucosamine. HP is found to primarily contain long repeating disaccharide units of –IdoUA2S-GlcNS6S-, while HS is found to be more diverse in its epimerization and sulfation patterns. Consequently, two points can be concluded from this, 1) that HP could be classified as a form of highly modified HS, and 2) its feasible for HS to display HP-like sequences within its polysaccharide chain. The disaccharide units obtained from HP contain on average 2.7 sulfate groups, compared to an average of 0.6-1 sulfate groups seen within the disaccharide units of HS (21). The individual monosaccharides within HS and HP isolated from natural sources are found to be present at various levels. The majority of the glucosamine residues found in HS are either *N*-acetylated (GlcNAc) or *N*-sulfated (GlcNS), with only 1-7% of the glucosamine residues existing in the *N*-unsubstituted form ($GlcNH_2$), thus allowing HS to display primary amine groups (22). Structural studies have shown that the presence of a 6-*O*- sulfated glucosamine and a 2-*O*-sulfated iduronic acid (IdoUA2S) are

common among the monosaccharides found in HS, while 3-*O*-sulfated glucosamine and 2-*O*-sulfated glucuronic acid (GlcUA2S) residues are a rare component found in HS (23).

Heparan Sulfate Proteoglycans (HSPGs) – Core Proteins

Heparan sulfate proteoglycans (HSPGs) exists on the cell surface of mammalian cells as well as in the ECM in abundant quantities. HSPGs consist of a core protein to which one or more GAG chains are attached at specific sites. They have also been found to have a variety of diverse functions. These functions range from mediating cell adhesion and migration, to regulating proliferation and differentiation (2, 24-27). Even though it is generally considered that the specific HS chains are the moieties that interact with various proteins and allow HSPGs to be diverse in its biological functions, the core protein component is also important as it determines the localization and presentation of the proteoglycan and its HS chains on the cell surface and in the ECM. The majority of core proteins contain up to 5 conserved HS sites, consisting of a SGXG or SG sequence, where X refers to any amino acid, with this sequence usually being preceded by various acidic residues (28). HSPGs can be classified into two groups, membrane bound and secreted proteoglycans. The major membrane bound HSPGs include syndecans and glypicans, which are encoded by multiple genes, while the major secreted HSPGs that make up the ECM include perlecans and agrins, which are encoded by a single gene respectively.

Syndecan

Syndecans are classified as type I transmembrane proteins, meaning that they contain a single membrane-spanning domain with the C-terminus oriented towards the cytoplasm of

the cell and the N-terminus is oriented towards the ECM. This core protein has the ability to display either HS or CS/DS polysaccharide chains; however the majority of GAG chains are HS. Syndecans have been found to have an average molecular weight between 20-45 kDa, and have been found to be present in four isoforms, namely syndecan-1, syndecan-2 (fibroglycan), syndecan-3 (N-syndecan) and syndecan-4 (amphiglycan or ryudocan) (2, 24, 29). These isoforms contain a large ectodomain, a cytoplasmic domain and a highly conserved transmembrane region. Within their cytoplasmic region, the isoforms have two conserved domains linked together by a variable region. This variable region is unique for each individual isoform, allowing for isoform specific protein interactions to occur (30). The different isoforms of syndecan have been shown to be expressed in a developmental and cell type-specific pattern. Recent *in vitro* and *in vivo* data suggest that syndecans are involved in the regulation of various events including leukocyte-endothelial interactions, extravasation, formation of chemokine gradients and growth factor signaling (31).

Glypican

Glypicans are members of the membrane bound HSPG family that displays exclusively HS. However, unlike syndecans, glypicans are attached to the cellular membrane via a glycosylphosphatidylinositol (GPI) anchor. The presence of the GPI anchor results in variable localization patterns and differentiation of its metabolism pathways when compared to other HSPGs families (32, 33). The glypican family is comprised of at least six different isoforms glypican-1 (glypican), glypican-2 (cerebroglycan), glypican-3 (OCI-5), glypican-4 (K-glypican), glypican-5 and -6. There is limited sequence homology between the glypican isoforms, however all glypicans share 14 conserved cysteine residues and have 2 or 3 GAG

attachment sites very close to the cellular membrane, thus suggesting that all members within this family share a similar tertiary structure (34). Studies have provided evidence to suggest that glypicans are involved in cell proliferation and cancer development. One example of this is found in a published report by Kleff and colleagues that provided evidence which showed that the expression of glypican-1 (but not other glypicans) is induced in human pancreatic and breast cancer cells (35). This suggests that glypicans may have isoform specific biological functions.

Perlecan

Perlecan, which consists of a core protein of approximately 400 kDa, is primarily found in the basement membrane (2). They have been shown to contain up to 3 GAG attachment sites which are primarily for HS, however CS can also be attached (36). This family of HSPGs is comprised of five domains; each domain has specific and unique functions. These domains allow perlecan to bind various basement membrane proteins, growth factors and integrins through its HS side chains and/or the perlecan core protein itself (2, 37-40). Through these binding interactions, perlecan HSPGs have been found to participate in lipid uptake and metabolism, cell adhesion, cellular growth and morphogenesis (38, 41).

Agrin

Agrin, consisting of a core protein of approximately 250 kDa, is found as a constituent of the basement membrane, specifically within neuromuscular junctions and renal tubular basement membranes (42-44). Agrin, like perlecan, has multiple domains with each

domain required for a specific function. The structural functions of these domains have been reviewed by Iozzo *et al*. (45). Agrin, unlike perlecan, displays exclusively HS. Moreover, this HSPG can display at least six HS chains and contains five *N*-glycosylation sites, allowing the possibility of agrin to display heterogeneity in various tissues. The biological functions of agrin HSPGs include aggregation of acetylcholine receptors and interaction with neural cell adhesion molecules, which led to the suggestion that agrin may play a role in the cell adhesion processes during neural development, including synaptogenesis (42-44).

Biosynthesis of heparan sulfate

The biosynthesis of HS results in the formation of a very diverse and heterogeneous polysaccharide chain. This structural diversity of HS is of great importance as the position of IdoUA residues and sulfation patterns within the polysaccharide chain is directly correlated to HSPGs ability to interact with proteins and/or ligands and permits participation in a wide variety of biological functions. In simple terms, the modifications within the HS polysaccharide chain determine the specific function of HSPGs. The HS polysaccharide can be comprised of 50-100 disaccharide units and with each disaccharide unit having the possibility to carry variable modifications, the complexity and diversity that HS can obtain within its sequence is obvious. The structural diversity of HS is achieved in the manner by which it is biosynthesized. The HS biosynthetic pathway is described as a non-template, enzymatic driven process, which is separated into three steps: a) biosynthesis of the tetrasaccharide linkage region, b) chain initiation/chain elongation, and c) chain modification. The majority of the key HS biosynthetic enzymes have been cloned, which has allowed detailed investigations of their roles in generating specific sequences of HS (46).

Step 1: Biosynthesis of the tetrasaccharide linkage region

HS biosynthesis occurs in the Golgi apparatus and is initiated by the attachment of a linkage region of four monosaccharides to the core protein at specific serine residues. The tetrasaccharide linkage region has a sequence of xylose-galactose-galactose-glucuronic acid (Xyl-Gal-Gal-GlcUA), where the Xyl is covalently attached to a specific serine residue within the core protein (figure 3). The linkage tetrasaccharide has the potential to be modified at various locations. The xylose residue can be phosphorylated at its C_2 position, while the two galactose residues may be sulfated at the C_4 or C_6 positions (47). However, studies have not found any sulfate groups on either Gal residue in HSPGs only in CSPGs have they been found. The individual sugar residues of the tetrasaccharide linkage sequence are added in a stepwise manner by the activities of four specific glycosyltransferases including, xylosyltransferase (XylT), galactoslytransferase I (GalT-I), galactoslytransferase II (GalT-II), and glucuronyltransferase I (GlcUAT-I). These glycosyltransferases have been cloned (48), which has served as an important technological tool for new avenues concerning the chemoenzymatic synthesis of oligosaccharides (49, 50).

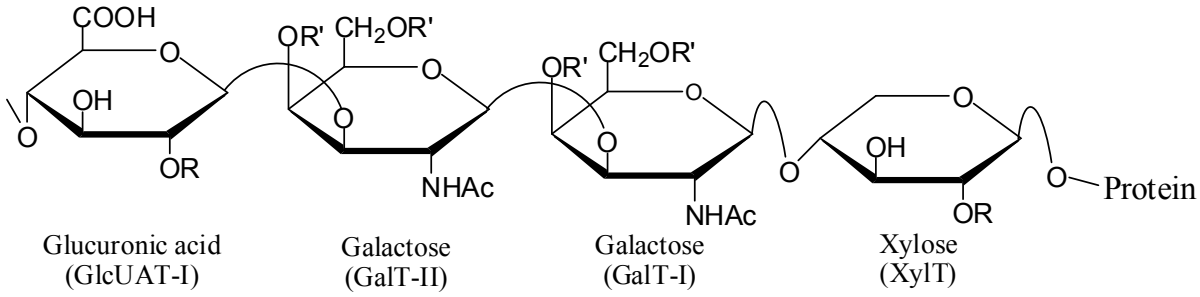

Figure 3: Biosynthesis of the tetrasaccharide linkage region. The tetrasaccharide linkage region (GlcUA-Gal-Gal-Xyl) is shown. The enzyme that is responsible for the transfer of each respective sugar unit is presented in parenthesis under the sugar unit. R = proton or sulfate, R' = proton or phosphate.

Xylosyltransferase (XylT)

XylT is the first enzyme to act in the biosynthesis of the tetrasaccharide linkage region. XylT catalyzes the transfer of D-xylose, from its donor substrate UDP-xylose to sequence specific serine residues within the core protein. Usually substitution occurs at serine residues within the following peptide sequence of SGXG, where X is any amino acid. However, additional recognition signals must be involved since not all SGXG sequences within the core protein are substituted (51-54). Like other glycosyltransferases, XylT has type II transmembrane topology which is consistent with its location in the Golgi apparatus where HS is synthesized. Studies have also shown that xylosylation does indeed take place in the pre-Golgi compartment (55, 56). Studies have also proved that XylT is involved in the biosynthesis of HS. Chinese hamster ovary (CHO) cells that are deficient in XylT were found unable to synthesize HS or CS, suggesting that XylT is responsible for the initiation of HS formation in CHO cells (57).

Galactosyltransferase I (GalT-I) and Galactosyltransferase II (GalT-II)

GalT-I is the second enzyme to act in the biosynthesis of the tetrasaccharide linkage region. This enzyme transfers the first of two galactose (Gal) residues onto the previously transferred xylose, while GalT-II is responsible for the addition of the second Gal residue. Both GalT-I and GalT-II catalyze their respective reactions by using UDP-galactose as a donor substrate and they both show type II transmembrane topology (47, 48, 58). Studies have been conducted to prove the importance and role of these enzymes in the formation of the linkage region as well as in total GAG synthesis. Transfection of GalT-I cDNA into CHO cells that are deficient in GalT-I was shown to restore GAG synthesis (59). GalT-II

was also shown to be an essential enzyme for the synthesis of GAGs (58). Concerning the substrate specificity, it was found that GalT-I does not exhibit activity toward a C_2 phosphorylated xyloside, which suggests that the presence of a 2-*O*-phosphorylated xylose residue on the acceptor substrate may disrupt substrate recognition by the enzyme (47, 60). Information concerning the physiological importance of GalT-I and also GAGs synthesis was also expanded upon when mutations of GalT-I resulted in progeroid-type Ehlers-Danlos syndrome in humans (61, 62).

Glucuronyltransferase I (GlcUAT-I)

The transfer of a GlcUA residue to the second Gal residue is the final biosynthetic step of the linkage region. This transfer is catalyzed by the key enzyme GlcUAT-I. GlcUAT-I carries out its function by using UDP-GlcUA as a donor substrate. The crystal structure of GlcUAT has been solved, which has provided structural information concerning its catalytic mechanism and the key amino acid residues that play a role in its substrate recognition (63). Site-directed mutagenesis studies have also been conducted which allowed for definitive evidence concerning the residues that are involved in the catalytic mechanism (47). According to experimental evidence, sulfation at various positions on the Gal residues have an effect on GlcUAT-I activity (47). This allowed researchers to propose that sulfation is a critical feature that allows a sequence to serve as a substrate for GlcUAT-I. Interestingly, studies concerning GlcUAT-I has provided evidence that this enzyme may be considered as a pharmacological target in the onset of osteoarthritis. GlcUAT-I plays an important role in priming hexuronic acid containing GAG synthesis. Any change in activity would likely affect the rate of GAG synthesis and consequently its proteoglycan biological properties.

Osteoarthritis is characterized by quantitative and qualitative modifications of proteoglycans and their GAG chains, which leads to alterations of the cartilaginous matrix (64). Since GlcUAT-I is a key player in the formation of the linkage region, this could implicate HSPGs as a therapeutic target for osteoarthrits treatment (65, 66).

Step 2: Chain Initiation/ Chain Elongation

After the tetrasaccharide linkage region is synthesized onto the core protein, another set of enzymatic reactions occurs which ultimately serves to synthesize and extend the HS backbone sequence that will serve as a precursor substrate for later modifications. The HS backbone is synthesized by glycosyltransferases that are encoded by the *EXT* (exostosin) gene family (67). To date, five different *EXT* genes have been identified *EXT1*, *EXT2* and 3 *EXT*-like genes *EXTL1*, *EXTL2*, *EXTL3*. All members of the *EXT* gene family of proteins are type II transmembrane proteins that are located in the Golgi apparatus thus enabling them to participate in HS biosynthesis (48, 68). The *EXT* gene family has been demonstrated to function as tumor suppressor genes with overlapping glycosyltransferase substrate specificities and are involved in HS biosynthesis (67-69). The biosynthesis of HS backbone sequence can be separated into two parts: 1) HS chain initiation and 2) chain elongation or polymerization. Chain initiation is carried out by *N*-acetyl-glucosaminyltransferase I (GlcNAcT-I) activity and chain elongation is carried out by two main polymerization enzymes *N*-acetyl-glucosaminyltranferase II (GlcNAcT-II) and glucuronyltransferase II (GlcUAT-II) (figure 4).

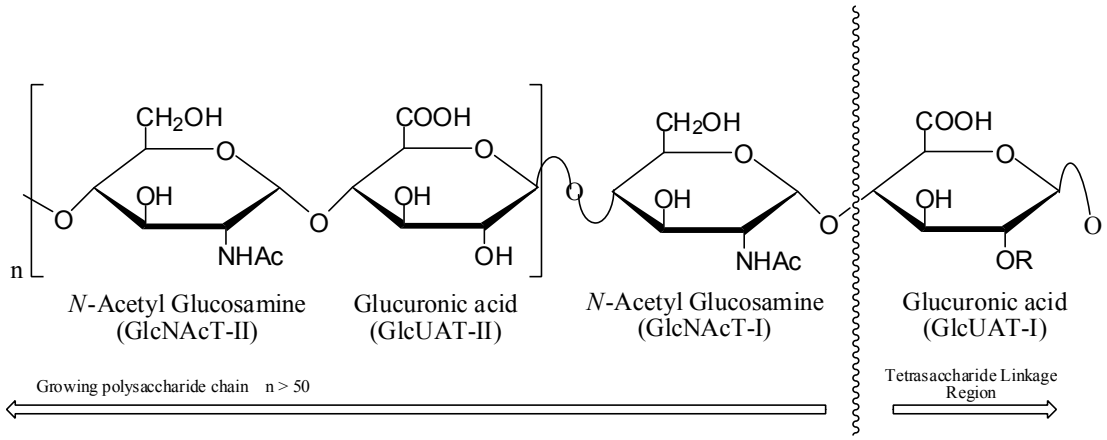

Figure 4: Enzymes involved in chain initiation and chain polymerization of the HS polysaccharide. Chain initiation is achieved by GlcNAcT-I, which serves to transfer of a GlcNAc residue to the non-reducing end of GlcUA residue. Chain polymerization occurs by the addition of alternating repeating units of GlcUA and GlcNAc residue by GlcUAT-II and GlcUAcT-II respectively.

N-Acetyl-glucosaminyltransferase I (GlcNAcT-I)

The critical enzyme responsible for the transfer of GlcNAc to the linkage region is GlcNAcT-I (70). This reaction is catalyzed *in vitro* by two *EXT* gene proteins, *EXTL2* and *EXTL3* (67). GlcNAcT-I transfers the initial GlcNAc residue to the GlcUA residue at the non-reducing end of preformed tetrasaccharide linkage region via a α1→4 linkage, thereby initiating HS formation (instead of other GAGs) allowing this catalytic transfer to serve as a molecular signal or an indicator of HS polymerization. *EXTL3* has been shown to possess both GlcNAcT-I and –II activities (48, 71). This unique feature allows for its possible participation in both chain initiation and chain elongation phases. On the other hand, *EXTL2* has only been shown to possess GlcNAcT-I activity, suggesting that it is primarily involved during the chain initiation phase (48).

D-Glucuronyltransferase II(GlcUAT-II) / *N*-Acetyl glucosaminyltransferase (GlcNAc T-II)

Once HS formation has been initiated by transfer of a GlcNAc residue onto the tetrasaccharide linkage region, two main HS polymerizing enzymes serve to elongate the HS backbone by alternatively adding the repeating disaccharide units of GlcUA and GlcNAc. These reactions are catalyzed by the GlcUAT-II and GlcNAcT-II. GlcUAT-II transfers a GlcUA residue to the previously transferred GlcNAc residue via a β1→4 linkage using UDP-GlcUA as a donor substrate. While GlcNAcT-II transfers a GlcNAc residue to the non-reducing end of the previously added GlcUA via a α1→4 linkage using its UDP sugar as a donor substrate. These two glycosyltransferases are products of *EXT2* and *EXT1* tumor suppressor genes respectively. These products have been found to exist in a large heteo-oligomeric complex within the Golgi, where the intricate roles of each gene product in HS polymerization is complex, however it has been reported that both need to be present in complex for successful polymerization to take place (48). Numerous studies have been conducted that provide positive evidence for all *EXT* genes in HS biosynthesis and development (48, 72, 73). Moreover, a great review has been published concerning the *EXT* gene family and cites relevant references that provide additional evidence for the involvement of the *EXT* gene family in HS biosynthesis and their biological importance (48).

Step 3: Chain Modification

After the HS chain is elongated with variable chain lengths of repeating disaccharide units of GlcUA and GlcNAc as determined by the activities of the polymerization enzymes mentioned above, chain diversity is further complicated as the backbone sequence of HS can serve as a precursor substrate for a variety of enzymatic modifications. These modifications

include *N*-deacetylation and *N*-sulfation of glucosamine (GlcN), C_5 epimerization of GlcUA acid to IdoUA, 2-*O*-sulfation of IdoUA and GlcUA, as well as 6-*O* and 3-*O*-sulfation of GlcN. The enzymes that are responsible for these modifications are *N*-deacetylase/*N*-sulfotransferase (NDST), C_5 epimerase (C5-Epi), 2-*O*-sulfotransferase (2-OST), 6-*O*-sulfotransferase (6-OST), and 3-*O*-sulfotransferase (3-OST) respectively. It is important to note here that none of these enzymatic modification reactions goes to completion, thereby adding yet another degree of diversity within the heterogeneous HS chain.

Sulfotransferases catalyze the transfer of a sulfo group to an acceptor site of numerous substrates, utilizing 3′-phosphoadensine 5′-phosphosulfate (PAPS) as a universal sulfo donor as shown in figure 5 (74).

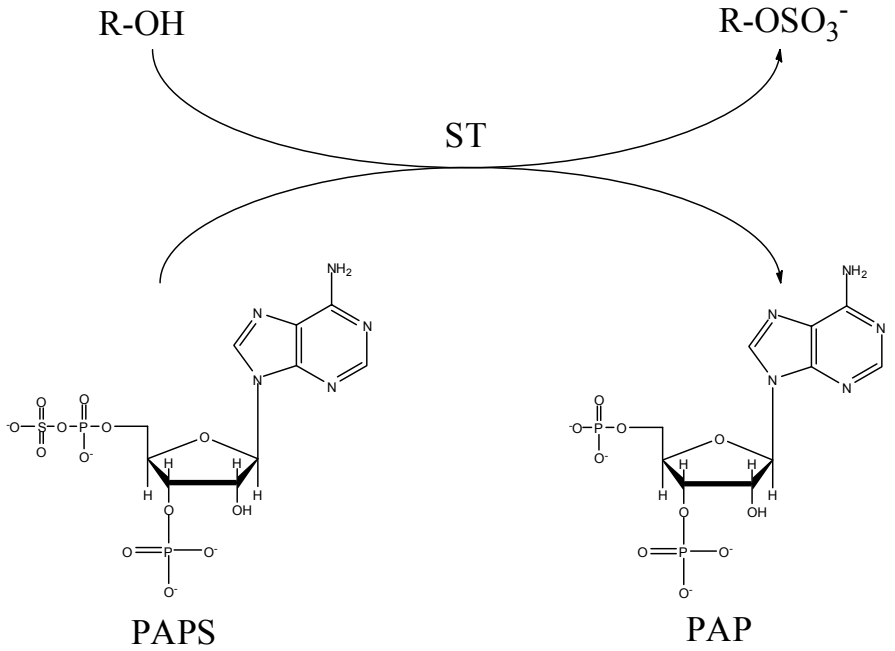

Figure 5: General catalyzed reaction of sulfotransferases. R-OH represents the awaiting substrate (i.e. HS), ST represent a sulfotransferase (i.e. NDST, 2-OST, 6-OST, or 3-OST) and $R\text{-}OSO_3^-$ represents the 3-*O*-sulfated product.

PAPS is a biologically active form of inorganic sulfate that serves as a sulfo donor in various biologically processes (75). It is interesting to note that a naturally-occurring defect in PAPS synthesis has been found to be lethal in mice (76). This fact suggests that sulfation of HS

along with various substrates of other sulfotransferases are biologically relevant for normal development. Specific Golgi-membrane sulfotransferases have the ability to transfer a sulfo group to glycosaminoglycans (i.e. HS), which converts the common polysaccharide chains to unique sites that can be recognized by biologically functional molecules, thus allowing HS to play a role in various biological processes (74). All HS sulfotransferases are present in multiple isoforms with the exception of 2-OST. NDST is present is four isoforms, 6-OST is present in three isoforms and 3-OST in seven isoforms. The majority of these enzymes and their multiple isoforms have been isolated and cloned (46). These isoforms have slightly different substrate specificities and unique tissue specific expression patterns (77-80). Different substrate specificities among isoforms allows for increased diversity within the HS chain. It is hypothesized that cells have the ability to regulate expression levels of various isoforms to synthesize HS chains with defined saccharide sequences required to achieve certain biological functions (81).

_N_-Deacetylase/_N_-Sulfotransferase (NDST)

NDST is a bifunctional enzyme with two distinct activities; *N*-deacetylation and *N*-sulfation (82). The *N*-deacetylase activity of NDST catalyzes the removal of acetyl groups from GlcNAc residues to generate unsubstituted glucosamine residues that display residues with free amino groups ($GlcNH_2$). The *N*-sulfotransferase activity of this enzyme can then catalyze the transfer of a sulfo group, from the universal sulfo donor PAPS, to the unsubstituted glucosamine at its *N*-position as shown in figure 6.

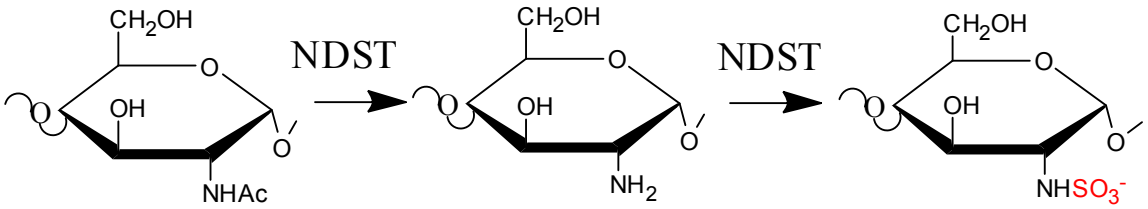

Figure 6: Bifunctional activity of NDST. The *N*-deacetylase activity of NDST catalyzes the removal of an acetyl group (Ac) from GlcN residue (left) to generate an unsubstituted GlcN residue with a free amino group ($GlcNH_2$) (middle). The *N*-sulfotransferase activity of NDST catalyzes the transfer of a sulfo group, from PAPS, to generate GlcNS (right). The SO_3^- group is colored in *red* for emphasis.

The action of NDST is a key component in the overall design of HS, as subsequent modifications of HS depend on the presence and/or absence of specific GlcNS residues within the polysaccharide chain. Depending on the activity of NDST, the HS polysaccharide chain can be divided into three domains; a highly modified domain (NS domain) containing a high degree of both *N*- and *O*-sulfate groups, a largely unmodified domain (NA domain) containing a short stretch of GlcNAc residues, and a domain that encompasses the two is considered a NS/NA domain. NDST is present in four isoforms; NDST1, NDST2, NDST3 and NDST4 (77, 83, 84). These isoforms have been found to have a noticeable difference in their relative degrees of *N*-deacetylase and *N*-sulfotransferase activities (77). Moreover, they display different expression patterns within tissues. NDST1 and NDST2 are found to be ubiquitously expressed, while NSDT3 and NDST4 are expressed in a tissue specific manner (77, 83, 85, 86). All isoforms of NDST are type II membrane proteins with four domains consisting of a cytoplasmic region, a transmembrane region, a stem region, followed by the catalytic domain which contains the independent active sites for *N*-deacetylase and *N*-sulfotransferase activities. The transmembrane and stem regions are thought to localize the enzyme in the Golgi whereby it can encounter the endogenous HS and allowed to participate in HS biosynthesis.

To date the crystal structure of only the *N*-sulfotransferase (NST) domain of NDST1 has been successfully solved (87). The overall structure of NST1 is roughly spherical with

an open clef, composed of a five-stranded parallel β-sheet with α-helices located on both sides (figure 7).

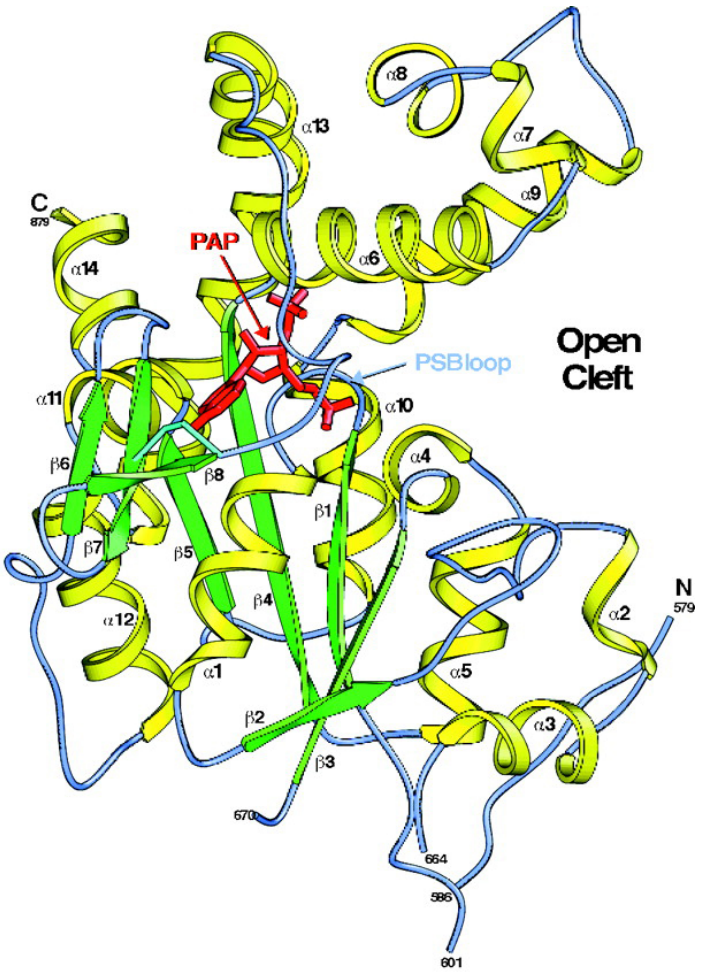

Figure 7. Overall structure of NST1. A ribbon representation of NST1 in complex with PAP. Helices are in *yellow*, β-strands in *green*, random coils in *blue*, disulfide bond in *light blue*, and PAP molecule in *red* (87).

A cavity formed between the 5'-phosphate binding loop (PSB-loop) and α6 defines the site for PAP binding. The open clef that runs perpendicular to the PAP binding cavity is large enough to accommodate a hexasaccharide chain. Based on the crystal structure, the α6 and random coil between β2 and α2 may constitute part of the putative substrate binding site.

Lys-614 of NST1 is known to be a conserved residue in other HS sulfotransferases (88, 89). Site-directed mutagenesis studies have also implicated Lys-614 as a critical residue for NST1 activity (figure 8) (89).

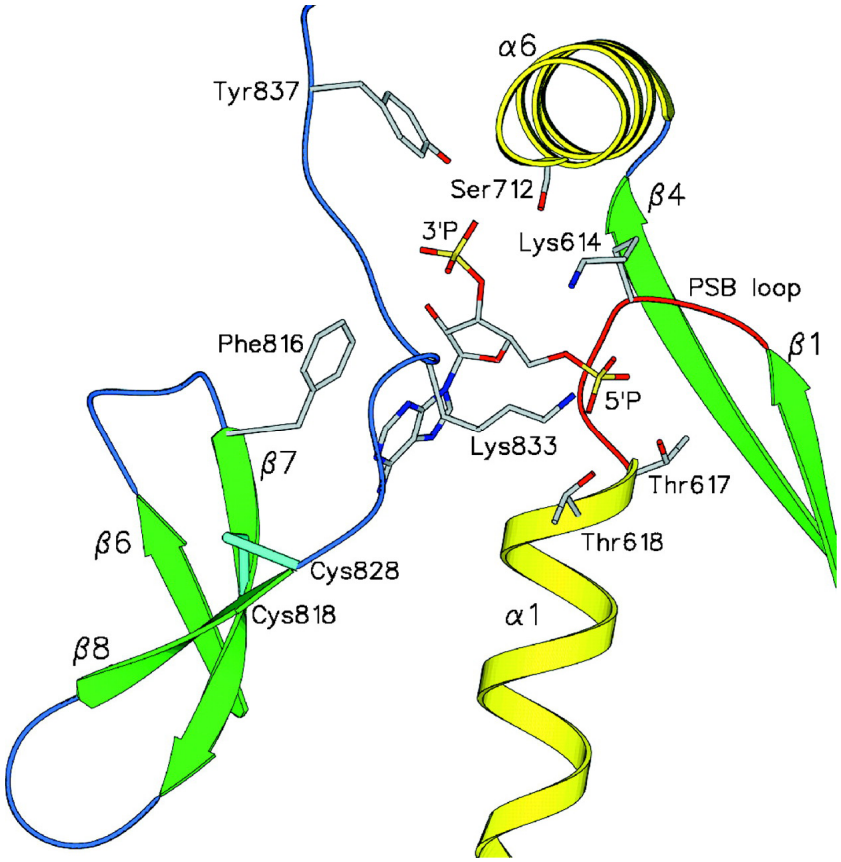

Figure 8. Ribbon diagram of the PAP binding site of NST1. Side chains that can interact with PAP are included. The disulfide bond is in *light blue* (87).

Even though Lys-614 has been implicated in the activity mechanism, the absolute structural role it plays in catalysis remains unsolved. However, the crystal structure of estrogen sulfotransferase (EST) in complex with PAP-vanadate has been solved (90) and has provided some structural insights into the possible catalytic mechanism for the sulfotransferase activity of NST1. Superimposition of the two crystal structures results in similar orientations of their PAP binding sites, especially Lys-614 in the NST1 complex and Lys-48 in EST complex (87, 91). Because of this similar orientation taken together with structural and mutational studies, it is proposed that Lys-614 may act as a proton donor in the NST1 catalytic mechanism, similar to the action of Lys-48 in the EST-PAP-vanadate complex (75, 90). Mutational studies have also been undertaken which suggest that additional residues are critical for NST1 activity (92).

Due to the high degree of sequence homology between NDST isoforms and with the crystal structure of NST1 as a template, molecular modeling techniques have allowed researchers to model the NST domains of the NDST2, NDST3, and NDST4 (77). The molecular models of the NDSTs showed varying charged distributions within their putative substrate binding sites. This suggests that the difference in their relative *N*-deacetylase and *N*-sulfotransferase activities may be due to their variable substrate selectivities. This idea was supported when multiple isoforms of NDST were overexpressed in human embryonic kidney 293 cells individually, resulted in the synthesis of HS with different *N*-sulfation patterns (93, 94).

N-deacetylation and *N*-sulfation of glucosamine residues is considered a prerequisite step for subsequent enzymatic modifications of HS and inactivation of this key step is expected to have very dramatic consequences for the overall structure and sulfation pattern of HS. Moreover, these dramatic changes are hypothesized to have a delirious effect on the relative function of HS. With this said, the generation of NSDT1 and NSDT2 knockout mice had yielded some very interesting results (84, 95). NDST2 null mice showed a phenotype that was restricted to connective tissue-type mast cells (96, 97). This was thought to be unusual considering that NSDT2 is ubiquitously expressed in many tissues. This observation suggested that is it a possibility that other isoforms of NDST can compensate for NSDT2 activity when it is not present. Results with NDST1 yielded very dramatic but expect results considering it is also ubiquitously expressed. Targeted mutations of NDST1 gene showed a dramatic reduction in *N*-sulfation of HS in various tissues (98). Also, which is of great interest, was the observation that NDST1 null mice die neonatally (98). These observations

taken from knockout studies suggest that NDST1 deficiency is lethal, and also implicates the participation of NDST1 and HS in the role of embryonic development.

Glucoronyl C_5 Epimerase (C5-Epi)

In the biosynthesis of HS, C5-Epi, which displays type II transmembrane topology (99), serves to change the configuration at the C_5 position of specific D-glucuronic acid (GlcUA) residues by converting them to L-iduronic acid (IdoUA) residues (100-102). This conversion step is relevant as IdoUA residues are biologically important for HS, as studies have shown these IdoUA residues play a role in promoting interactions with various proteins because of their conformational flexibility (103). Epimerization is a two step process (figure 9).

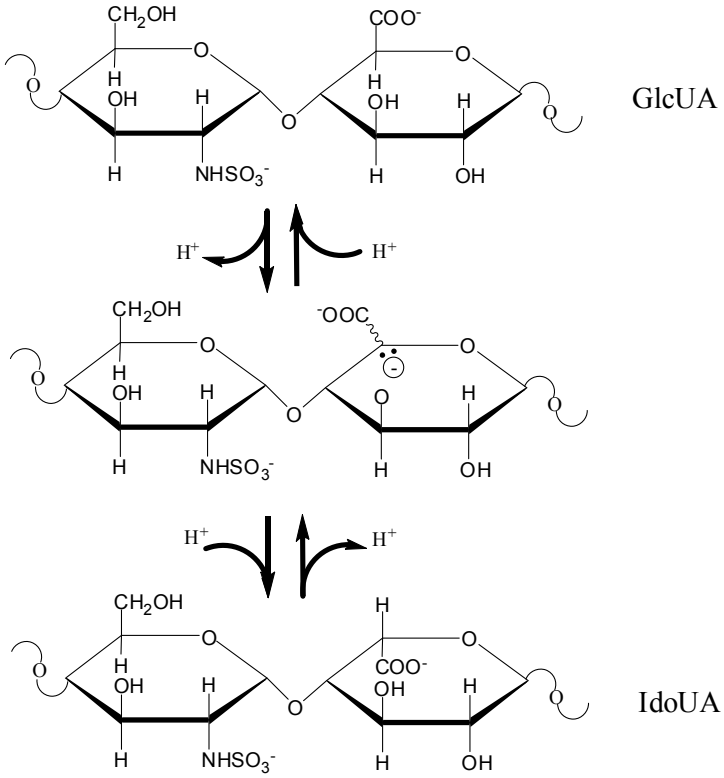

Figure 9: Basic mechanism for C_5 epimerization of GlcUA residues. C_5 epimerization involves abstraction of the C_5 proton of GlcUA (top) followed by re-addition of a proton from the medium to the resultant carbanion intermediate (middle) to generate IdoUA (bottom).

First, there is a removal of the C_5 proton of the GlcUA residue, resulting in the formation of a carbanion intermediate. This is followed by the re-addition of a proton at the C_5 position with the inversion of the stereocenter such that the carboxyl group is shifted across the plane of the sugar ring (100).

Substrate recognition by the epimerase depends on the *N*-sulfation pattern (i.e. NDST activity) of the HS precursor polysaccharide, whereby it is required that the adjacent GlcN residue towards the non-reducing end be *N*-sulfated (i.e. GlcNS-GlcUA). Moreover, if that non-reducing end bears a GlcNAc residue (i.e. GlcNAc-GlcUA), it is not a substrate for the epimerase (101, 104). Additionally, kinetic studies have shown that the epimerase will act on appropriate GlcUA residues (forward reaction) as well as the IdoUA residues (reverse reaction) (104). In a soluble *in vitro* system, epimerization of an appropriate substrate was found to be freely reversible, with the equilibrium favoring the retention of the GlcUA (100). However, when the reversibility of the epimerization reaction in a cellular system was studied, results suggested that C_5 epimerization by the epimerase is irreversible *in vivo*, suggesting that there may be some order in the biosynthetic system (102).

The action of C5-Epi during the biosynthesis of HS is followed by modification of the HS chain by various *O*-sulfotransferases. Immediately following C5-Epi, there is the action of 2-*O*-sulfotransferase (2-OST). It has been proposed that during HS biosynthesis, the biosynthetic enzymes may interact and form complexes with one another. This notion is corroborated by a report that provides evidence to suggest that C5-Epi and 2-OST forms a stable complex *in vivo* (105). When this complex is formed, the relative activity of C5-Epi is increased as compared to its activity when not complexed (105). This feature by which C5-Epi and 2-OST can form a stable complex, with increased activity may manifest itself by the

fact that 2-*O*-sulfation of IdoUA somehow prevents the reverse epimerization reaction back to the GlcUA unit (104).

Uronosyl 2-*O*-Sulfotransferase (2-OST)

2-OST catalyzes the transfer of a sulfo group from PAPS to the 2-OH position of specific uronic acid residues within HS (see figure 10).

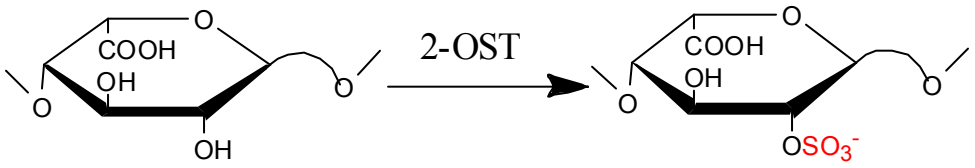

Figure 10. Reaction catalyzed by 2-OST. 2-OST can catalyze the transfer of a sulfo group from PAPS to the 2-OH position IdoUA to generate IdoUA2S, *as drawn*. 2-OST can also sulfate GlcUA acid but the catalytic transfer favors the sulfation of IdoUA. The SO_3^- is colored in *red* for emphasis.

The 2-*O*-sulfation has been deemed important as specific interactions between HS and a variety of proteins depend upon the degree of *O*-sulfation, specifically 2-*O*-sulfation's involvement in fibroblast growth factor (FGF) binding (106). Currently, 2-OST is unique among the other sulfotransferases that participate in the biosynthesis of HS in that it is presently found to exist in only one isoform. The substrate specificity of 2-OST has been investigated, using appropriate *N*-sulfated substrates (107, 108). From these investigations, evidence suggests that 2-OST has the ability to use IdoUA and GlcUA as substrates for 2-*O*-sulfation. However, in substrates containing both uronic acid residues in equal amounts, 2-OST strongly favored the 2-*O*-sulfation of IdoUA (107). In agreement with the propensity to generate IdoUA2S, 2-OST was also found to have approximately a five-fold higher affinity for IdoUA containing substrates when compared to that of GlcUA containing substrates (107). To date the crystal structure of 2-OST has not been solved, thus the mechanism by which 2-OST recognizes its substrate and transfers a sulfo group is not completely known.

However, based on the high sequence homology with other sulfotransferases (NST1 and 3-OST-1 and 3-OST-3) in which the crystal structures have been solved, it is hypothesized that the sulfuryl transfer mechanism of 2-OST is similar.

The 2-*O*-sulfation of appropriate residues within HS is of biological importance as implicated in mutational studies. Genetic studies have shown that mice that are deficient in 2-OST die during the neonatal period due to defective kidney development and it was proven that the HS chains lacked 2-*O*-sulfate groups (109, 110). Also, 2-OST deficient mice showed skeletal as well as eye morphological defects (84). However, in these 2-OST deficient mice no lung defects could be detected suggesting that different sulfation patterns of HS are important for the development of different tissues, since NDST deficient mice were found to development lung defects (111). Since subsequent chain modifications are dependent on *N*-sulfation, NDST deficient mice will have a reduced degree of 2-*O*-sulfation. However, in these mice (NDST deficient) with reduced 2-*O*-sulfation, kidneys were found to develop normally suggesting that the reduced amounts of 2-*O*-sulfation may be sufficient for kidney development (84, 109, 110). These studies provide evidence to suggest that variable degrees of different types of sulfation may allow HS to have variable biological effects.

Glucosaminyl 6-*O*-Sulfotransferase (6-OST)

6-OST serves to catalyze the transfer of a sulfo group from PAPS to the 6-OH position of specific glucosamine (GlcN) residues within the HS polysaccharide chain (figure 11).

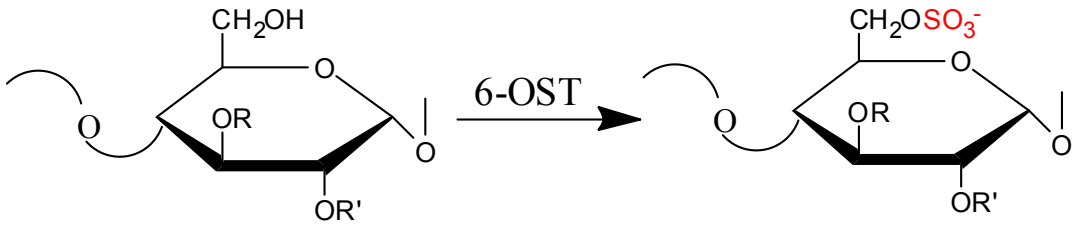

Figure 11: Reaction catalyzed by 6-OST. 6-OST catalyzes the transfer of a sulfo from PAPS to the 6-OH position of GlcN. R' represents sulfate or acetyl group, R represents proton. The SO_3^- is colored in *red* for emphasis.

Three isoforms of 6-OST (6-OST-1, -2 and -3) have been cloned and characterized (112). All three isoforms display type II transmembrane topology and have approximately 50-55% sequence homology to each other (112). The tissue expression patterns among the 6-OST isoforms are variable, where 6-OST-1 is found to be highly expressed in liver, 6-OST-2 is primarily expressed in brain and spleen, and 6-OST-3 is rather ubiquitously expressed (78). Using recombinant enzymes, the substrate specificities of the different 6-OST isoforms have been investigated (78, 113). In those studies, investigators used various *O*-desulfated and polysulfated oligosaccharides as potential substrates for 6-*O*-sulfation. Results obtained suggested that all 6-OST isoforms can catalyze the 6-*O*-sulfation of glucosamine residues contained within the following sequences –GlcUA-GlcNS- and –IdoUA-GlcNS-. In addition, results also suggested that all isoforms had a higher preference for the 6-*O*-sulfation of IdoUA-containing sequences with or without 2-*O*-sulfation. Additionally, 6-*O*-sulfation of GlcNAc residues was also found to be achievable with all three isoforms of 6-OST (113). Based on the investigations, it can be concluded that the three isoforms have similar substrate specificities with only minor differences within their target preference or recognition.

The interaction of HS with FGF is critical for the growth factor to bind to the cell surface. Various structural motifs or sulfation patterns provide the necessary binding sites for these interactions to occur. It has been found that HS lacking 6-*O*-sulfation lost its capability to stimulate FGF-mediated cell proliferation (114). Disaccharide analysis of FGF

activating and non-activating oligosaccharides yielded a significant difference. Based on disaccharide analysis, the difference between these fractions were that the activating fractions contained 6-*O*-sulfated disaccharides whereas the non-activating fractions did not (114). These results suggest that in addition to 2-*O*-sulfation of IdoUA residues, there is a requirement for 6-*O*-sulfation of glucosamine residues within HS for the promotion of HS-mediated FGF activity.

Glucosaminyl 3-*O*-Sulfotransferase (3-OST)

The final modification, and also the most rare, in the biosynthesis of HS is catalyzed by the activity of 3-OST. 3-OST serves to catalyze the transfer of a sulfo group from PAPS to the 3-OH position of specific glucosamine residues within HS (figure 12).

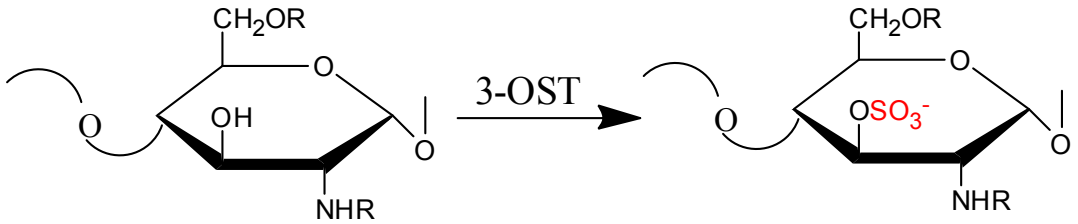

Figure 12: Reaction catalyzed by 3-OST. 3-OST catalyzes the transfer of a sulfo from PAPS to the 3-OH position of GlcN residues to generate 3-*O* sulfo GlcN. R represents sulfate or acetyl group. The SO_3^- is colored in *red* for emphasis.

To date, 3-OST is found to be expressed in seven isoforms which are present at different levels in a tissue specific manner (Table 1) (79). It is on this premise that suggests 3-OST is important in the biosynthesis of tissue-specific HS. The isoforms of 3-OST that have been cloned and characterized are 3-OST-1, -2, -3_A, -3_B, -4, -5, and -6. The isoforms of 3-OST have been found to have 50-80% homology within their sulfotransferase domain (79). In particular, 3-OST-3_A and 3-OST-3_B have nearly identical amino acid sequence in the sulfotransferase domain (115). All isoforms of 3-OST, except 3-OST-1, are classified as type II transmembrane proteins, which suggest that they can be localized in the Golgi so as to

be in the proper vicinity to participate in HS biosynthesis. 3-OST-1 is found to lack this transmembrane region; however its ability to participate in HS biosynthesis suggests it is or can be localized to the Golgi via an alternative mechanism, possibly through interactions with other proteins that reside in the Golgi compartment (79).

Table 1: Tissue Expression and Known Biological Function of 3-OST Modified HS

3-OST Isoform	Tissue Distribution	Known Biological Function
3-OST-1	Heart, brain, lung, kidney	Anticoagulant HS
3-OST-2	Brain	HSV-1 entry receptor
3-OST-3_A	Heart, placenta, lung, liver, kidney	HSV-1 entry receptor
3-OST-3_B	Heart, brain, lung, liver, kidney	HSV-1 entry receptor
3-OST-4	Brain	HSV-1 entry receptor
3-OST-5	Brain, spinal cord, skeletal muscle	Anticoagulant HS and HSV-1 entry receptor
3-OST-6	Liver, kidney	HSV-1 entry receptor

By invoking their catalytic activity during the final stages of HS biosynthesis, the isoforms of 3-OST are generally considered to be more driven in terms of their substrate specificities compared to that of other HS biosynthetic enzymes. The studies of 3-OSTs and their substrate specificities using recombinant enzymes demonstrate that these enzymes transfer a sulfo group to the 3-OH position of glucosamine residues that is linked to different sulfated uronic acid residues (81, 116, 117) (figure 13). The substrate specificities of 3-OST-1, 3-OST-3 and 3-OST-5 have been studied more extensively and are presented here for clarity as opposed to the presentation of all 3-OST isoform substrate specificities.

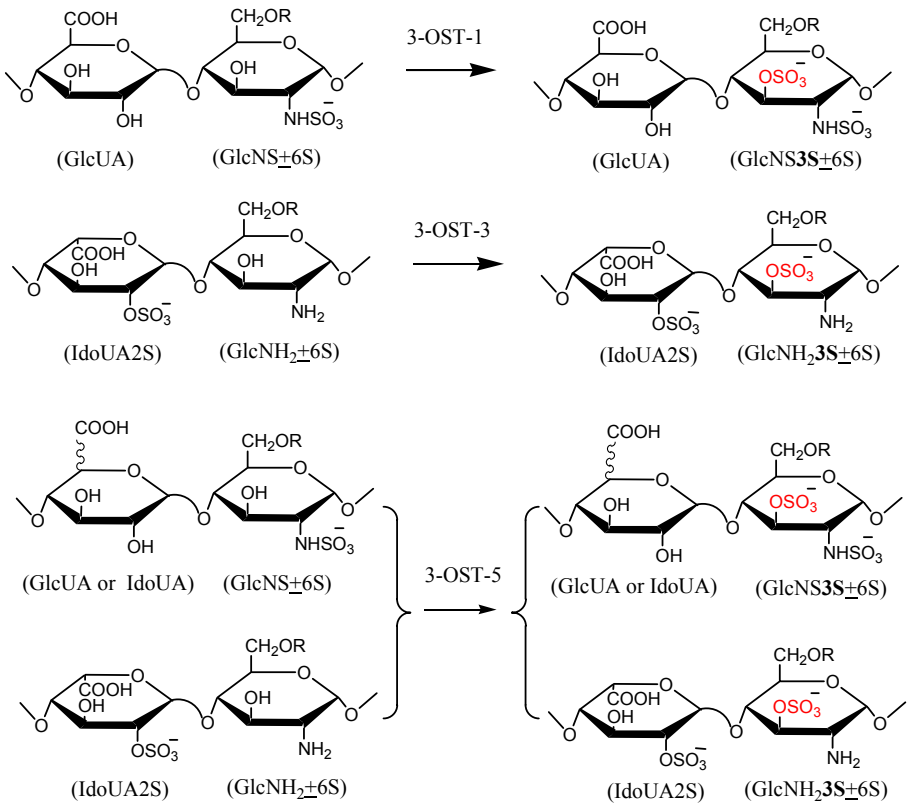

Figure 13: Substrate specificities of 3-OST-1, 3-OST-3 and 3-OST-5 (116). 3-OST-1 transfers a 3-*O*-sulfo group to *N*-sulfated glucosamine (GlcNS±6S) residues that are linked to non-sulfated glucuronic acid (GlcUA) residues at its nonreducing end. 3-OST-3 transfers a 3-*O*-sulfo group to *N*-unsubstituted glucosamine ($GlcNH_2$±6S) residues that are linked to 2-*O*-sulfo iduronic acid (IdoUA2S) residues at its nonreducing end. 3-OST-5 transfers a 3-*O*-sulfo group to glucosamine (GlcNS±6S or $GlcNH_2$±6S) residues that are linked to either a non-sulfated or sulfated iduronic (IdoUA±2S) or non-sulfated glucuronic acid (GlcUA) residue on its nonreducing end.

The addition of the 3-*O*-sulfo group is hypothesized to generate binding sites within HS for a number of biologically important proteins. This hypothesis is supported by that fact that 3-OST-1 modified HS has the ability to bind to antithrombin (AT) and possess anticoagulant activity, whereas 3-OST-3 modified HS can bind to herpes simplex virus envelope glycoprotein D and assist in viral infection by serving as an entry receptor for HSV-1 (118, 119). Additionally, studies have shown that 3-OST-5 seems to be a more promiscuous enzyme, as it is able to generate HS sequences that can bind to AT as well as glycoprotein D.

The crystal structures of 3-OST-1 (120) and 3-OST-3 (121) have been solved and along with the elucidation of the structure of NST1, have provided some structural

information concerning the catalytic mechanism and substrate recognition properties of the HS sulfotransferases. In a published report, 3-OST-1 was crystallized in a binary complex with the donor product PAP (figure 14).

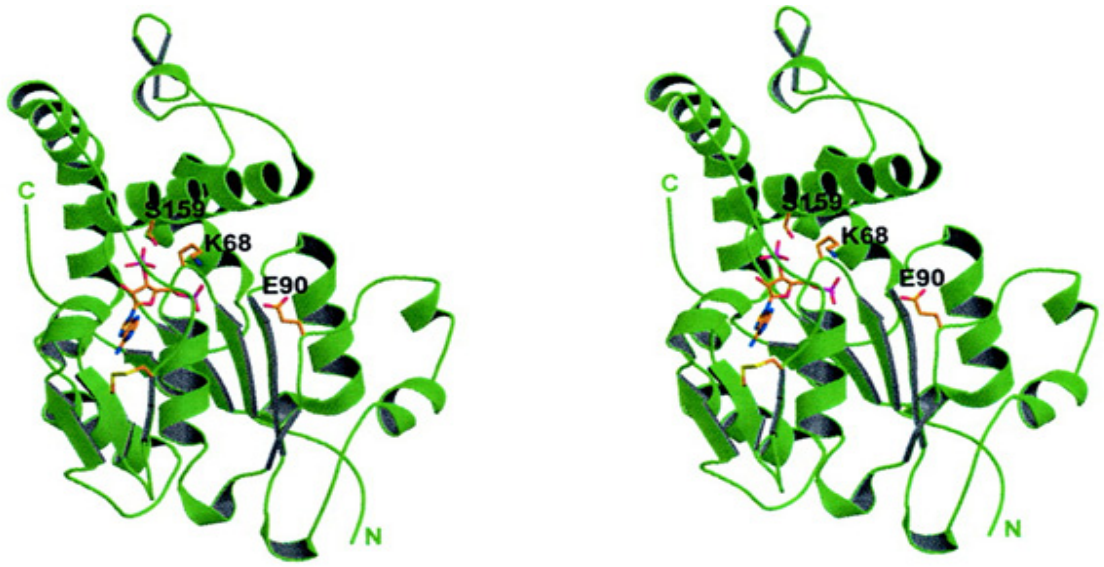

Figure 14: Stereo diagram of the PAPS binding site of 3-OST-1 (120). Also pictured are the donor product PAP, conserved residues Ser-159 and Lys-68, and the catalytic Glu-90 that interact with the 3'- and 5' phosphates of PAP respectively. The conserved histidine is not shown.

The structure of the 3-OST-1-PAP complex is roughly spherical that contains a relatively large open clef. Additionally, as consistent with all known sulfotransferases, the structure is centered around an α/β motif (75). Detailed observations of the crystal structure along with mutational studies revealed critical residues for PAPS binding and enzymatic activity of 3-OST-1 (120). These studies also suggest potential residues that may dictate or direct substrate specificity along with evidence that suggest 3-OST-1 undergoes a conformational change upon HS binding (120, 122).

The crystal structure of 3-OST-3 was solved in a ternary complex with PAP and a *N*-sulfated tetrasaccharide substrate (121) (figure 15).

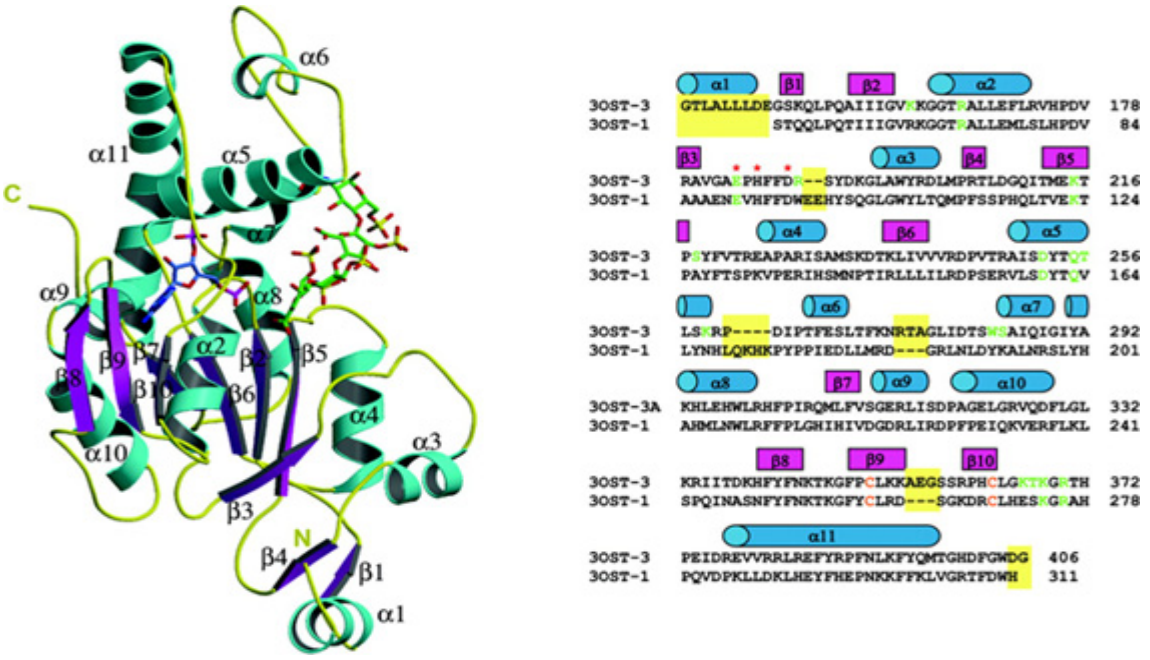

Figure 15: Ribbon diagram of the crystal structure of ternary complex 3-OST-3/PAP (blue)/tetrasaccharide (green) and sequence alignment of human 3-OST-3 and mouse 3-OST-1 (121). ß-strands and a-helices are purple and cyan respectively. Structural alignment of 3-OST-3 with 3-OST-1 is shown. Cyan barrels represent residues in helices and purple represents regions in B-strands. Residues that are structurally dissimilar are shaded with a yellow background. Residues that form interactions with the tetrasaccharide are colored green and the cysteines that form a disulfide bond are colored orange. Red asterisks represent the three residues that may form a catalytic triad in the 3-OSTs.

The overall structure of 3-OST-3 was found to be very much similar to that of 3-OST-1, with minor differences that were not found to contribute to the enzyme substrate specificity as they were found to be external of the conserved sulfotransferase domain. The elucidation of this ternary complex combined with mutational studies identified residues that are involved in substrate recognition during catalysis (121). It also provided atomic details concerning the reaction mechanism of HS sulfotransferases. When PAPS is superimposed onto PAP, the acceptor hydroxyl group of the substrate is located 2.9 Å from the sulfur atom of PAPS and on the opposite of the sulfur from the leaving group PAP (see figure 16).

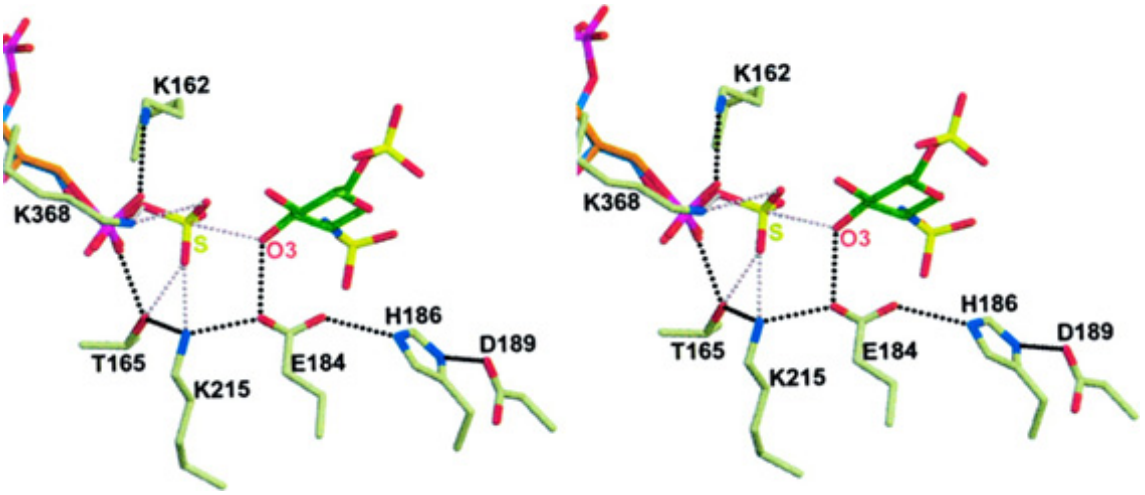

Figure 16: Active site of 3-OST-3 with PAPS superimposed (121). Stereo diagram of the superposition of the PAPS (orange) from the crystal structure of human estrogen sulfotransferase in to the active site of 3-OST-3 (123). The PAP (blue) and the acceptor substrate (*green*) are pictured, as are residues that may play a catalytic role. Possible hydrogen bonds between 3-OST-3 and its substrate are displayed as *black dashed lines*. Possible interactions between 3-OST-3 and the donor sulfuryl group based on the superposition are displayed as *pink dashed lines*. Also displayed as a *pink dashed line* is the line of attack of the O-3 oxygen of the sugar to the donor sulfur atom of the PAPS molecule.

The location of the sulfate group is consistent with a SN_2 like displacement mechanism. Given that Glu-184 is 2.8 Å from the 3-OH position of the substrate, it is reasonable to suggest that this residue likely functions as a catalytic base serving to deprotonate the 3-OH position allowing for a nucleophilic attack on the sulfate group. This glutamate residue is conserved among all the 3-OSTs and NSTs, suggesting its essential role for the catalytic function of HS sulfotransferases. Studies have shown that if this conserved glutamate residue is mutated, activities of NST-1 and 3-OST-1 (92, 120) and 3-OST-3 (121) are completely lost. A hydrogen bonding network that involves Glu-184, His-186, and Asp-189 is observed in the ternary complex (figure 16). This hydrogen bonding pattern is considered to be a catalytic triad. Mutational studies have provided results that have shown His-186 and Asp-189 to be essential for the sulfotransferase activity of 3-OST-3 (121). It is interesting to note that a similar hydrogen bonding network is observed in 3-OST-1 but not in NST-1 (87, 120). This result suggests that this "catalytic triad" may be linked to 3-OST activity.

Currently the crystal structure of 3-OST-5 has not been solved. When the crystal structure of 3-OST-5 is available, it may provide some structural information to corroborate the promiscuous nature of 3-OST-5 and the presence of the catalytic triad will strengthen the notion that it is linked to 3-OST activity.

Interesting and important information concerning the roles of 3-*O*-sulfated HS in biological events can be learned from using knockout mice. Currently, only 3-OST-1 has been successfully knocked out and results show no obvious phenotype (124, 125). From the published reports, it was also concluded that 3-OST-1 generates the majority of anticoagulant HS. Evidence was also provided that allowed for the conclusion that there is an unexpected phenotype exhibited by 3-OST-1 deficient mice in that they do not display an obvious procoagulant phenotype. This would suggest that 3-*O*-sulfotransferases may have some redundancy associated within its various isoforms as suggestive by the fact the 3-OST-5 can generate anticoagulant HS as well.

Section III: Common Analytical Approaches for Structural Analysis of HS

It is widely known that HS plays a role in many biological processes. However, due to the heterogeneity and structural diversity that HS displays within its polysaccharide chain, the elucidation of the structural-functional relationship of HS remains largely unresolved. The structural analysis of HS has come a long way; however under current technologies it is still impossible to completely characterize biologically relevant full length HS polysaccharides sequences. Even though it is not possible to study the structure activity relationship of HS at the polysaccharide level, is possible to characterize HS at the oligosaccharide to disaccharide levels.

The initial step in the analysis of a HS sequence is usually a study of its disaccharide components in which the relative composition and purity can be analyzed using multiple analytical techniques that include various HPLC chromatography methods and capillary electrophoresis (126, 127). There are only a few choices available to depolymerize HS into its disaccharide components with high specificity. The common methods for degrading the HS polysaccharide into its oligosaccharide or disaccharide components are enzymatic or chemical degradation. It is important to note here that utilizing these methods have revealed various disaccharide components that play a role in allowing HS to posses anticoagulant activity as well as the ability for HS to be used as an entry receptor for the HSV virus (128-130).

Heparin Lyases

The use of heparin lyases are the most commonly used enzymatic approach for the degradation of HS into its disaccharide substituents. Heparin lyases exist in multiple

isoforms that can be isolated from *Flavobacterium heparium* and are commercially available. Additionally, these isoforms can be expressed as recombinant proteins using traditional molecular cloning techniques. The multiple isoforms of heparin lyases have been found to have different substrate specificities which has aided in their use for the structure analysis of biologically relevant HS (figure 17)

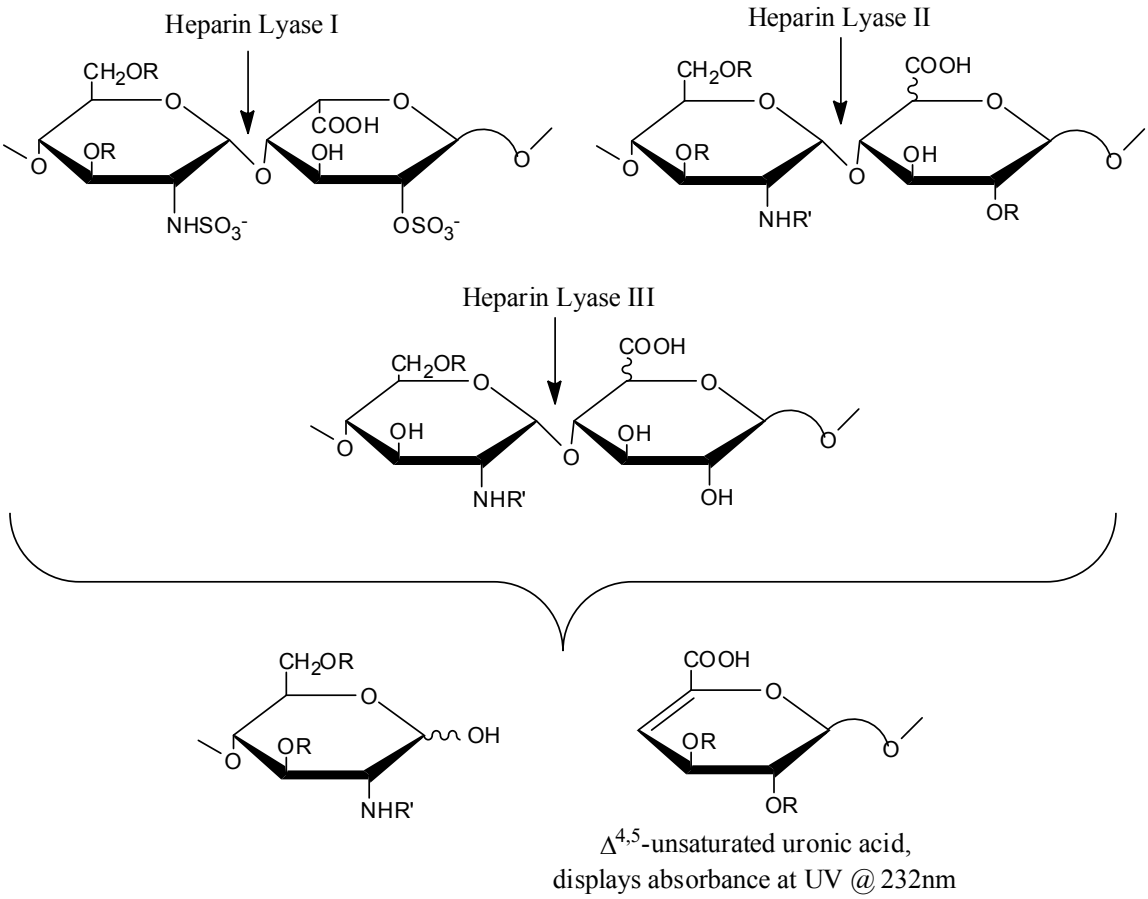

Figure 17: Substrate specificities of heparan lyases. R represents (SO_3^-) or H; R' represents (SO_3^-), an acetyl or H.

Because heparin lyases are endoglycosidases, these enzymes cleave specific internal glycosidic linkages between the hexuronic acid and glucosamine residues within HS (131). The substrate specificity of the isoforms allows the lyases to recognize their cleavage sites within unique saccharide context (132). Briefly, heparin lyase I cleaves the glycosidic linkage between 2-*O*-sulfated iduronic acid and *N*-sulfated glucosamine residues in highly

sulfated domains within HS. Heparin lyase III cleaves the glycosidic linkage between glucuronic acid and either *N*-acetylated or *N*-sulfated glucosamine in less sulfated domains within HS when compared to that of heparin lyase I. Heparin lyase II displays less structural specificity in terms of its substrate recognition with the ability to cleave both heparin lyase I and heparin lyase III sites displayed within HS. The major advantage for using heparin lyases to degrade HS is that the degradation results in the formation of a $\Delta^{4,5}$-unsaturated uronic acid at the non-reducing end of the product which gives it characteristic absorbance at 232 nm (figure 17). The limitation here is that there is a loss of structural configuration about the C_5 carbon of the hexuronic acid, which does not allow for the correct assignment of IdoUA or GlcUA residues in the precursor structure.

Nitrous Acid Digestion

Another approach commonly used to degrade the HS polysaccharide is by chemical means using nitrous acid as shown in figure 18. Nitrous acid digestion of HS generates 2,5-anhydromannose residues via nitrous acid reaction with glucosamine, which can be stabilized by conversion to 2,5-anhydromannitol by a reducing agent. The selectivity of the nitrous acid reaction is found to be pH dependent. Briefly, at high pH (4.5-5.5) nitrous acid degradation is selective towards *N*-unsubstituted glucosamine residues by reacting with the free amino group. Conversely, at low pH (1.5) this reaction is more selective toward *N*-sulfated glucosamine residues (133). The advantage in using this chemical degradation method is that the configuration about the C_5 carbon of the hexuronic acid is retained, which allows for subsequent assignment of IdoUA versus GlcUA residues using HPLC disaccharide analysis. The limitation here is that the degraded products do not contain any

intrinsic UV absorbance properties, thus the incorporation of a radiolabel tag or fluorescent motif is required before analysis.

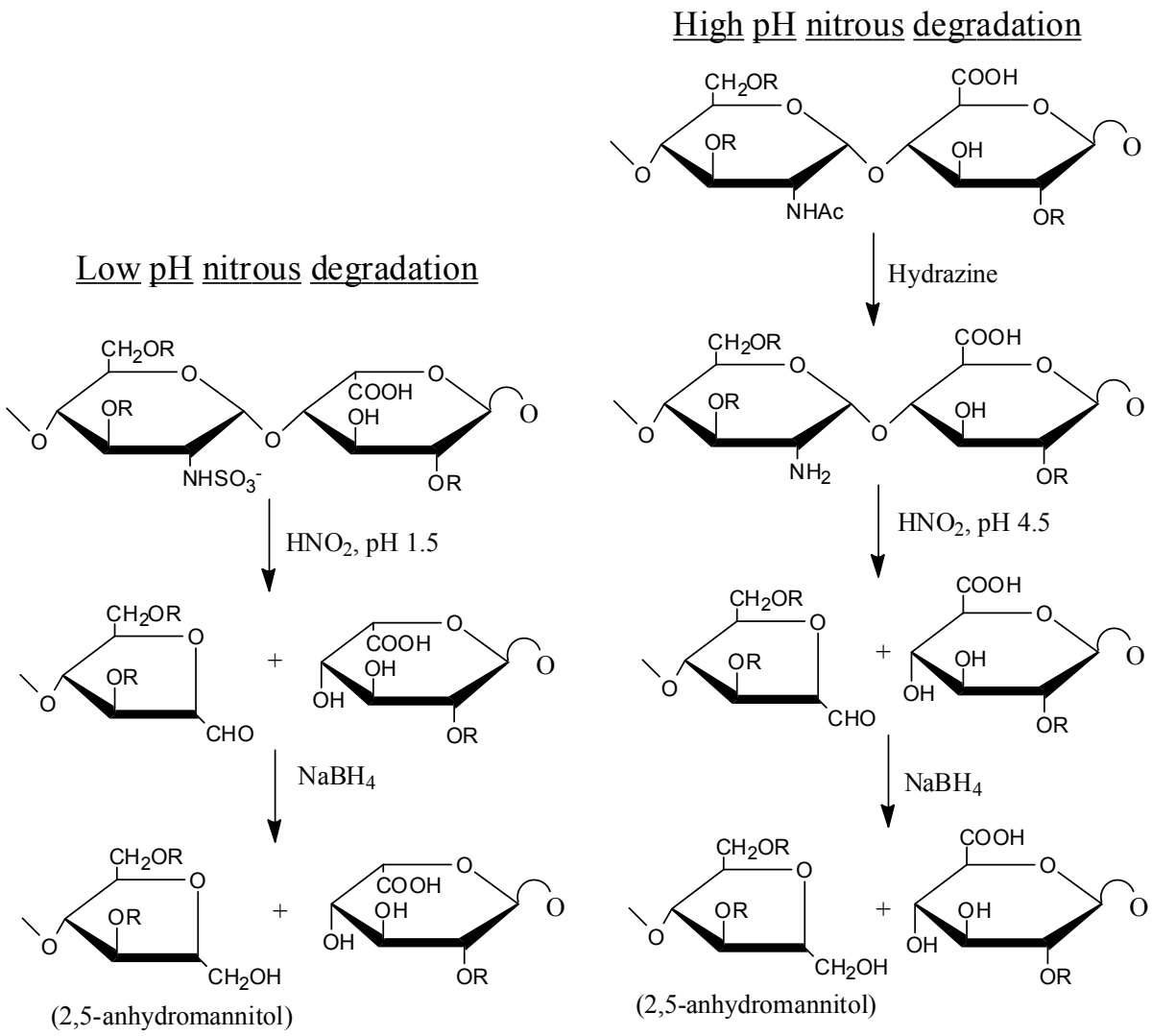

Figure 18: Degradation of HS with nitrous acid. Nitrous acid cleaves the linkage of *N*-sulfated glucosamine and uronic acid at pH 1.5. Nitrous acid cleaves the linkage of *N*-unsubstituted glucosamine and uronic acid at pH 4.5-5.5. *N*-acetylated glucosamine is converted to *N*-unsubstituted glucosamine via deacetylation by incubating HS with hydrazine.

Sequencing Approach

Another approach for the structural analysis of HS oligosaccharides can be described as a multifaceted sequencing approach. This strategy is divided up into two sections; reducing end analysis and non-reducing end analysis. By using each component of this strategy it is possible to systemically determine the identity of a HS saccharide sequence if given a sufficient amount of material. Briefly, reducing end analysis involves the incorporation of a tag onto the reducing end of the oligosaccharide via reaction with its hemiacetal group. Reducing tags can include a fluorescent tag, a radiolabeled tag, or a mass tag (109, 134, 135). After the incorporation of either of the above tag moieties, it is then possible to subject the tagged derivative to a series of digestions with heparin lyases or with nitrous acid under partial or exhaustive conditions. The reducing end tag will allow for the determination of whether the resulting disaccharide (or oligosaccharide) originated from the reducing end as it with have different characteristics upon analysis with appropriate standards. Non-reducing end analysis involves the use of a series of exoenzymes that only react with the non-reducing end of the saccharide sequence. These exoenzymes include various sulfatases, hexauronidases, and α-hexaminidases. Accordingly, based on the substrate specificities of the exoenzymes one can determine the identity of each residue after its systematic cleavage. It is important to note here that cleavage of a residue will change the characteristics of the material in the form of a shift during analysis on HPLC and other analytical techniques.

In addition to the above approaches, the use of various mass spectrometry techniques has greatly aided in the characterization and study of HS oligosaccharides sequences. These techniques include the use of matrix-assisted laser desorption/ionization (MALDI-MS) and

nanoelectrospray ionization (nESI) mass spectrometry (136-138). The great advantage of these techniques is that they offer analysis to be conducted on femto- to picomole amounts of material. This aspect is critical due to the complex and difficult nature that exists in the isolation of complex HS oligosaccharides. The characterization of HS polysaccharide sequences at the disaccharide to oligosaccharide levels using enzymatic and chemical degradative approaches combined with MS techniques have revealed some structural relationships between various HS components that affect binding or activation of various proteins.

Section IV: Heparan Sulfate Protein Interactions

Heparan sulfate has been shown to interact with and modulate the activities of many different proteins. These proteins include cytokines, growth factors, adhesion molecules, ECM proteins, as well as enzymes (31, 139, 140). The majority of these proteins can interact with HS via ionic interactions primarily with lysine and arginine residues located within primary consensus sequences known as "Cardin-Weintraub" sequences (141). These consensus sequences are as follows: XBBXBX and XBBBXXBX; where B is a basic amino acid and X is any hydrophilic amino acid. As a result, these sequences have been used as an initial screen to identify regions within proteins that can potentially bind HS. However, as this is a simplified generalization, it is important to note that not all HS binding sequences are contiguous; the 3-D structure of a protein has an effect on HS binding and may orient the necessary residues from different regions of the protein in close proximity as to play a role in HS binding. The interactions between HS and different types of proteins have been reviewed extensively (142, 143). It is a misconception to imply that HS binding interactions are merely non-specific ionic interactions. Current investigations provide evidence to suggest that HS binding interactions are indeed specific. Herein, the focus of this section will be to highlight the two most heavily studied HS binding proteins, antithrombin (AT) and fibroblast growth factor (FGF), as investigations have led to some specific structural features of HS that play a important role its ability to bind to AT and FGF.

Antithrombin (AT)

AT is a single-chain glycoprotein, present in the plasma, with a molecular weight of 58 kDa. AT, a member of the serpin (serine protease inhibitor) superfamily of proteins, displays its primary regulatory function within the blood coagulation cascade (figure 19).

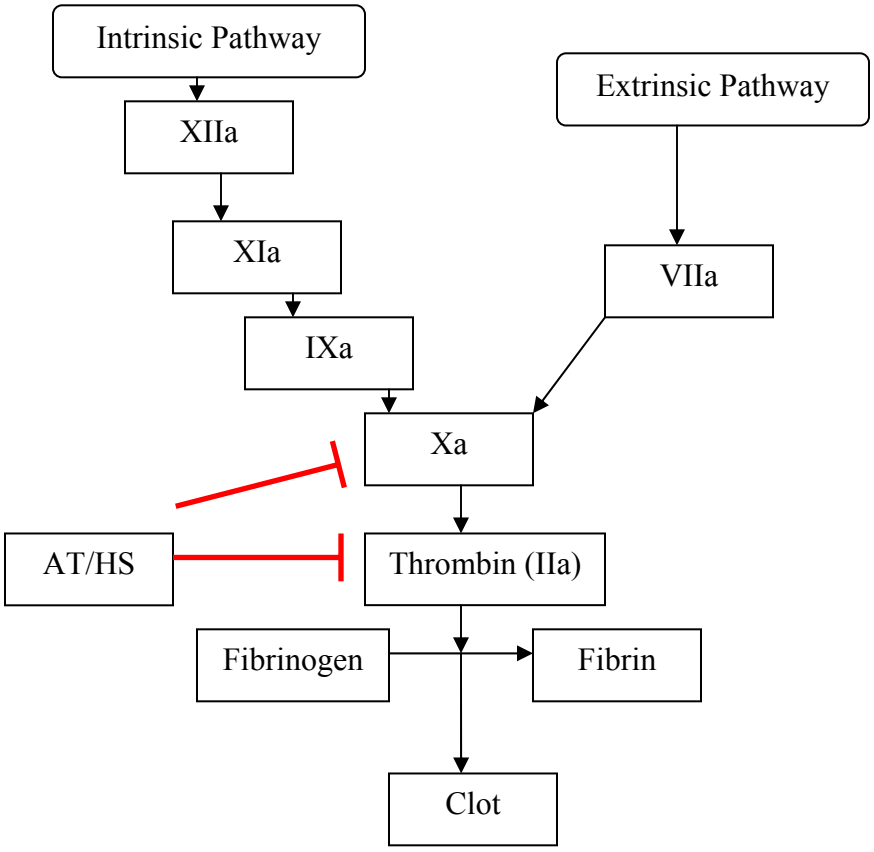

Figure 19: Simplified representation of the blood coagulation cascade. As shown the cascade can be initiated by two distinct pathways: the intrinsic pathway and the extrinsic pathway. The cascade is made up of various proteases as illustrated above. They converge on the activation of factor X into Xa. 'a' denotes active species. The *red* line represents inhibitory action of AT/HS complex factor Xa and to a lesser extent on thrombin.

As illustrated in figure 19, the blood coagulation cascade can be separated into two distinct pathways: the intrinsic pathway and the extrinsic pathway. The intrinsic pathway is initiated when there is an exposure of collagen to a vessel surface; while the extrinsic pathway is initiated at the site of the injury in response to the release of a tissue factor (Factor III). Although the pathways are initiated by distinct processes, they do converge on a

common pathway (Factor Xa activation) that ultimately leads to the activation of thrombin via hydrolysis. Thrombin is serine protease that once activated by factor Xa, can convert fibrinogen to fibrin. Fibrin then has the ability to form cross-links thereby generating and stabilizing a fibrin mesh or commonly known as a blood clot.

The activity of AT is critical for the regulation of the blood coagulation cascade, which is critical for maintaining proper blood flow, while preventing excessive bleeding or thrombosis (144). The importance of AT was observed in genetic studies whereby AT-deficient mice resulted in death from massive thrombosis (145). Additionally, there is a correlation between functional AT and diseases, specifically individuals with functionally defective AT were found to be susceptible to thromboembolic diseases (146). As mentioned previously, AT displays its primary role as a protease inhibitor in the regulation of blood coagulation proteinases. AT has a natural ability to bind to and inhibit both factor Xa and thrombin but at a relatively slow rate. The activity of AT has been found to be enhanced by binding to HS/HP. Briefly, it has been demonstrated that once AT binds to HS, it undergoes a conformational change at its reactive center thereby resulting in an accelerated inactivation of factor Xa (147) and an increased affinity for thrombin (IIa) (148). This enhances the formation and stabilization of AT/IIa complexes which results in the inhibition of factor IIa activity in the blood coagulation cascade.

HP has been therapeutically used as an anticoagulant for many years. During that time very little was known about the specific structural features that allow for HP to bind to AT. HP usage as an anticoagulant has been shown to have a few side effects, specifically platelet aggregation and blockage of veins (149). It was hypothesized that a synthetic derived oligosaccharide could serve to decrease the side affects associated with HP

administration. As a result of impressive structural analysis, the determination of the minimum saccharide sequence required for AT binding has been elucidated (figure 10) (150).

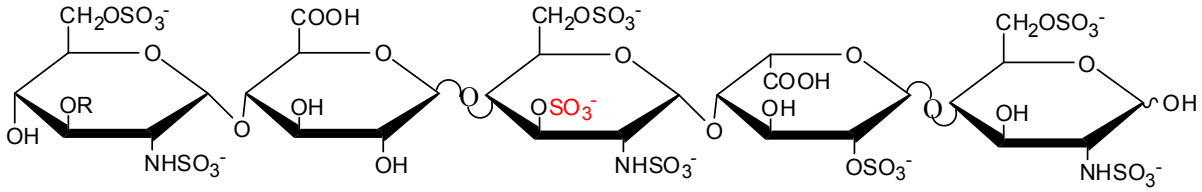

Figure 20: AT binding pentasaccharide. The critical 3-*O*-sulfo group on the internal glucosamine is shown in *red* for emphasis. The pentasaccharide has K_d = 10-50 nM .

This unique pentasaccharide sequence is a rare component of HS/HP as it contains a 3-*O*-sulfo group on its internal glucosamine residue. This pentasaccharide has a binding affinity to AT of 10-50 nM. The pentasaccharide alone can achieve the accelerated inactivation of factor Xa by binding to and inducing a conformation change in AT. However, in order for thrombin (IIa) to be effectively inactivated, longer HP chains are necessary as it can bridge AT and thrombin generating a ternary complex (151). It is important to note here that the 3-*O*-sulfo group can be transferred to HP/HS by the catalytic activity of 3-OST-1 and 3-OST-5. The addition of the 3-*O*-sulfo group has been found to enhance AT binding affinity by 20,000-fold (152). Moreover, targeted disruption of 3-OST-1 results in the decreased ability of HP/HS to bind to AT, which suggests that the 3-*O*-sulfo group plays an important role in binding. The crystal structure of AT in complex with the pentasaccharide has been solved and has provided structural information regarding the amino acid residues involved in binding (148, 153).

Due to the high anticoagulant activity of the pentasaccharide, a synthetic HP pentasaccharide which only contains the AT binding region of HP, is now being used as an anticoagulant with reduced side effects under the name of Arixtra®. The elucidation of the specific sequence required for AT binding has opened the door for the increased study regarding the structure of HS-protein interactions. Currently, research is underway to

determine the minimum structural motifs that are displayed by HS in order for it to acquire the ability to interact with a variety of proteins, with hopes that the structural functional relationships, once elucidated, will serve to aid in the development of HS-related compounds that will modulate a variety of biological processes.

Fibroblast Growth Factor (FGF)

The FGF family of proteins is comprised of approximately 20 members. Studies have shown that HS provides binding sites for members of the FGF family and have the ability to modulate FGF-mediated signaling events which have a role in cell proliferation, differentiation and angiogenesis (154, 155). The majority of investigations to date, in terms of the structural requirements of HS that allow for binding, have been focused on two members of the FGF family namely FGF1 and FGF2. The FGF signaling cascade involves FGF binding to its cell surface receptor (FGFR), which leads to receptor oligomerization. This is followed by phosphorylation/activation of downstream signaling molecules, which initiates the signaling cascade. HS binding has been implicated in this pathway by enhancing the formation of FGF-FGFR complexes and stabilization of FGFR oligomers (156).

Several crystal and co-crystal structures of FGFs with different HS oligosaccharides and FGFRs have been solved (154, 157-159). The structure of various FGF-HS oligosaccharide complexes suggest that FGF1 and FGF2 have different HS-mediated oligomerization modes in terms of the stoichiometries of the respective complexes. Crystal structures have also implicated specific sulfate groups that are involved in FGF binding and/or FGF signaling (figure 21) (160).

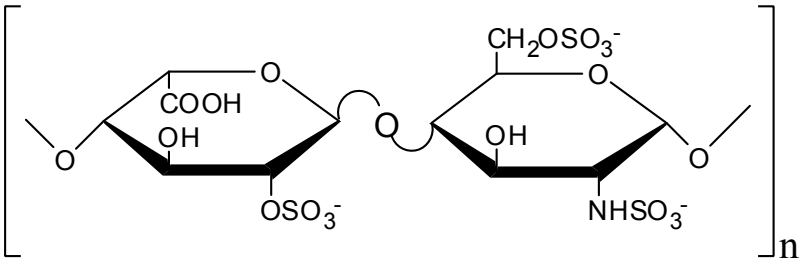

Figure 21: Repeating disaccharide unit –IdoUA2S-GlcNS6S- implicated in FGF binding. n>2 needed for binding, while n>5 needed for dimerization and cell signaling.

The oligosaccharide sequences contained within the crystal structures were primarily of the repeating disaccharide unit of [-IdoUA2S-GlcNS6S-]. Analysis of the structures by NMR and surface plasmon resonance (SPR) techniques determined the following: 1) the 2-*O* sulfate on iduronate and *N*-sulfate on the glucosamine residues are critical for both FGF1 and FGF2 binding and signaling, and 2) the 6-*O* sulfate on the glucosamine is critical for FGF1 binding and signaling; however it was found not to be necessary for FGF2 signaling (160). This suggests that there may be some specificity between different growth factors for specific HS sulfated sequences. Additionally, it was shown that saccharide length plays an important role in HS ability to facilitate growth factor dimerization (160). This is important as dimerization of the growth factor is essential for the initiation of FGF-mediated signaling events.

While extensive structural studies have focused on HS ability to bind to FGF1 and FGF2, studies are currently being initiated that focus on HS ability to bind to the other members of the FGF family as well as other growth factors (161). Using a library approach, investigators are now beginning to uncover the structural-functional relationships between HS and growth factor binding. Once elucidated, it may lead to the development and generation of specific HS sequences or HS inspired compounds that can modulate specific growth factor functions.

Section V: HS Involved in Viral Infections

HS is expressed on the cell surface by virtually all cell types. It is known that under physiological pH, HS is a highly sulfated molecule that displays numerous negative charged groups along its carbohydrate chain. Because of its rather ubiquitous presentation on the cell surface, HS is considered an ideal target for initial interactions between the virus and potential target cells. These initial interactions could take place through various basic motifs of the viral envelope proteins and the negatively charged HS chain. To date HS has been found to be involved in the viral infection mechanisms of at least 16 viruses some which are listed in Table 2 (3). The most well known pathogenic viruses including the epstein-Bar virus (EBV) (162), hepatitis C virus (HCV) (163), human immunodeficiency virus (HIV) (164) and herpes simplex virus (HSV) (165), utilize HS during their infections mechanisms. As a result, this has sparked an increased interest in the study of HS by the pharmaceutical and industry sectors to develop antiviral drugs by targeting HS.

Table 2: Heparan sulfate involved in viral infections.

Pathogenic Viruses (Human)	***Diseases manifestations/implications***
Herpes simplex virus (HSV)	Perioral and genital lesions and encephalitis
Dengue virus	Dengue hemorrhagic fever
Human immunodeficiency virus (HIV)	Acquired immunodeficiency syndrome
Epstein Barr virus (EBV)	Burkitt's Lymphoma
Cytomegalovirus (CMV)	Small pox
Human papillomavirus (HPV)	Cervical cancer
Varicella zoster virus (VZV)	Chicken pox and shingles
Hepatitis C virus (HCV)	Liver cancer and cirrhosis
Pathogenic Viruses (Animal)	
Foot and mouth disease virus (FMDV)	Highly infectious disease in animals that can cause economic problems for humans
Pseudorabies virus and Swine fever virus	Infections found primarily in pigs
Sindbis virus	Fatal diseases in neonatal/adult mice

Herpes simplex viruses (HSV) are DNA viruses and are members of the neurotropic subgroup (alphaherpesviruses) of the herpes family. Infection with HSV type 1 (HSV-1) and HSV type 2 (HSV-2) are common among humans and display different phenotypes (166). Infections with HSV-1 results in the formation of localized lesions in and around the mouth, while HSV-2 results in the formation of lesions around the genital region. The infection of the epithelial can cause characteristic herpetic lesions, blindness and infection in the central nervous system can cause life-threatening encephalitis. It is estimated that the incidence of herpes-related encephalitis is about 2.3 cases per million people per year (167). The current FDA approved treatment for HSV infection is the administration of two nucleoside analogs valacyclovir and acyclovir, which are designed to terminate DNA viral replication (168).

The early stage infection of target cells is a two-step process: attachment to cells and entry into cells (figure 22) (169, 170). It has been known that cell surface HS plays an important role in assisting the attachment as well as in inducing the entry of the virus (165, 171). This knowledge is evident from the observation that removing HS from the cell surface severely reduces the susceptibility of those cells to HSV infection (172). The attachment step primarily involves the interaction of HS and viral envelope glycoprotein C (gC) and/or glycoprotein B (gB) (173). Previous studies have provided evidence to suggest that specific sulfated saccharide sequences probably contribute to the binding of HS to gC (174, 175). Evidence has been provided to suggest that the shortest gC binding fragment consist of 10-12 monosaccharide units that contains at least one 2-*O* and one 6-*O*-sulfate groups (175).

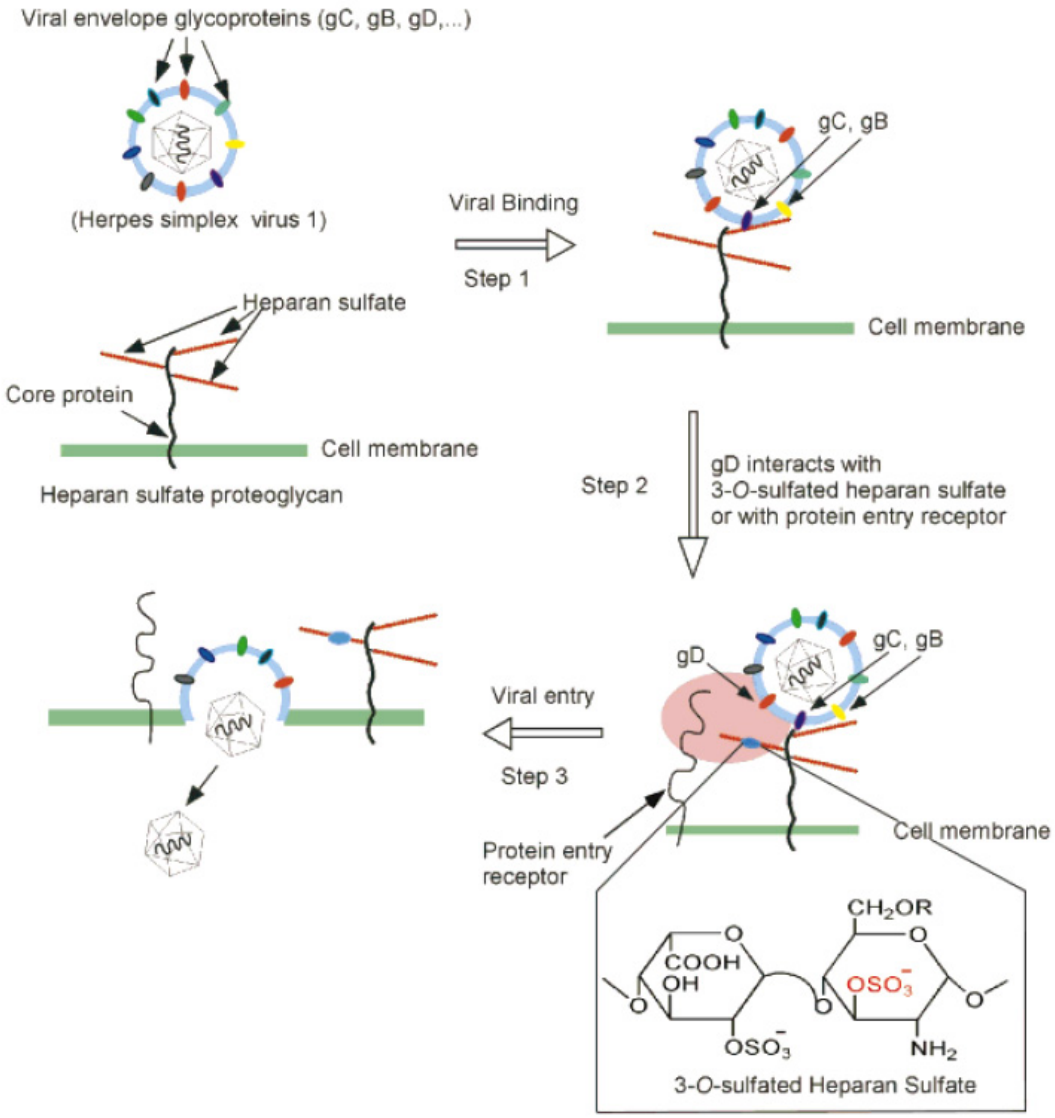

Figure 22: HSV-1 viral binding and entry mechanism (3). Step 1, the virus attaches to its targets cells through the interactions of viral envelope proteins, glycoprotein C (gC) and glycoprotein B (gB) with cell surface HS. Step 2, glycoprotein D (gD) interacts with cell surface entry receptors to trigger the fusion of the cell membrane. The entry receptors include 3-*O*-sulfated HS or other protein entry receptors. Step 3, the interaction of gD and entry receptor triggers the uncharacterized fusion mechanism which leads to infection.

Attachment of the viral particle to the target cell alone is not enough to cause the infection; fusion of the viral envelope with the cellular membrane is also required. Following attachment, HSV-1 enters into target cells by interacting with specific cell surface entry receptors. It is hypothesized that binding of cell surface receptors to viral envelope protein glycoprotein D (gD) initiates a fusion mechanism via an unknown pathway in concert with other viral glycoproteins including gB, gH, and gL that allows for subsequent infection

to occur (176). gD is a type 1 viral membrane glycoprotein that is made up of 369 amino acids (177). The core of gD (residues 56 to 184) has a V-like immunoglobulin (Ig) fold. This is encompassed by extensions at the N- and C-termini which make up the principle functional domains of the protein (178, 179). Three families of HSV-1 entry receptors are present on the cell surface and all have the ability to bind to gD in the micromolar range (170). Herpesvirus entry mediator (HVEM) and nectin-1 represent two families of those receptors, which belong to the tumor necrosis factor family and immunoglobulin superfamily respectively (169, 180).

The 3-*O*-sulfated HS, which is generated by 3-OST-2, -3, -4, -5 and -6 represents the third family of HSV-1 known entry receptors (80, 118, 171). This receptor is unique as it is a polysaccharide that contains a specific saccharide structure. It is of great importance the observation that a specific 3-*O*-sulfated HS can serve as an entry-receptor for HSV-1 in the absence of the HVEM and nectin-1 protein receptors that were mentioned previously (130). Wild-type CHO cells do not contain 3-*O*-sulfated HS and are resistant HSV infection. However, when the cDNA of 3-OST-3 was transfected into CHO cells, it rendered the cells susceptible to viral entry. On the contrary, the transfection of the cDNA of 3-OST-1 into CHO cells did not result in HSV entry (130). It is important to note here the 3-OST-1 modified HS does not bind to gD, while 3-OST-3 modified HS does bind to gD with a binding affinity of 2 μM (130). Based on the known difference in substrate specificities between 3-OST-1 and 3-OST-3, and the above evidence it suggests that a specific HS saccharide sequence can serve as an entry receptor of HSV-1.

The structure of a gD-binding HS derived octasaccharide was isolated from a 3-OST-3 modified HS oligosaccharide library and characterized using a combination of mass

spectrometry and chemical and enzymatic degradation approaches (181) . The proposed structure of the gD binding HS octasaccharide was found to be ΔUA-GlcNS-IdoUA2S-GlcNAc-UA2S-GlcNS-IdoUA2S-$GlcNH_2$3S6S (figure 23).

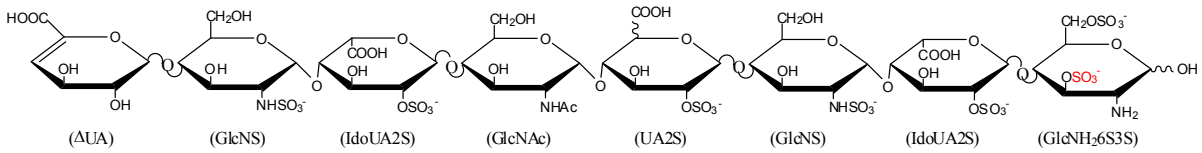

Figure 23: Structure of the gD binding HS octasaccharide. This octasaccharide was demonstrated to bind to gD with a K_d value of 18 μM. The abbreviated name of monosaccharide unit is shown under each sugar unit. The critical 3-*O*-sulfo (shown in red) is on the reducing in $GlcNH_2$ residue.

In that study, the above octasaccharide was found to have a binding affinity to gD of 18 μM. Supporting the role of 3-*O*-sulfated HS in assisting HSV-1 entry, two putative 3-*O*-sulfonated HS binding sites on gD were observed in the co-crystal structure of gD and HVEM as shown in figure 24 (178).

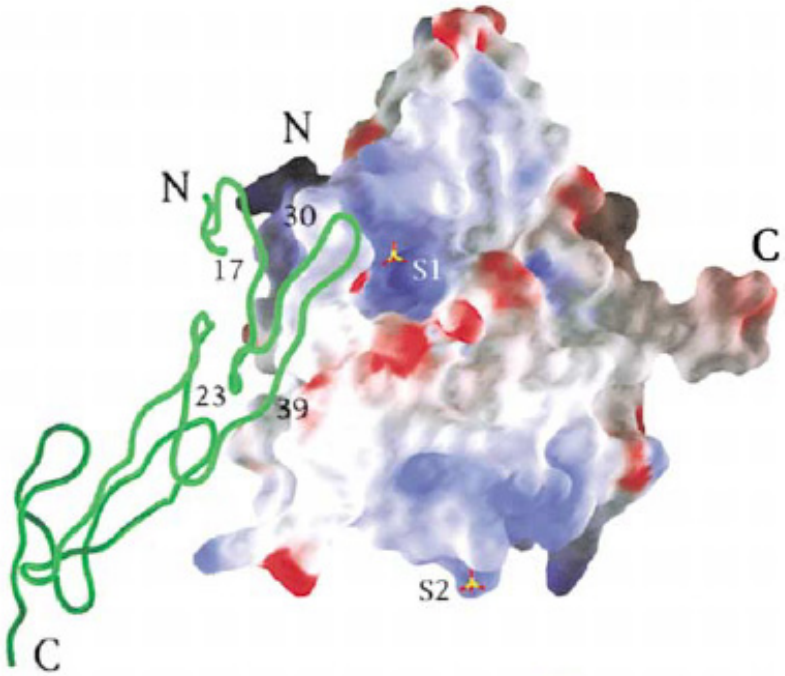

Figure 24: Crystal structure of gD in complex with HVEM (178). Electrostatic potential energy surface of gD in complex with HVEM. Positive potential colored in *blue*, neutral potential colored in *gray* and negative potential colored in *red*. S1 and S2 represents sulfate ion bound in complex and are potential sites of 3-*O*-sulfated HS binding.

One potential binding site is located within a deep positively charged pocket, while another is located on a relatively flat surface covered with numerous basic amino acid residues. It is hypothesized that these two sites have the ability to interact with HS utilizing various electrostatic interactions. One of the putative 3-*O*-sulfated HS binding sites is located at the N-terminal of gD. Viruses expressing wild type gD are able to infect target cells expressing 3-OST-3, thereby displaying 3-O-sulfated HS. However, it has been shown that viruses carrying gD mutations at the N-terminal are unable to infect target cells expressing 3-OST-3, confirming the location of a 3-*O*-sulfated HS binding site as predicted by the crystal structure (182, 183).

Because HS has been found to participate in a wide variety of viral infection mechanisms, it is possible that investigations concerning the structural characteristics of HS that promote these infections can lead to polysaccharide based antiviral agents for the treatment of various viral infections.

Section VI: Statement of Problem

Heparan sulfate (HS) is a highly sulfated polysaccharide that has been found to exist on the surface of mammalian cells in substantial quantities. Unique saccharide sequences of HS have been shown to bind specifically to a number of biologically relevant proteins, thus allowing HS to play a role in numerous biological processes. Previous studies have shown that 3-OST-3 generates 3-*O*-sulfated HS that can bind to gD and facilitate HSV viral entry into target cells, thus implicating 3-*O*-sulfated HS as a HSV entry receptor. Once gD binds to its cellular receptor, an uncharacterized fusion mechanism is initiated that allows the HSV viral particle to fuse with its target cell which leads to infection. If the specific 3-*O*-sulfated oligosaccharide sequence that is thought to be responsible for triggering this fusion event is elucidated, it may provide new insights to prevent HSV viral infections by inhibiting viral entry through its polysaccharide based receptors.

Due to the structural heterogeneity of HS, characterization of unique and biologically relevant sequences is a labor intensive process as it is difficult to obtain sufficient amounts of purified oligosaccharides to complete structural and functional analysis. This is the primary reason why the study of the structural-functional relationships of HS is considered an under-developed area compared to that of proteins and nucleic acids. The chemical synthesis of a gD binding octasaccharide was demonstrated to be unsuccessful due to a stereoselectivity problem (184); suggesting that an alternative approach is required. The goals of this dissertation are to provide additional structural information concerning HS mediated gD binding and to prepare sufficient amounts of a gD binding oligosaccharide to investigate its potential to inhibit HSV viral fusion.

Using structurally defined HP oligosaccharides substrates and purified 3-OST-3 enzyme, we have determined the minimal size required for gD binding and developed a novel approach to express recombinant gD. Milligram quantities of recombinant gD were expressed and purified from *E. coli*. utilizing a chaperone assisted bacteria expression system. This allowed us to conduct binding analysis between gD and the 3-*O*-sulfated HP oligosaccharides. Based on the results of the binding analyses, the 3-*O*-sulfated HP octasaccharide was concluded to be the minimum size for required of gD binding with a K_d value of 19 μM. The structural characterization of this 3-*O*-sulfated HP octasaccharide was achieved using chemical and enzymatic modifications with results suggesting the structure is ΔUA2S-GlcNS6S-IdoUA2S-GlcNS6S-IdoUA2S-GlcNS3S6S-IdoUA2S-GlcNS6S (3-*O*-sulfation site recognized by 3-OST-3 is underlined). Coupling a PAPS regeneration system with 3-OST-3 modification, nearly 130 μg of this octasaccharide has been synthesized. This amount of material should allow us to determine its efficacy in inhibiting HSV infection in a cell-based assay.

Herpes viral infections are prevalent in humans. HS plays intimate roles during the infection. Developing a HS-based antiviral drug could be a viable approach to treat HSV infection. Understanding the structure-activity relationship of HS in promoting HSV infections is essential for achieving this goal. This thesis represents the first attempt to prepare a structurally defined 3-*O*-sulfated octasaccharide that could potentially interrupt HSV entry. Further development of this project could uncover a new way to treat diseases related to HSV infections.

CHAPTER II

MATERIALS AND METHODS

Purification of HS from bovine kidney acetone powder

The large scale purification of HS from bovine kidney acetone powder was carried out by modifying and optimizing a previously published method (185). Initially, 200 g of bovine kidney acetone powder (ICN) was homogenized (Fisher Scientific-PowerGen 1800D) at 13,000 rpm for 45 mins. in 4 L of distilled water. The homogenate was autoclaved for 1 hr then cooled on ice. Protease digestion was carried out with the addition of 1 g of protease (Type VIII: Bacterial, Sigma P-5380) dissolved in 20 mM Tris and incubated with shaking at 37°C for 48 hours. After centrifugation at 3400 rpm for 30 minutes, 2 times volume of cold ethanol was added to the supernatant in the presence of 150 mM NaCl and 0.25 M CH_3COOH and placed at 4°C overnight. After centrifugation at 3400 rpm for 30 mins., the pellet was dissolved in 1 L of 20 mM Tris pH 7.85 and redigested with protease in a similar manner as before. Remaining proteins were removed via precipitation by the addition of trichloroacetic acid (TCA) to a final percentage of 10%. The material was centrifuged and the pH of the supernatant was adjusted to 7.85 using NaOH pellets followed by ethanol precipitation which was carried out as before. The pellet was dissolved in 20 mM Tris pH 7.85 and was subjected to beta elimination with the addition of 1 ml of 10 M NaOH/0.89 M $NaBH_4$ and incubated with shaking at 45°C. The elimination reaction was neutralized with the addition of 1 ml of 10 M CH_3COOH and adjusted to pH

7.85. The resultant material was filtered through a 0.2 μm filter and subjected to ethanol precipitation as before. The pellet was dissolved in 50 ml of ammonium acetate, pH 7 and digested with 3.3 units of chondroitnase ABC (purchased from Sigma C-2905) and incubated at 37°C overnight. The material was centrifuged at 12,000 rpm for 30 mins. to remove any insoluble material.

HS Purification - FPLC-DEAE Anion Exchange Chromatography

The HS was purified by utilizing DEAE anion exchange chromatography using an AKTA-FPLC system. A 10-20 ml DEAE column was packed and equilibrated with 20 mM sodium acetate, 250 mM NaCl, pH 5 (buffer A). After sample loading, the column was washed with 8 column volumes (CV) of buffer A at a flow rate of 3 ml/min. The desired material was eluted over a linear gradient using 1 M NaCl, pH 5 (buffer B) over the course of 20 CV while 4 ml fractions were collected with online UV detection at 280 nm. The purified HS was desalted by dialysis against 4 L of 20 mM ammonium bicarbonate overnight using MWCO 12-14,000 membrane.

Quantification of Purified HS - Alcian Blue Assay

The amount of HS purified from bovine kidney acetone powder was quantified using an alcian blue assay as previously described (186). Briefly, the alcian blue dye stock solution was made by dissolving 1 mg of the dye with 100 ml of 18 mM H_2SO_4, a 1/100 dilution of the resulting dye stock solution should have an A_{600nm} of ~1.4. If not, additional dye was added. This was followed by centrifugation at 10,000 rpm for 30 mins. to remove insoluble dye particles. Standards and unknown samples were prepared in duplicated with standards of

HS (ICN) ranging from 0-3 µg. All samples were brought up to 10 µl with distilled water, followed by the addition of 10 µl of reagent A. Reagent A contained a 1:1 ratio of 8 M guanidine-HCl and 54 mM H_2SO_4, 0.75% Triton X-100, this solution was prepared fresh with each use. To this, 100 µl of working dye was added to all samples bringing the final volume of the samples to 120 µl. The working dye solution contained 18 mM H_2SO_4, 0.25% Triton X-100, and 5% dye stock solution, which was filtered through a 0.2 µm filter and the resultant solution was centrifuged at 10,000 rpm for 10 mins. to remove any insoluble material. The samples were mixed thoroughly and centrifuged at 14,000 rpm for 30 mins. The supernatant was removed and the pellet was dissolved with 500 µl of 8 M guanidine-HCl afterwards, the samples were analyzed at a wavelength of 600 nm.

Preparation of HS oligosaccharide library

A diverse HS-derived oligosaccharide library was prepared by incubating HS (bovine kidney) with limited amounts of heparin lyase III (Hep III) followed by resolution of sized fractions on a Bio-Gel P-6 column (Bio-Rad) as previously described (114). In a typical optimized preparation, twenty separate digestions (5 mg HS/digestion) were incubated with 6.1 mU of Hep III per digestion. Each digestion mixture (1 ml) consisting of 50 mM NaH_2PO_4 and 100 µg/ml BSA, pH 7 was incubated at 37°C for 24 hr. Digestions were then terminated by heating at 100°C for 15 mins. All reaction mixtures were centrifuged at 13,000 rpm to remove any insoluble material and after combining the supernatants from all reactions, the sized fractions were resolved by loading on into Bio-Gel (Bio-Rad) P-6 size exclusion column (2.5 × 200 cm) equilibrated with 0.5 M ammonium bicarbonate at a flow of 0.5 ml/min as 4.5 ml fractions were collected. The digestion in terms of the amount of

Hep III used, was optimized so as to yield a partial digestion with the maximum amount of the hexasaccharide pool as this material contained the gD binding octasaccharide as previously published (181).

Isolation of gD_{306t} DNA from Baculovirus

The isolation of gD_{306t} (gD) viral DNA began with the isolation of the baculovirus viral particles that contain the gD gene of interest using the Invitrogen protocol. This was accomplished by mixing, by inversion, 750 µl of amplified baculovirus with 750 µl of cold (4°C) 20% PEG in 1 M NaCl in a sterilized eppendorf tube with incubation on ice for 30 mins. The tube was then centrifuged for 10 mins. at 4°C to pellet the viral particles while the supernatant was discarded. The viral particles were then reconstituted in 100 µl sterile distilled water. The isolation of the gD DNA from the viral suspension began with the addition of 143 µl of solution A (Invitrogen) to the viral particles and vortex for 1 second to mix and then incubated at 65°C for 6 mins. Next, 58 µl of solution B (Invitrogen) was added and vortex for 5 seconds which was followed by adding 258 µl of chloroform and mixing. The resultant solution was centrifuged at 13,000 rpm for 10 mins. at 4°C to separate aqueous and organic phases. The aqueous phase (containing DNA) was transferred into a separated sterilized centrifuge tube for subsequent DNA precipitation. The gD viral DNA precipitation began with the addition of 500 µl of 100% ethanol (-20°C) mixed by inversion followed by centrifugation at 13,000 rpm for 5 mins. To the pellet, 500 µl of 70% ethanol (-20°C) was added, followed by another round of centrifugation as before. The supernatant was decanted and the resulting pellet was allowed to air dry for 5 mins. The gD viral DNA was reconstituted in 20 µl of sterile distilled water and was ready for cloning and expression.

Expression and Purification of gD – Chaperone Bacterial Expression System

The introduction of a His_6 tag at the C-terminus of gD_{306t} (Lys_{26}-His_{332}) (gD) was achieved in the following manner. The purified gD viral DNA was amplified by the polymerase chain reaction (PCR) using the 5′-specific primer, 5′-ATTATTATCATATGAAATATGCCTTGGCGGATGC-3′ (*Nde*I site underlined), and the 3′-specific primer, 5′-ATAATATAAAGCTTATGGTAAGGCGTCGCGGCGT-3′ (*Hind*III site underlined). The resulting PCR construct was inserted into the pET21b vector (Novagen) using the with *Nde*I/*Hind*III restriction sites. The resulting plasmid was sequenced to confirm the reading frame (at the University of North Carolina at Chapel Hill DNA Sequencing Core Facility). The gD-pET21b plasmid was transformed into CHAP-Origami B competent cells. Bacterial transformations were completed by mixing 50 µl of Origami B competent cells with 1-10 ng of plasmid DNA. The samples were allowed to incubate on ice for 10-30 mins., and then were placed at 42°C for 30 seconds. The samples were then returned to ice for another 1-2 mins. 100-200 µl of pre-warmed SOC media was then added, and the samples were allowed to incubate at 37°C for 1 hour (1 L SOC contains 20 g tryptone, 5 g yeast extract, 2 ml of 5 M NaCl and 2.5 ml of 1 M KCl). The transformation was then plated on LB-agar plates (supplemented with the appropriate antibiotics) and allowed to grow at 37°C overnight.

Expression of gD was carried out in CHAP-Orgami B cells (Novagen). CHAP-Orgami B competent cells containing the gD-pET21b plasmid were grown in LB media with 12.5 µg/ml tetracycline (Tet), 15 µg/ml kanamycin (Kana), 20 µg/ml chloamphenicol (Chl), and 50 µg/ml carbenicillin (Carb) at 37°C. When the $O.D_{600nm}$ reached 0.6-0.8, the temperature was reduced to 22°C for 10 mins. Isopropyl-β-thiogalactopyranoside (IPTG)

was then added to a final concentration of 200 μM IPTG and arabinose was added to a final concentration of 1 mg/ml and allowed to shake for 20 hr at 22°C. Cells were harvested by centrifugation at 7,000 rpm for 10 mins. and resuspended in the sonication buffer containing 25 mM Tris, 500 mM NaCl, and 15 mM imidazole at pH 7.5. The cells were lysed by sonication and cell debris was removed by centrifugation at 14,000 rpm for 30 mins. The cell lysate was processed for purification of the desired protein.

Purification of gD-FPLC-Nickel Chromatography

The initial step in gD purification was performed by utilizing nickel chromatography using an AKTA-FPLC system. A 7 ml nickel sepharose column was packed and equilibrated with a buffer containing 25 mM Tris, 500 mM NaCl, and 15 mM imidazole at a pH of 7.5 (buffer A). After sample loading, the column was washed at a flow rate of 3 ml/min with buffer A for 10 column volumes (CV). The eluted protein was monitored with an online UV detector at 280 nm, elution was carried out using a linear gradient in a buffer containing 25 mM Tris, 500 mM NaCl, and 250 mM imidazole (buffer B) from 0-100% B over the course of 7 CV, while 3 ml fractions were collected. This was followed by an additional wash with 100% B for 15 mins. The desired fractions were collected, pooled, and subjected to concentration using Amicon® Ultra MWCO 10,000 centrifuge tubes.

Purification of gD-FPLC-Size Exclusion Chromatography

The concentrated protein from the nickel column was subjected to size exclusion chromatography using an AKTA-FPLC system. A pre-packed HiLoad™ 16/60 Superdex™ prep grade size exclusion column (Amersham Biosciences) was equilibrated with a buffer

containing 20 mM Tris, 1 M NaCl pH 7 (degassed). After a maximum of 3 ml of concentrated protein was loaded, the protein was eluted under isocratic conditions with 120 ml of the equilibration buffer at a flow rate of 1 ml/min. The eluted protein was monitored with an online UV detector at 280 nm as 2 ml fractions were collected. Final protein concentration was determined by UV absorbance at 280 nm, where 1.0 absorbance unit = 1.0 mg/ml).

SDS-PAGE Electrophoresis

Protein purity was determined using SDS-PAGE using precasted Tris-Tricine SDS-PAGE (16.5% resolving gel, 4% stacking gel, 8.6 × 6.8 cm (W × L), BioRad). Samples (10 µl) were diluted with an equal volume of sample buffer (200 mM Tris-HCl, pH=6.8, 2% SDS (BioRad). Gels were run at 110V for 1 hour, and then stained with coomassie blue (0.4%) for 30 mins. Gels were destained using 10% acetic acid.

Preparation of 3-O-sulfated HP oligosaccharides

To prepare 3-*O*-sulfated HP oligosaccharides, individual reactions consisting of 1-5 µg of the oligosaccharide (either tetra-, hexa-, or octasaccharide), was mixed with approximately 140-240 ng of purified 3-OST-3 enzyme (121), [^{35}S]PAPS (of known specific activity) in a buffer containing 50 mM MES, 1% Triton X-100, 5 mM $MgCl_2$, 10 mM $MnCl_2$, 100 µg/ml BSA, pH 7, in a final volume of 65 µl. The reaction was incubated for 1.5 hrs. at 37°C. The enzymatic reaction was stopped by boiling at 100°C for 2 mins. The resultant solution was centrifuged at 14,000 rpm for 2 mins. to remove any insoluble materials. The supernatant was then subjected to a 200 µl DEAE column equilibrated with 150 mM NaCl.

The column was washed with 4×1 ml UPAS (50 mM NaAcO, 150 mM NaCl, 0.1% Triton X-100, 6 M Urea, and 1 mM EDTA, pH 5), then 3×1 ml 150 mM NaCl, and the desired 3-*O*-[^{35}S]sulfated oligosaccharide was eluted with 1 ml of 1 M NaCl. The resultant 3-*O*-[^{35}S]sulfated oligosaccharides were desalted in the appropriate manner depending on their size. The 3-*O*-[^{35}S]sulfated hexa- and octasaccharides were dialyzed against 3 L of 20 mM ammonium bicarbonate overnight MWCO 3500, while 3-*O*-[^{35}S]sulfated tetrasaccharide was subjected to bio-gel P-2 size exclusion chromatography.

Determination of gD binding affinity - Immunoprecipitation Approach

The assay for determining the binding of various sized 3-*O*-[^{35}S]sulfated HP oligosaccharides to gD was carried out by an immunoprecipitation procedure using purified gD and an anti-gD monoclonal antibody (130). In separated reactions, either 3-*O*-[^{35}S]sulfated tetra-, hexa-, or octasaccharide (1-10 pmole) was incubated in 50 µl of buffer containing 50 mM Tris, 0.001% Triton X-100, pH 7.4 (binding buffer), and 20 µg gD at room temperature for 30 mins. The anti-gD monoclonal antibody DL6 (5 µl) was added and the reaction mixture was incubated on ice for 1 hour, followed by the addition of protein A-agarose beads (50 µl of pre-washed/pre-equilibrated beads) with agitation at 4°C for an additional hour. The protein A-agarose beads were then washed stepwise with 0, 25, 50, 150, 250, 500, and 1000 mM NaCl in the above binding buffer all while monitoring the elution of [^{35}S]sulfated oligosaccharides as increasing NaCl was used. The binding of HS to gD was assayed in a similar manner, with washing protein-A beads with 150 mM NaCl in binding buffer and eluting bound material with 1 M NaCl in above binding buffer.

Determination of gD binding affinity – Affinity Co-Electrophoresis (ACE)

To quantitatively determine the binding affinity between the 3-OST-3 modified HP derived oligosaccharides and gD, an affinity co-electrophoresis approach was utilized in a similar manner as previously described (130, 187). Briefly, purified gD was cast in 1 % low melting point agarose (GIBCO) separation zones in a degassed gel buffer containing 125 mM sodium acetate and 50 mM 3-(*N*-morpholino)-2-hydroxypropane-sulfonic acid, pH 7, at six final concentrations ranging from 0 to 60 μM of gD in each zone. In separate experiments, the 3-*O*-[^{35}S]sulfated octasaccharide or 3-*O*-[^{35}S]sulfated hexasaccharide, of known [^{35}S] specific activity was loaded into each separation zone and the gel was subjected to electrophoresis at 350 mA for 3 hrs in circulated cold gel buffer. The gel was dried using a Bio-Rad GelAir dryer, analyzed on a PhosphorImager (Amersham Biosciences, Storm 860) and exposed to radioactive developing film at -80°C for 1 week to observe the migration of 3-*O*-[^{35}S]sulfated HP derived oligosaccharide. The binding affinity between the 3-*O*-[^{35}S]sulfated oligosaccharide and gD was calculated as a K_d value by plotting R/gD versus R, where the retardation coefficient $R = (M_0 - M)/M_0$. Here M_0 is representative of the migration of free 3-*O*-[^{35}S]sulfated oligosaccharide, and M is the observed migration of the 3-*O*-[^{35}S] oligosaccharide in the presence of a specific concentration of gD located in a separation zone. Based on the Scatchard equation, the calculation of the slope from the resulting plot yields $-1/K_d$.

Heparin Lyase digestion

The digestion of unlabeled or 3-*O*-[^{35}S]sulfated HP derived oligosaccharides were carried out as previously described (188). Digestions were carried out in 100 μl of 40 mM

ammonium acetate (pH 7) containing 1 mM $CaCl_2$ with limited amounts of heparin lyase I, II, and III, which are expressed and purified using a bacterial expression system. The digestion mixtures were incubated at 37°C overnight, and the reactions are terminated by heating at 100°C for 2 mins. The resultant material was centrifuged for 5-10 mins. at 13,000 rpm to remove insoluble materials and was subsequently ready for HPLC analysis.

HPLC-PAMN chromatography

Materials were analyzed using PAMN chromatography. The elution profile was monitored as the 3-*O*-[^{35}S]sulfated material was applied to a silica-based polyamine (PAMN) HPLC column (0.46 × 25 cm, Waters) (121). The column was equilibrated with 300 mM KH_2PO_4, and the radioactive material was eluted with a linear gradient of KH_2PO_4 from 300 mM to 1 M in 60 min at a flow rate of 0.5 ml/min, followed by a continuous state of washing at 1 M for up to 100 mins. The [^{35}S] elution profile was monitored using an online radioactive detector.

HPLC-DEAE-NPR chromatography

Materials were analyzed using DEAE-NPR chromatography. The elution profile of the 3-*O*-[^{35}S]sulfated material or unlabeled material was monitored as the material was applied to a nonporous DEAE-NPR HPLC column (0.46 × 7.5 cm, Tosohass). The DEAE-NPR column was equilibrated with 100 mM NaCl in 50 mM Tris-HCl, pH 7 at a flow rate of 0.4 ml/min. The desired material was eluted using a linear gradient of 1 M NaCl, pH 7 over the course of 100 mins. while radioactivity and/or UV was monitored using an online detectors.

Non-Reducing End Labeling – $\Delta^{4,5}$Glycuronate-2-sulfatase

Non-reducing end labeling was employed to distinguish disaccharide products that result from the non-reducing upon digestion with heparin lyases and was carried out in as previously described (121). The 3-*O*-[^{35}S]sulfated HP oligosaccharides were digested with appropriate amounts of $\Delta^{4,5}$-glycuronate-2-sulfatase (2ase) (Seikagaku Corporation) warranted for complete digestion. A typical digestion mixture consisted of the 3-*O*-[^{35}S]sulfated HP oligosaccharide and 2ase in a total volume of 100 µl of 50 mM imidazole-HCl buffer (pH 6.5) that was subsequently incubated at 37°C overnight. The 2ase digestion was terminated by heating at 100°C for 2 mins. after which the reaction mixture was centrifuged at 13,000 rpm to remove any insoluble materials. The resulting supernatant was ready for HPLC analysis.

Reducing End Labeling – [2-AB] (2-aminobenzamide)

The derivatization of the 3-*O*-[^{35}S]sulfated HP oligosaccharides with 2-AB was achieved in a similar manner as previously described (189, 190). Briefly, a given amount of 3-*O*-[^{35}S]sulfated HP oligosaccharide (5-100 µM) was dried to completion using a speed-vac centrifuge dryer (LABCONCO). An aliquot (5-20 µl) of a freshly prepared derivatization reagent mixture (0.35 M [2-AB]/1 M $NaCNBH_4$/30% (v/v) acetic acid in DMSO) was added to the dried sample and incubated for 3 hr at 65°C (Eppendorf Thermomixer R). The resultant reaction mixture was purified via paper chromatography by spotting the mixture on to a section of Whatman 3MM paper. The paper sections with UV absorbance as visualized under a UV light source are cut and placed into an eppendorf tube. The paper strips were washed with 1 ml of acetonitrile 3 times by centrifugation at 10,000 rpm for 3 mins. while

the desired labeled oligosaccharide was eluted with 1 ml of distilled water. The resultant material was then dried to completion and reconstituted in 50-100 µl distilled water to allow for further analysis.

Preparation of larger quantities of 3-O-sulfated HP octasaccharide

Scale up preparation of the 3-*O*-sulfated HP octasaccharide was achieved using a PAPS regeneration system as similarly described (191). Regeneration reactions consisted of 1 ml of the following: 50 mM MES pH 7, 40 µM PAP, 1 mM PNPS, 50 µl purified AST-IV, and 10 µg of purified 3-OST-3 was incubated at room temperature for 15 mins. The coupling efficiency was monitored by measuring the concentration of PNP at O.D. 410 nm. Once equilibrium was reached 50 µg of the HP octasaccharide substrate was added and the resultant mixture was rotated at room temperature overnight. Reactions were terminated by boiling for 2 mins. at 100°C. Insoluble materials were removed by centrifugation at 13,000 rpms for 10 mins. The resultant material was loaded onto a 1 ml DEAE column that was equilibrated with 150 mM NaCl. The column is washed with 5 × 2 ml with UPAS (without Triton X-100), then 5 × 10 ml with 150 mM NaCl, and the material was eluted with 3 × 2 ml with 1 M NaCl. The resultant material was dialyzed against 20 mM ammionium bicarbonate for 8 hrs. using a MWCO 3500 membrane. The dialyzed material was dried to completion and dissolved in distilled water.

Electrospray Ionization Mass Spectrometry

The 3-*O*-sulfated HP octasaccharide, unmodified HP octasaccharide, and Arixtra® was dialyzed against 25 mM ammonium acetate using a microdialysis apparatus with MWCO

1000 membrane. The samples were then dried to completion on a speed-Vac device and reconstituted in doubled-deionized water to a known final concentration. In separate analysis experiments, the unmodified HP octasaccharide (10 μM), the 3-*O*-sulfated HP octasaccharide (20 μM), and Arixtra® (100 μM) contained in 70% acetonitrile and 10 μM imidazole was introduced by direct infusion (10 μl/min) into the electrospray ionization mass spectrometer (Agilent 11090 MSD-Trap at the Mass Spectroscopy Core at the University of North Carolina at Chapel Hill School of Pharmacy). Experiments were performed in negative ionization mode (2000V at 200°C, dry gas at 15 psi, nebulizing gas at 5 L/min.)

CHAPTER III

DETERMINATION OF THE MINIMAL REQUIRED LENGTH OF THE GLYCOPROTEIN D BINDING HEPARIN OLIGOSACCHARIDE

Introduction

HS is presented on the cellular surface and is a common receptor for numerous viruses. It is believed that defined sulfated sequences provide binding sites for the herpes simplex viral envelope protein gD as evident by the observation that 3-*O*-sulfated HS generated by 3-OST-3, not 3-OST-1, interacts with gD to induce viral entry (130, 175, 178). It is hypothesized that gD binding to its cellular receptor initiates a currently unknown fusion mechanism between the virus and the cell. Due to the heterogeneity contained within HS sequences, it is extremely difficult to obtain substantial amounts of a homogenous sequence required to complete characterization and cell based assays. Herein, the structurally similar but much less diverse HP oligosaccharides of various sizes were 3-*O*-sulfated by purified 3-OST-3 enzyme and investigated to determine the minimal length required for binding to gD. The gD binding interactions of the 3-*O*-sulfated HP oligosaccharides were investigated both qualitatively and quantitatively using immunoprecipitation and affinity co-electrophoresis approaches respectively. As a result, gD was expressed and purified from bacteria in sufficient quantities that were necessary for the completion of this study.

Purification of gD FPLC-Nickel Chromatography

Truncated form of gD-1 (Lys_{26}-His_{332}) (gD) was cloned into a pET21b vector. The resultant protein has a (His_6)-tag on its C-terminus, which facilitates its purification using nickel chromatography. The procedure for the expression of gD is described in Chapter II, which was carried out in *E. coli*. co-expressing the chaperone proteins GroEL and GroES. The cells were lysed by sonication and the supernatant was applied to a nickel column. The protein was eluted from the column with an imidazole gradient and the elution profile is shown in figure 25.

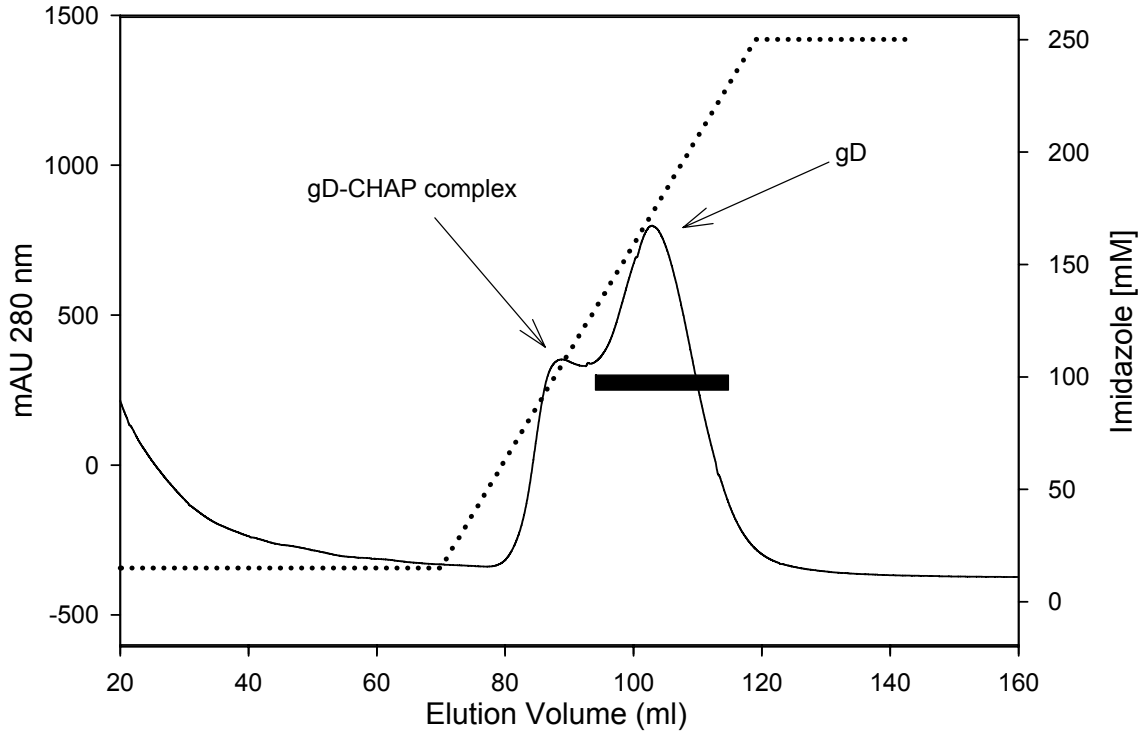

Figure 25. FPLC nickel chromatogram of bacterial gD. The bacterial cell lysate from a 5 L culture containing gD was subjected to a 7 ml nickel column. The column was eluted using an imidazole gradient while 3 ml fractions were collected. The *solid line* represents the absorbance of the eluent monitored with an online UV detector at 280 nm, while the *dotted line* represents the imidazole gradient. The *black* bar represents the fractions that were pooled and collected for further purification. gD-CHAP represents the gD and chaperone complex.

As shown in figure 25, there are two partially resolved peaks. The first peak was indicative of a gD-CHAP complex, while the second peak contained the purified gD protein. However, due to the over expression of CHAP proteins, the recombinant gD after nickel column purification undoubtedly contained some CHAP proteins as determined by SDS PAGE (data not shown). To obtain pure gD additional purification steps were necessary. It was observed that greater than 90% of the protein from the bacteria lysate did not bind to the nickel column suggesting that this step was successful.

Purification of gD-FPLC-Size Exclusion Chromatography

The next step in the purification scheme was designed to purify based on the molecular sizes. To this end, the pooled fractions from the nickel column were concentrated and subjected to size exclusion chromatography. The size exclusion purification profile is shown in figure 26. The purified gD migrated at a molecular weight of 35 kDa as observed by a symmetric peak between 52 and 61 ml. This molecular weight was very close to the calculated molecular weight of recombinant gD (37 kDa). It is known that the CHAP proteins are present in hexametric form with an apparent molecular weight greater than 400 kDa (192). Indeed a peak was observed in the exclusion volume at 42 ml and this peak predominately contained CHAP proteins as determined by SDS-PAGE (data not shown).

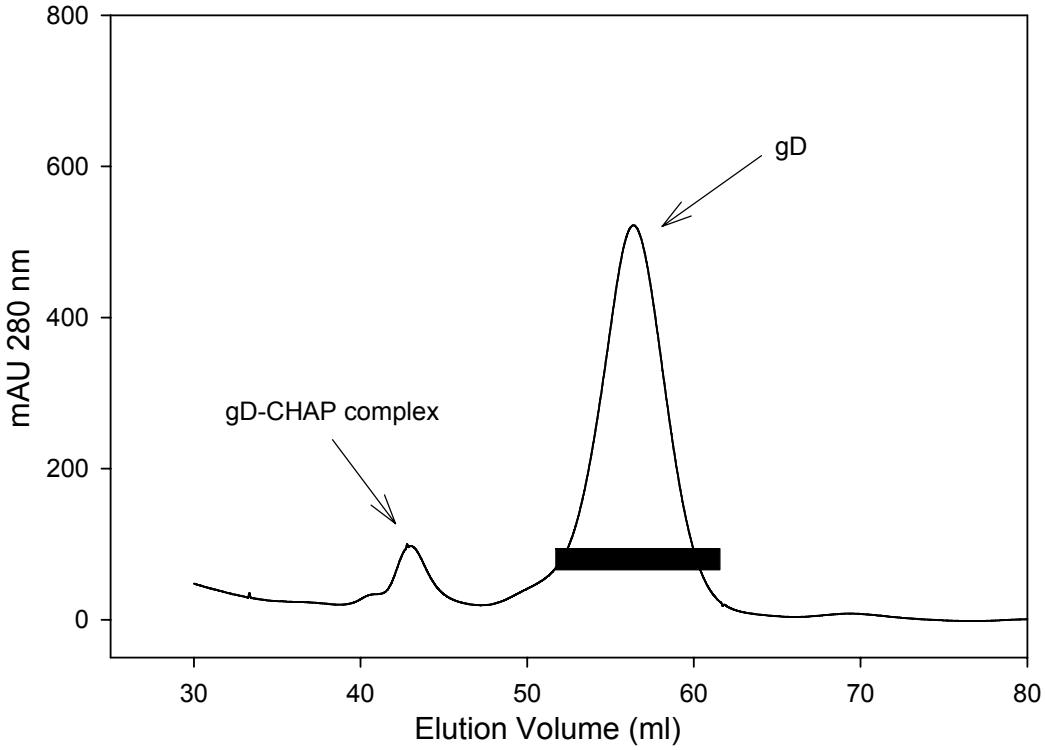

Figure 26. FPLC-size exclusion chromatogram bacterial gD. The concentrated protein was subjected to size exclusion chromatography, while 3 ml fractions were collected. Elution conditions are described in "methods" section. The *solid* line represents protein concentration monitored by an online UV detector at 280 nm. The *black* bar represents the fractions that were pooled. The peaks corresponding to the gD-CHAP complex and purified gD are labeled.

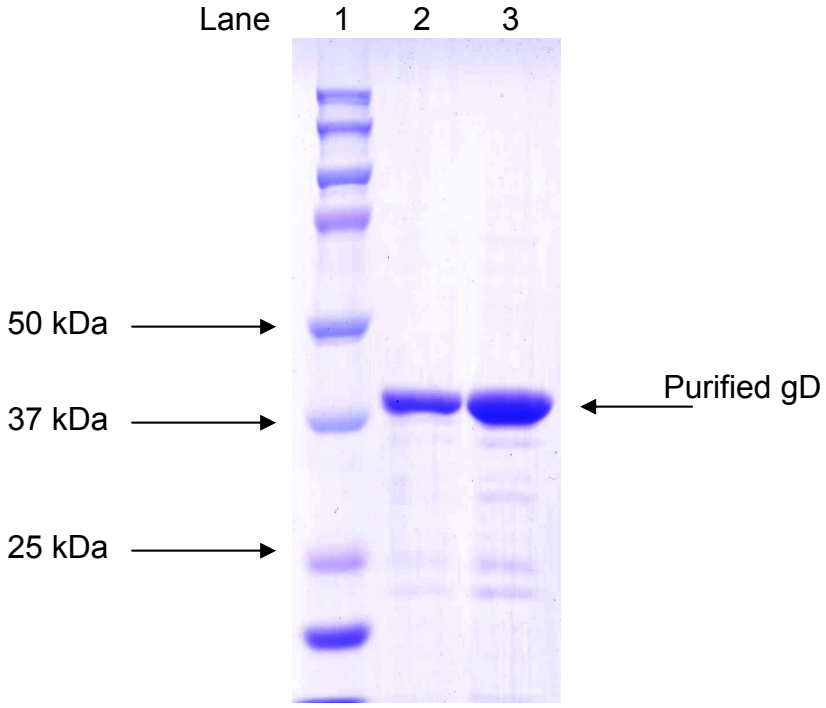

Figure 27. SDS-PAGE analysis of the purified gD. SDS analysis was conducted on the purified gD protein as described in "methods" section. Lane 1 is the molecular weight ladder and lane 2 is 4 µg of purified gD and lane 3 is 8 µg of purified gD.

The gD protein after the size exclusion chromatography purification step was analyzed by SDS-PAGE and the gel is shown in figure 27. The result suggested that the recombinant gD protein was approximately 85% pure. Polypeptides smaller than gD were observed as higher amounts of purified gD were loaded onto the gel (figure 27, lane 3). It was hypothesized that these lower molecular weight polypeptides were a result of proteolytic digestion during the purification. Nonetheless, these polypeptide contaminants did not significantly affect the binding of 3-*O*-sulfated HS to gD as demonstrated below. This purification procedure allowed for the recovery of 5 mg of purified gD from a liter of bacterial culture.

Comparison of HS binding to gD expressed in bacteria and gD expressed in insect cells

Recombinant gD has been expressed in insect cells and purified, and this gD preparation has been widely used in previously published reports (178, 181). Three *N*-glycosylation sites are present on the gD expressed in insect cells and are distant from the putative HS binding site based on the crystal structure (193). So it was hypothesized that the bacteria expressed gD lack of glycosylation would not have an effect on its binding to HS. To prove this hypothesis, the two preparations of gD proteins were compared in terms of their binding to 3-*O*-sulfated HS using a gD immunoprecipitation approach with the specific anti-gD monoclonal antibody DL6 as previously described (130).

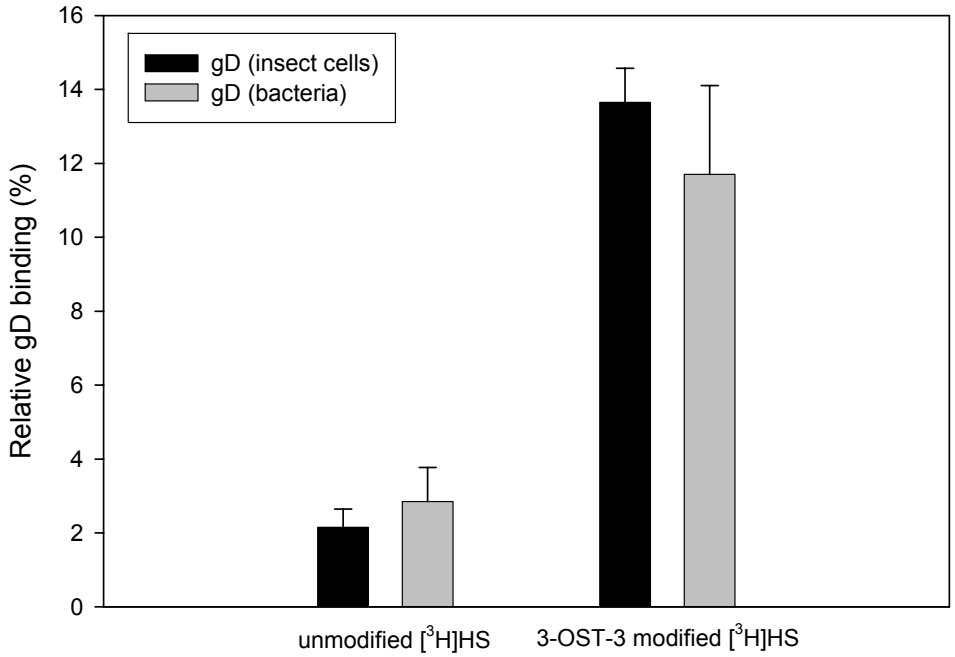

Figure 28. The binding of unmodified and 3-OST-3 modified HS to gD expressed in bacteria and insect cells. The binding of HS to differently expressed gD was carried out (in duplicate) at pH 7.4 by using an immunoprecipitation approach as described in the "methods" section. The unmodified [^{3}H]HS was prepared from wild type CHO cells grown in media containing [^{3}H]glucosamine. The 3-OST-3 modified [^{3}H]HS was prepared by incubating unmodified [^{3}H]HS with purified 3-OST-3 enzyme. The binding experiment was carried out by incubating the unmodified [^{3}H]HS and 3-OST-3 [^{3}H]HS with 20 μg gD, where *black bar* represents gD from insect cells and *gray bar* represents gD from bacteria. The HS-gD complex was captured by anti-gD antibody DL6 on protein-A agarose. Protein-A beads were equilibrated and washed with buffer containing 150 mM NaCl. The relative binding is displayed as the percentage of [^{3}H] counts recovered upon 1 M NaCl elution. Error bars are representative of the standard deviation.

The result shown in figure 28 demonstrated that 14% of the 3-OST-3 modified HS bound to gD expressed in insect cells, similarly 12% of the 3-OST-3 modified HS bound to gD expressed in bacteria. This result suggests that the gD expressed in bacteria and the gD expressed in insect cells are comparable in terms binding to 3-OST-3 modified HS. Consistent with previously published reports, the unmodified HS showed a much lower binding percentage to gD (figure 28).

Overall, these results demonstrate that gD expressed in bacteria can be used to determine the binding of 3-*O*-sulfated HS. Additional functional assays to prove the similarity between the gD expressed in bacteria and the gD expressed in insect cells are being conducted in Dr. Shukla's laboratory (The University of Illinois at Chicago-UIC). Preliminary results indicate that these two gD preparations are indeed similar.

Preparation of 3-O-[^{35}S]sulfated HP oligosaccharides

Because the 3-*O*-sulfo group introduced by 3-OST-3 is critical for gD binding, a series of 3-*O*-sulfated HP oligosaccharides were prepared in order to determine the minimal length required for this interaction. Three purified oligosaccharides including tetra-, hexa-, and octasaccharides were purified from heparin lyases digested heparin by Dr. Linhardt (Rensselaer Polytechnic Institute-RPI). The structures and purity were confirmed by MS and NMR in Dr. Linhart's laboratory (194). To prepare 3-*O*-sulfated HP oligosaccharides, purified 3-OST-3 enzyme was incubated with the oligosaccharides in the presence of [^{35}S]PAPS and the products were purified by DEAE chromatography. The procedure of the preparation of 3-*O*-sulfated HP oligosaccharides and the structures of the oligosaccharide substrates are shown in figure 29.

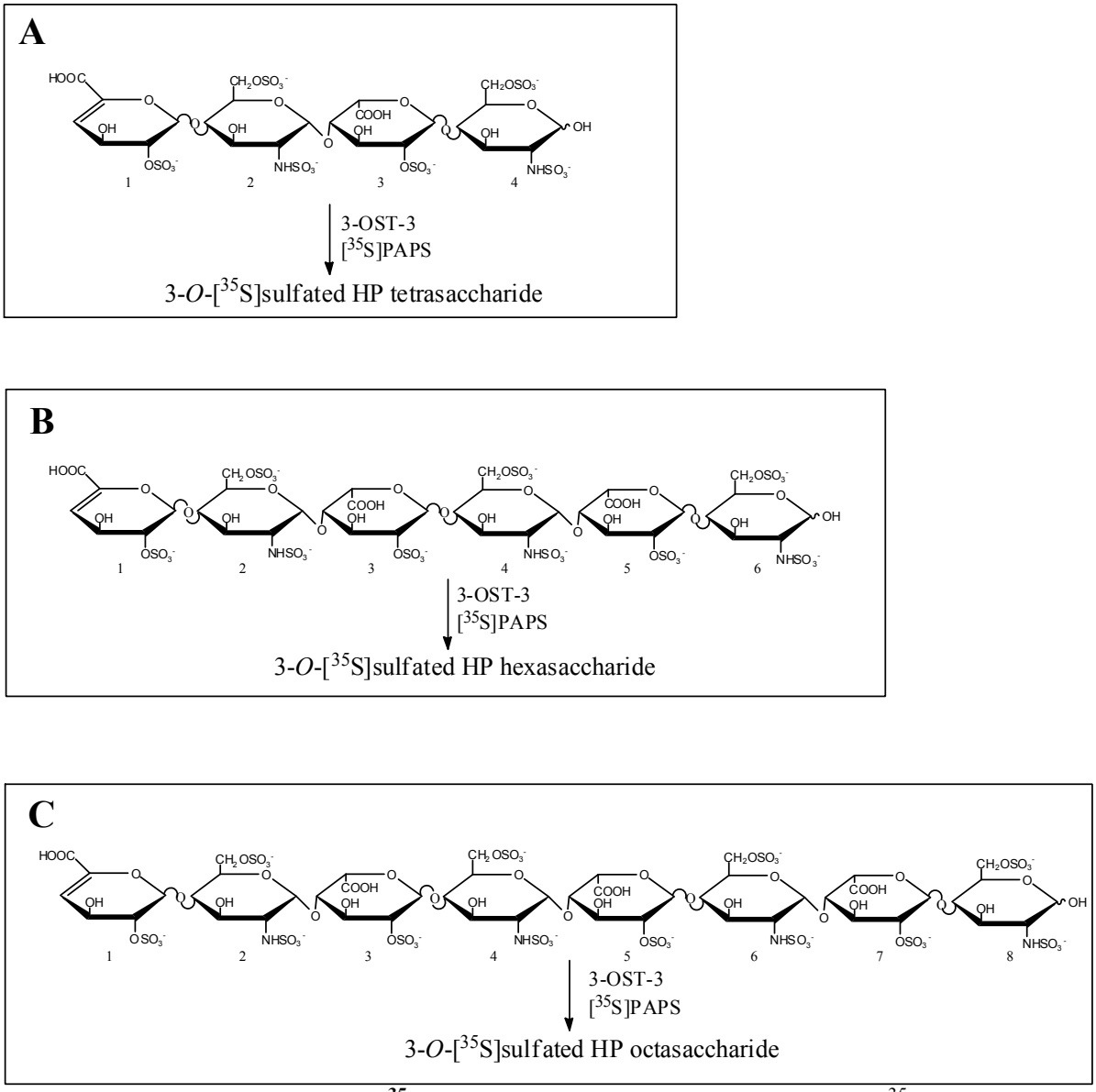

Figure 29. Preparation of 3-*O*-[^{35}S]sulfated HP oligosaccharides. 3-*O*-[^{35}S]sulfated HP oligosaccharides of various sizes were generated by incubating purified 3-OST-3 enzyme and [^{35}S]PAPS with the respective unmodified HP oligosaccharide substrate. *Panel A* shows the generation of 3-*O*-[^{35}S]sulfated HP tetrasaccharide, *panel B*, shows the generation of 3-*O*-[^{35}S]sulfated HP hexasaccharide and *panel C* shows the generation of 3-*O*-[^{35}S]sulfated HP octasaccharide. Residue numbers are presented under each sugar unit for clarity.

The susceptibility of these HP oligosaccharides to 3-OST-3 modification is shown in figure 30. It appeared that the HP octasaccharide was the best substrate among these HP oligosaccharides accepting 44 pmole sulfate/μg of substrate. The HP tetrasaccharide was the least susceptible to 3-OST-3 modification. A previous study demonstrated that full length HP is not a substrate for 3-OST-3 (195). However, the data presented above suggests that smaller oligosaccharides of HP can serve as a substrate for 3-OST-3. As a result, it is hypothesized that upon depolymerization of full length HP into its smaller oligosaccharide components a structural feature that may inhibit 3-OST-3 activity is lost. Nevertheless, the susceptibility of the HP oligosaccharides to 3-OST-3 modification allowed for the preparation of 3-*O*-sulfated HP oligosaccharides to determine the minimal size of the gD binding site. It should be noted that the position of the 3-*O*-sulfo groups on the HP oligosaccharides upon 3-OST-3 modification is not completely known with the exception of the tetrasaccharide substrate. Previous studies demonstrated that the 3-OST-3 enzyme transfers a 3-*O*-sulfo group to the 3-OH position of the glucosamine located at residue 2 (121).

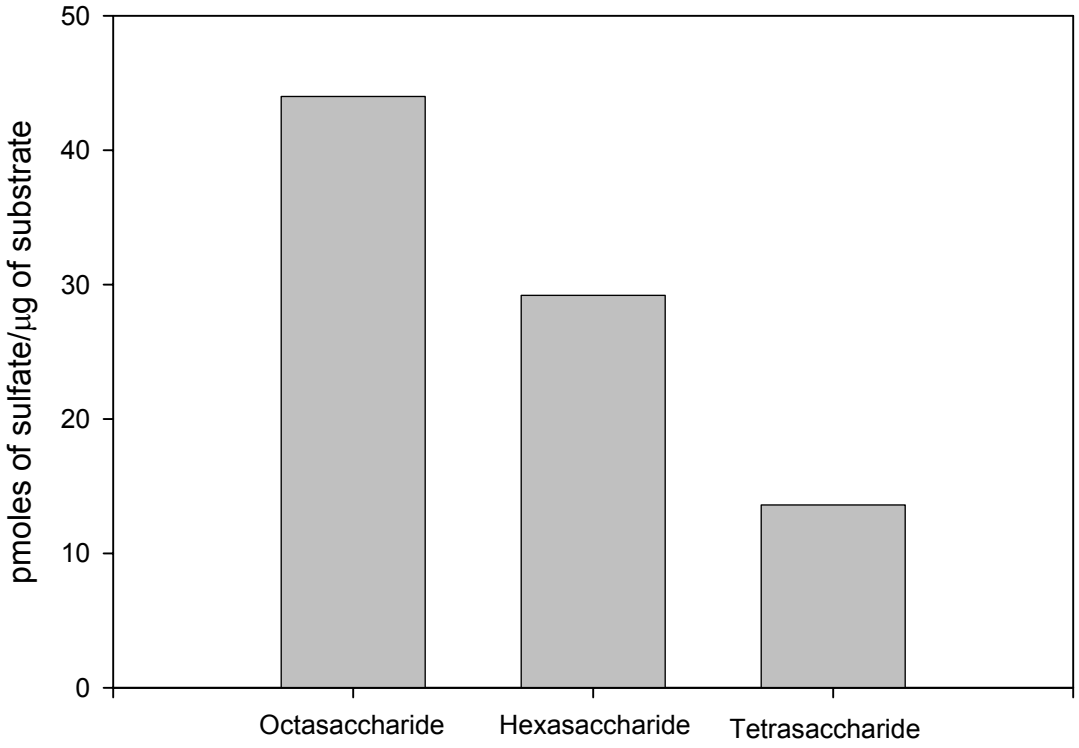

Figure 30. Susceptibility of HP derived oligosaccharides to 3-OST-3 modification. Individual modification reactions consisting of 10 μg of substrate (octa-, hexa-, or tetra-) were incubated with 440 ng purified 3-OST-3, 15 μM cold PAPS, and [^{35}S]PAPS at a specific activity of 4000 cpm/pmole in reaction buffer (see methods section). The amount of pmoles transferred was calculated by the amount of [^{35}S] counts recovered after purification. No error bars are presented as trial was done once.

The binding of 3-O-[^{35}S]sulfated HP oligosaccharides to gD (Immunoprecipitation Approach)

The binding of 3-*O*-[^{35}S]sulfated HP oligosaccharides to gD was investigated using an immunoprecipitation approach. The 3-*O*-[^{35}S]sulfated HP oligosaccharides of various sizes were incubated with gD and the complex of gD/3-*O*-[^{35}S]sulfated HP oligosaccharides were captured using anti-gD antibody on protein A agarose. The 3-*O*-[^{35}S]sulfated HP oligosaccharides were eluted from protein A agarose beads using increasing amounts of NaCl from 0 mM to 1 M. The elution profile is shown in figure 31. For the 3-*O*-[^{35}S]sulfated HP tetrasaccharide only 5% of the [^{35}S]counts were eluted with buffer containing 150 mM NaCl. In contrast more than 40% of the [^{35}S]counts of the 3-*O*-[^{35}S]sulfated HP octasaccharide were eluted with buffer containing 150 mM NaCl. About 20% of the [^{35}S]counts from the 3-*O*-[^{35}S]sulfated HP hexasaccharide was eluted under the same conditions. These observations suggest that the binding affinity to gD depends on the size of the oligosaccharide. This suggestion was further strengthened by determining the binding constants using affinity co-electrophoresis as described below.

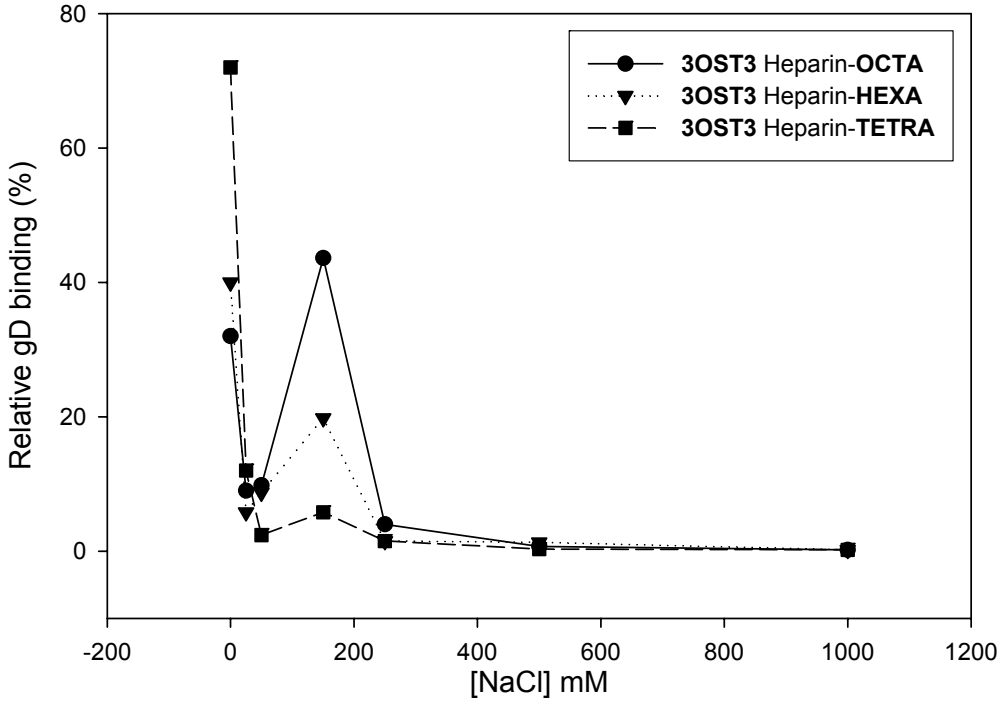

Figure 31. Binding of various sized 3-*O*-[^{35}S]sulfated HP oligosaccharides to gD using immunoprecipitation approach. 3-*O*-[^{35}S]sulfated HP of various sizes (30 pmoles, 20 pmoles, and 11 pmoles for octa-, hexa-, and tetra- oligosaccharides respectively) were incubated in binding buffer pH 6, and 20 µg gD at room temperature. The anti-gD monoclonal antibody DL6 was added and incubated at 4 °C for 1 h followed by addition of the protein A-agarose gel and agitated at 4 °C for an additional hour. The protein A agarose gel (Pierce) was then washed with increasing amounts of NaCl from 0 mM to 1 M. During each washing concentration (x-axis) 5 × 500 µl was used to elute. Relative gD binding is presented as the percentage of [^{35}S] counts recovered upon the indicated NaCl wash (y-axis).

Affinity Co-electrophoresis-(ACE)

Affinity Co-Electrophoresis (ACE) is used to determine the binding constant by monitoring the electrophoretic mobility of a ligand in the presence of different concentrations of a receptor (187). This technique can be used to measure the interactions between glycosaminoglycans and proteins in both high and low binding affinities. Specifically, it has been used to determine the binding constants between HS and fibroblast growth factor (the K_d for FGF binding is nM range), antithrombin, and gD (the K_d for gD binding is μM range) (130, 181, 196).

The diagram shown in figure 32 illustrates how ACE technique is applied. The protein of interest is casted in separation zones at various concentrations. Trace amounts of a ligand is loaded at the top of the separation zones in pre-formed wells (Figure 32, panel A). With the anode positioned at the bottom of the gel, once the current is applied the ligand migrates through the separation zones while being retarded via its binding affinity towards the protein (figure 32, panel B). At appropriate protein concentrations, the electrophoretic migration of the ligand is retarded in a concentration dependent manner. Based on the distance traveled by the ligand through various protein concentrations, the binding constant (K_d) can be calculated using the Scatchard analysis. In fact the protein concentration at which the ligand is half-shifted from being fully mobile is close to the K_d value.

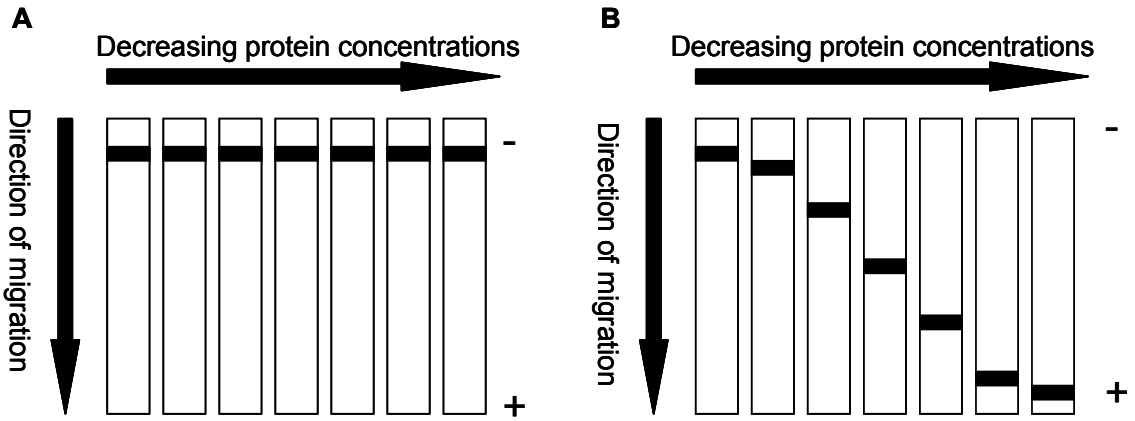

Figure 32. Schematic representation of Affinity Co-electrophoresis. *Panel A* represents gel before electrophoresis, *panel B* represents gel after electrophoresis. The protein is cast at various concentrations within an agarose gel. The radiolabeled ligand, *black bars*, is introduced at the top of the gel. During electrophoresis, the radiolabeled ligand migrates through the gel zones and is slowed by binding to the protein cast in the gel. Based on the migration pattern, a plot is generated from which an affinity constant may be derived (see text).

The main advantage for using ACE to determine the binding affinity between a GAG and a specific protein is that ACE requires small amounts of GAG and GAG has high mobility under electrophoretic conditions. More importantly, the interactions between GAG and its target protein often meet the requirements for accurate K_d determination using this technique (187). For example, the interaction between the GAG and its protein is not affected by the present of the gel. The complex of GAG/protein versus free GAG can be easily separated under electrophoretic conditions. Furthermore, the association and dissociation rates of GAG and proteins are fast compared to the electrophoresis time.

gD Binding of 3-O-[^{35}S]sulfated HP octasaccharide-(ACE)

The binding constant of the interaction between gD and 3-*O*-[^{35}S]sulfated HP octasaccharide was determined using ACE. The 3-*O*-[^{35}S]sulfated HP octasaccharide was prepared as described above by incubating the HP octasaccharide with purified 3-OST-3 enzyme in the presence of [^{35}S]PAPS and purified using DEAE chromatography. The 3-*O*-

[^{35}S]sulfated HP octasaccharide was separated under electrophoresis conditions through agarose gel zones containing gD concentrations ranging from 0 to 60 μM. The migration profile of the 3-*O*-[^{35}S]sulfated HP octasaccharide was visualized using Phosphor-Imager (not shown) and by autoradiography (figure 33, panel A).

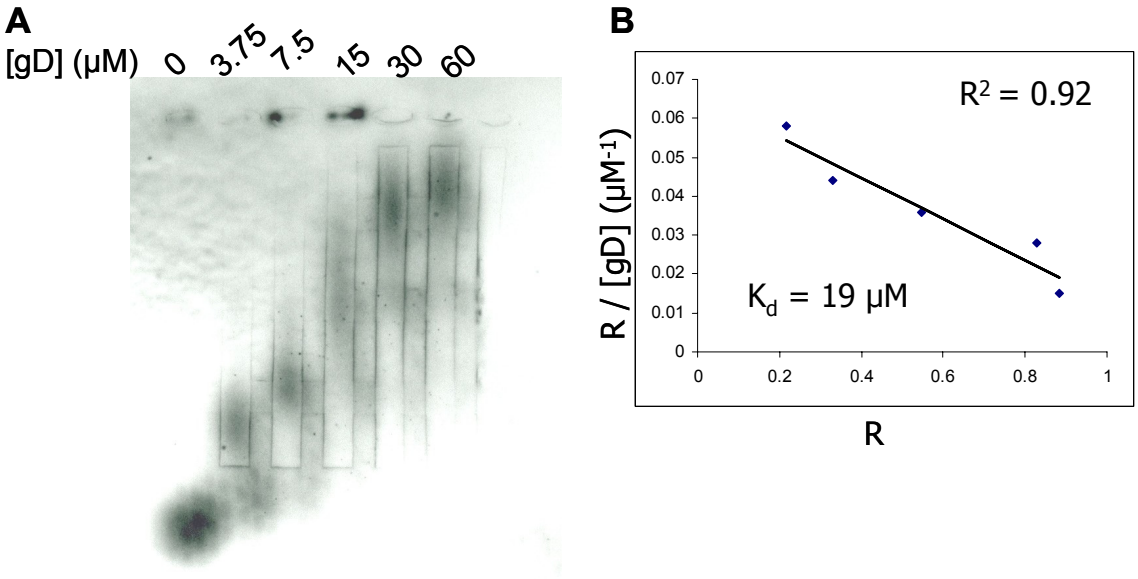

Figure 33. Determining the Binding Constant (K_d) between gD and 3-*O*-[^{35}S]sulfated HP octasaccharide. *Panel A* presents the autoradiography of the agarose gel in which purified 3-*O*-[^{35}S]sulfated HP octasaccharide was subjected to electrophoresis through separation zones containing gD at concentrations indicated. Approximately 28,000 cpm (4×10^{-12} mol)/lane of 3-*O*-[^{35}S]sulfated HP octasaccharide was loaded into each separation zone. *Panel B* represents the plot of $R/[gD]_{total}$ versus R, where $R = (M_0\text{-}M)/M_0$. M_0 is the migration of free 3-*O*-[^{35}S]sulfated HP octasaccharide and M is the observed migration of 3-*O*-[^{35}S]sulfated HP octasaccharide in the presence of gD at various concentrations. According to the Scatchard equation, the plot in *Panel B* should yield a straight line with a slope of $-1/K_d$. The linear coefficient value of the plot is indicated as R^2 in *Panel B*.

It was clear that the migration of the 3-*O*-[^{35}S]sulfated HP octasaccharide was retarded by gD in a concentration dependent manner (figure 33, panel A). For example, it was observed that the 3-*O*-[^{35}S]sulfated HP octasaccharide was almost completely retarded at 60 μM, while being fully mobile when no gD was present. The relative migration distances of the 3-*O*-[^{35}S]sulfated HP octasaccharide at various concentrations of gD, along with the Scatchard equation, were used to determine the K_d value to be 19 μM (figure 33, panel B).

Two interesting points were noted. First, that the concentration 3-*O*-[^{35}S]sulfated HP octasaccharide was much lower than the gD contained with the separation zones. This allowed us to determine the K_d value. If the amount of the 3-*O*-[^{35}S]sulfated HP octasaccharide were close to the K_d value, deviations from linearity would occur at low values of R (at low protein concentrations) which may lead to an overestimation of K_d (187). Secondly, the 3-*O*-[^{35}S]sulfated HP octasaccharide was nearly fully retarded at high concentration of gD suggesting that does this preparation was pure in terms of gD binding affinity. The structural homogeneity of the 3-*O*-[^{35}S]sulfated HP octasaccharide would facilitate the characterization of the position of the 3-*O*-sulfo group as described in Chapter IV.

gD Binding of 3-O-[^{35}S]sulfated HP hexasaccharide-(ACE)

The binding constant between gD and the 3-*O*-[^{35}S]sulfated HP hexasaccharide was also investigated using ACE. The 3-*O*-[^{35}S]sulfated HP hexasaccharide was prepared by incubating the HP hexasaccharide with 3-OST-3 enzyme in the presence of [^{35}S]PAPS and purified using DEAE chromatography. The 3-*O*-[^{35}S]sulfated HP hexasaccharide was resolved under the same conditions as the 3-*O*-[^{35}S]sulfated HP octasaccharide as described above. The migration profile 3-*O*-[^{35}S]sulfated HP hexasaccharide is shown in figure 34.

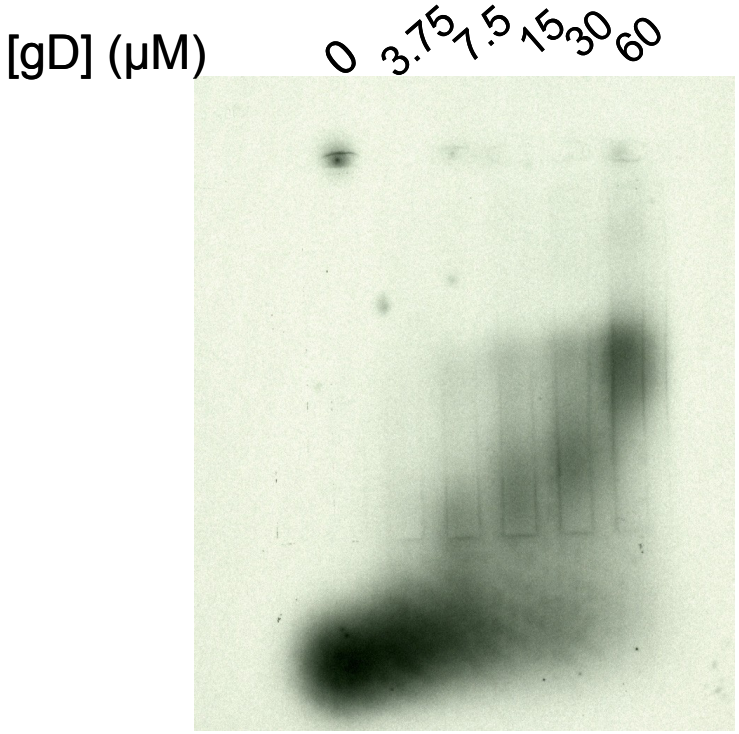

Figure 34. Migration profile of 3-*O*-[^{35}S] HP hexasaccharide on ACE gel. Shown is the autoradiography of the agarose gel in which 3-*O*-[^{35}S]sulfated HP hexasaccharide was subjected to electrophoresis through separation zones containing gD at concentrations indicated. Approximately 27,000cpm (4.2×10^{-12}mol)/lane of 3-*O*-[^{35}S]sulfated HP hexasaccharide was loaded into each separation zone. Graphical analysis was unable to be performed due to no substantial retention of migration.

The retardation of the 3-*O*-[^{35}S]sulfated HP hexasaccharide on the gel was much less obvious when compared to that of the 3-*O*-[^{35}S]sulfated HP octasaccharide. Specifically, at the highest gD concentration tested, 60 μM, the 3-*O*-[^{35}S]sulfated HP hexasaccharide migrated approximately halfway through the separation zone. A higher concentration of gD was attempted to be casted into the gel, however the gel failed to be solidified uniformly under such conditions. As a result, full retardation of the 3-*O*-[^{35}S]sulfated HP hexasaccharide could not be obtained. Thus, the K_d value could not be determined with confidence. Based on its migration pattern shown in figure 34, the K_d was estimated to be greater than 115 μM. This suggests that by reducing the size of the oligosaccharide from an octasaccharide to a hexasaccharide results in a greater than six fold decrease in its binding affinity. Because the binding affinity between the gD and 3-*O*-[^{35}S]sulfated HP

tetrasaccharide was believed to be lower than that of the 3-*O*-[^{35}S]sulfated HP hexasaccharide, we decided not to determine its affinity to gD.

The binding constant data are consistent with the results from immunoprecipitation binding experiments (figure 31). These data support the conclusion that gD binds to 3-*O*-[^{35}S]sulfated HP oligosaccharides in a size dependent fashion. Our results suggest the 3-*O*-[^{35}S]sulfated HP octasaccharide is the minimum size required for gD binding. Because this octasaccharide has the highest affinity to gD, its structure was determined as described in Chapter IV.

Conclusions

Various studies concerning the structure of gD and its binding to its receptors have been conducted previously. The majority of these studies used recombinant forms of gD that was expressed in insect cells using a baculovirus expression approach (178, 181). The complexities associated with the baculovirus expression of gD prompted us to search for a more efficient expression method. As presented above, the ectodomain of gD (Lys_{26}-His_{332}) was cloned and expressed in large quantities in *E. coli*. with a yield of 5 mg per liter of culture. This expression was achieved by co-expressing bacteria chaperone proteins. From the binding of 3-*O*-sulfated HS to gD expressed in bacteria and gD expressed in insect cells, data presented above suggested that the recombinant gD from bacteria expression was functional. To our knowledge, using a bacteria expression system to prepare HSV envelope proteins has not been reported previously. The bacteria expression of other HSV envelope proteins including gB and gC are currently under investigation in our laboratory. This novel

approach to express HSV envelope proteins could be used to develop a vaccine against HSV infections.

Results demonstrated that the 3-*O*-[^{35}S]sulfated HP oligosaccharides bound to gD in a size dependent manner, with the 3-*O*-[^{35}S]sulfated HP octasaccharide having the minimum length required for detectable gD binding. This conclusion was based on our success in obtaining purified 3-*O*-sulfated HP oligosaccharides of various sizes and the expression of gD in bacteria. The high susceptibility of the HP oligosaccharides to 3-*O*-sulfation allowed for the determination of the minimal required length for binding using immunoprecipitation and ACE approaches. The binding affinity of the 3-*O*-[^{35}S]sulfated HP octasaccharide was found to have a K_d value of 19 μM. This value was very similar to the K_d value determined for the previously characterized HS gD binding octasaccharide which was found to be 18 μM (181). In the previous study, the HS octasaccharide was the only oligosaccharide isolated from the 3-OST-3 modified oligosaccharide library. Thus, no information concerning the size requirement for gD binding was investigated.

It is well known that full length HP/HS can inhibit HSV infections. However, because of its heterogeneity, it has been shown to cross react with numerous proteins. As a result it is not considered as an ideal compound to inhibit HSV infections. Our goal is to generate a HP based oligosaccharide that can bind to gD and inhibit viral fusion between the virus and its target cells. The gD binding 3-*O*-sulfated HP octasaccharide serves as an excellent lead compound for further investigations. Two questions at this point remained unanswered. The first was what the precise structure of the 3-*O*-sulfated HP octasaccharide is. The second was whether this octasaccharide can inhibit viral infection. The next chapter describes the characterization of the 3-*O*-sulfated HP octasaccharide.

CHAPTER IV

STRUCTURAL CHARACTERIZATION OF THE GLYCOPROTEIN D BINDING 3-*O*-SULFATED HEPARIN OCTASACCHARIDE

Introduction

In the previous chapter, we determined that the 3-*O*-sulfated HP octasaccharide had a high binding affinity to gD. In this chapter the structural characterization of this 3-*O*-sulfated HP octasaccharide is described. The focus of the structural characterization was to determine the number and location of the 3-*O*-sulfo groups on the 3-*O*-sulfated HP octasaccharide. The purity of the 3-*O*-sulfated HP octasaccharide was determined by anion exchange HPLC. The structure was determined utilizing a combination of chemical and enzymatic degradations. In order to investigate the possibility of using the HP oligosaccharide to inhibit HSV infections, relatively large quantities of the 3-*O*-sulfated HP octasaccharide were needed. By coupling a sulfo donor regeneration system with 3-OST-3 modification, about 130 μg of the characterized gD binding 3-*O*-sulfated HP octasaccharide was generated for cell based viral entry assays. Once cell based assays are completed, results will determine whether the 3-*O*-sulfated HP octasaccharide can inhibit viral fusion via its binding affinity for gD. This will provide novel evidence as to the feasibility of inhibiting HSV viral infections by disrupting interactions with its polysaccharide based cellular receptors.

Determination of the purity of 3-O-[^{35}S]sulfated HP octasaccharide

DEAE-NPR anion exchange HPLC chromatography was used to assess the purity of the 3-*O*-[^{35}S]sulfated HP octasaccharide. The 3-*O*-[^{35}S]sulfated HP octasaccharide was prepared by incubating the HP octasaccharide with purified 3-OST-3 enzyme in the presence of [^{35}S]PAPS. The unmodified HP octasaccharide and the 3-*O*-[^{35}S]sulfated HP octasaccharide were well resolved on DEAE-NPR column as shown in figure 35. The unmodified HP octasaccharide has absorbance at 232 nm which was used to monitor its elution position. The 3-*O*-sulfated HP octasaccharide contained a [^{35}S] label which was used to monitor its elution position.

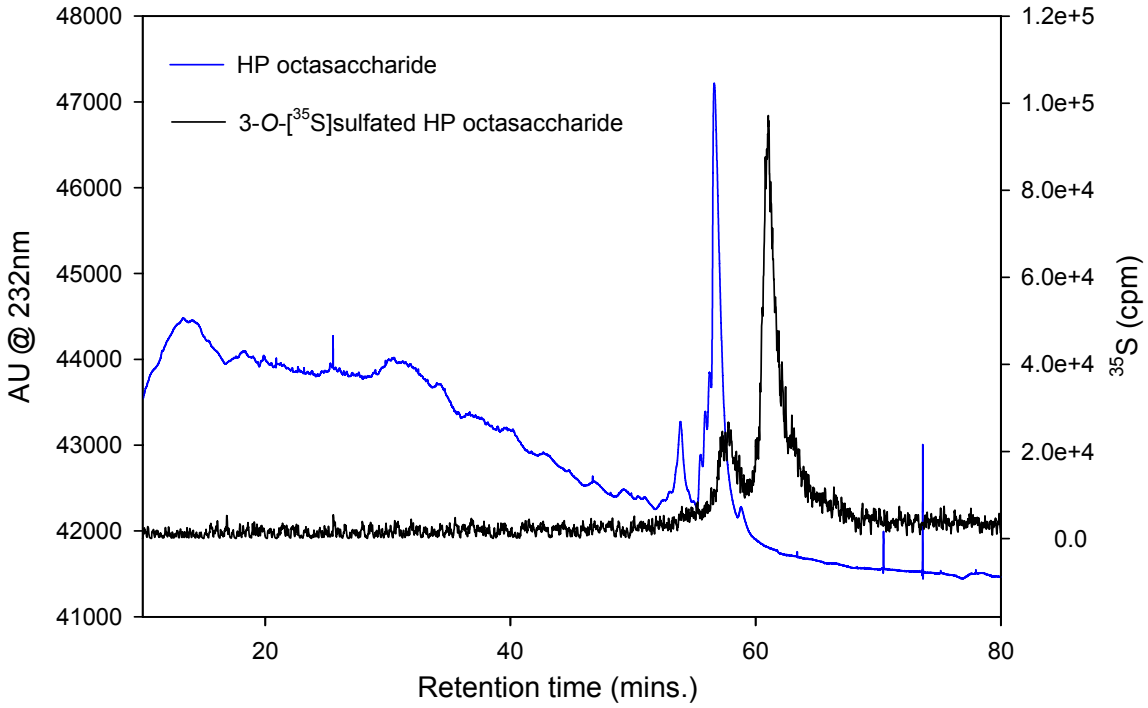

Figure 35. Anion exchange HPLC-DEAE-NPR chromatogram of 3-*O*-[^{35}S]sulfated HP octasaccharide. Approximately 3 ug of unmodified HP octasaccharide and approximately 56,000 cpm of 3-*O*-[^{35}S]sulfated HP octasaccharide was subjected to HPLC-DEAE-NPR chromatography as described under "methods section". The x-axis shows retention time in (mins.), the *right y-axis* monitors [^{35}S] using online detection and *left y-axis* monitors the online UV detection at 232 nm.

The separation of the HP oligosaccharides on the DEAE-NPR column was based on their negative charge densities. As expected, the unmodified HP octasaccharide eluted as a major UV peak at 57 mins. (figure 35, blue line). The 3-*O*-[^{35}S]sulfated HP octasaccharide eluted as a major [^{35}S] labeled peak at 62 mins. (figure 35, black line). The higher retention time observed for the 3-*O*-[^{35}S]sulfated HP octasaccharide on the DEAE-NPR column compared to that of the unmodified HP octasaccharide was indicative of it carrying additional sulfo groups. Two [^{35}S] labeled peaks were observed with retention times of 58 and 62 mins. The ratio of the intensities of the two [^{35}S] labeled peaks were calculated to be 1:4, suggesting the purity of the 3-*O*-[^{35}S]sulfated HP octasaccharide was 80%. The minor [^{35}S] labeled peak that eluted at 58 mins. was believed to be due to the 3-*O*-sulfation of the minor component present in the starting material. Indeed a minor component was observed in the starting material that eluted at 55 mins. (figure 35, blue line). Taken together these results suggest that the 3-*O*-[^{35}S]sulfated HP octasaccharide was sufficiently pure for structural characterization.

To eliminate the remote possibly that the minor contaminant in the 3-*O*-[^{35}S]sulfated HP octasaccharide preparation was responsible for binding to gD, we compared the DEAE-NPR profiles pre- and post gD affinity fractionation. The gD affinity fractionation was carried out using an immunoprecipitation approach as described in Chapter III. The resultant 3-*O*-[^{35}S]sulfated octasaccharide was resolved by DEAE-NPR chromatography. The results demonstrated that the major [^{35}S] labeled component was present in the high affinity fraction suggesting that this component was indeed responsible for the binding to gD (chromatograms not shown).

Structural characterization of 3-O-[^{35}S]sulfated HP octasaccharide

The unmodified HP octasaccharide contained four glucosamine residues, thereby giving it four potential sites for 3-*O*-sulfation by 3-OST-3 as shown in figure 36. These four positions include residues 2, 4, 6, and 8. Here we described the results to identify which residue carried the 3-*O*-sulfo group. The 3-*O*-[^{35}S]sulfated HP octasaccharide was prepared by incubated the HP octasaccharide with purified 3-OST-3 in the presence of [^{35}S]PAPS. The structural characterization was accomplished using a combination of chemical and enzymatic degradations from both non-reducing and reducing ends. Non-reducing end analysis permitted the identification of whether the 3-*O*-[^{35}S]sulfo group was present on either residue 2 or 4. Reducing end analysis permitted the identification of whether residue 6 or 8 carried the 3-*O*-[^{35}S]sulfo group

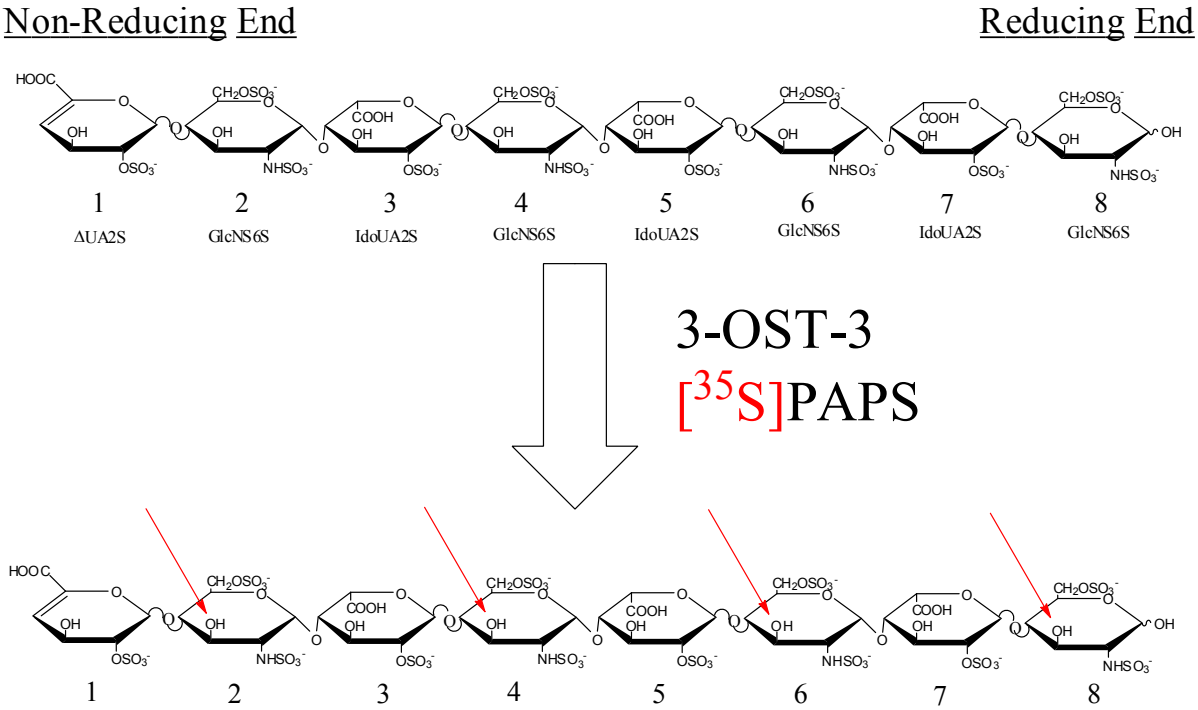

Figure 36. Potential 3-*O*-sulfation sites in HP octasaccharide. The unmodified HP octasaccharide (*top*) is comprised of repeated disaccharide units of –[IdoUA2S-GlcNS6S]-. After 3-OST-3 modification, in the presence of [^{35}S]PAPS, a [^{35}S]sulfo group is transferred to the 3-OH position of a specific glucosamine residue within the HP octasaccharide (*bottom*). The residues are numbered from 1 to 8, starting with the non-reducing end, *1* to the reducing end, *8*. The *red* arrows show the potential sites for 3-*O*-sulfation. The abbreviated notations are presented under the corresponding residue in the unmodified HP octasaccharide for clarity.

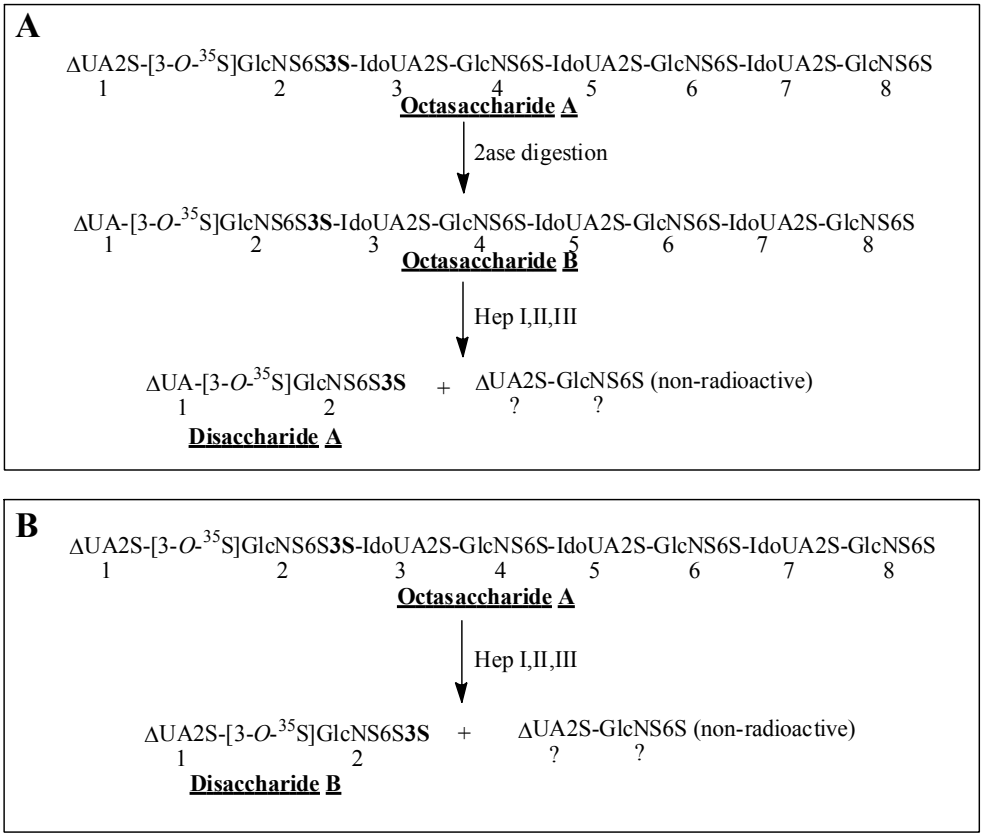

Figure 37. Strategy for the determination of reside 2 as the 3-*O*-sulfation site. *Panel A*, if an 3-*O*-[^{35}S]sulfated HP octasaccharide that carries the 3-*O*-[^{35}S]sulfo group on reside 2 (octasaccharide A, *panel A*) is digested with 2ase, the result with be octasaccharide E. If octasaccharide E is digested with a mixture of heparin lyases the result would be disaccharide A. *Panel B*, if octasaccharide A is directly digested with a mixture of heparin lyases, the result would be disaccharide B. If the HPLC elution profile for disaccharide A and B are different, then residue 2 carries the 3-*O*-[^{35}S]sulfo group. If the HPLC elution profile is similar, then residue 2 does not carry the 3-*O*-[^{35}S]sulfo group. The "?" represents unknown residue number.

Non-reducing end analysis

Non-reducing end analysis takes advantage of the substrate specificity of $\Delta^{4,5}$ glycuronate-2-sulfatase (2ase), an exolytic sulfatase (197). This enzyme is known to specifically to remove the 2-*O*-sulfo group from ΔUA2S, which is present at the non-reducing end of the 3-*O*-[^{35}S]sulfated HP octasaccharide. Subjecting the 3-*O*-[^{35}S]sulfated HP octasaccharide to heparin lyases digestion with or without pretreatment of 2ase permitted the determination of whether the 3-*O*-[^{35}S]sulfo group was on residue 2 or 4.

The initial hypothesis was that 3-OST-3 transferred a sulfo group to the 3-OH position of the glucosamine residue on the non-reducing end of the HP octasaccharide (figure 36, residue 2). This hypothesis was based on a previous study in which the 3-OST-3 enzyme sulfated a HP tetrasaccharide substrate (121). The strategy for the determination of whether residue 2 contains the 3-*O*-[^{35}S]sulfo group is described in figure 37.

The digestion of the 3-*O*-[^{35}S]sulfated HP octasaccharide with a mixture of heparin lyases should yield a [^{35}S] labeled disaccharide with a structure of ΔUA2S-[3-*O*-^{35}S]GlcNS6S3S (figure 37, panel B, disaccharide B). Digestion of the 3-*O*-[^{35}S]sulfated HP octasaccharide with 2ase will yield an octasaccharide that contains a ΔUA residue on the non-reducing end (figure 37, panel A, octasaccharide B). The extent of the 2ase digestion can be monitored by DEAE-NPR as the starting octasaccharide (figure 37, panel A, octasaccharide A) and the digested octasaccharide (figure 37, panel A, octasaccharide B) elute with different retention times. Subjecting octasaccharide B to a mixture of heparin lyases would yield a [^{35}S] labeled disaccharide with a structure of ΔUA-[3-*O*-^{35}S]GlcNS6S3S (figure 37, disaccharide A). The identities of disaccharides A and B would be determined by co-elution with standards on HPLC. To determine whether residue 4 contained the 3-*O*-[^{35}S]sulfo group, the 3-*O*-[^{35}S]sulfated HP octasaccharide would be converted to [^{35}S] labeled tetrasaccharide by partial digestion with a mixture of heparin lyases. This digestion would be combined with or without pretreatment of 2ase.

The experiments as described were conducted. Treatment of the 3-*O*-[^{35}S]sulfated HP octasaccharide with 2ase was completed, and the product was analyzed by DEAE-NPR (figure 38). As shown in figure 38 (panel A), when the 3-*O*-[^{35}S]sulfated HP octasaccharide was digested with 2ase (3.1 U), the elution profile that resulted suggested that only a partial

digestion was achieved. The undigested 3-*O*-[^{35}S]sulfated HP octasaccharide eluted a 63 mins. while the digested material eluted at 57 mins. As shown in figure 38, panel B, when the 3-*O*-[^{35}S]sulfated HP octasaccharide was digested with a larger amount of 2ase (10 U), one major [^{35}S] labeled peak was observed that eluted at 57 mins. The observable shift from 63 mins. to 57 mins. suggested that the 2-*O*-sulfo group was removed from the non-reducing end of the octasaccharide. The observation of one [^{35}S] labeled peak resulting from the 2ase digestion of the 3-*O*-[^{35}S]sulfated HP octasaccharide suggested that the digestion was greater than 95% complete. Furthermore, the 2ase treated 3-*O*-[^{35}S]sulfated HP octasaccharide was degraded with a mixture of heparin lyases and yielded a [^{35}S] labeled disaccharide. The resultant [^{35}S] labeled disaccharide was resolved using anion exchange PAMN chromatography and was eluted at 50 mins. (figure 39, panel B). This position was where the disaccharide standard with a structure of ΔUA2S-[3-*O*-^{35}S]GlcNS6S3S was eluted under the same condition. This ΔUA2S-[3-*O*-^{35}S]GlcNS6S3S standard was generated by subjecting the previously characterized 3-*O*-[^{35}S]sulfated HP tetrasaccharide to a mixture of heparin lyases as previously described (121). The untreated 3-*O*-[^{35}S]sulfated HP octasaccharide was also degraded with a mixture of heparin lyases and the resultant [^{35}S] labeled disaccharide was also eluted at 50 mins. on the same HPLC column as shown in figure 39, panel A. These results suggest that the 3-*O*-[^{35}S]sulfated HP octasaccharide gave identical [^{35}S] labeled disaccharide products after heparin lyase digestion regardless of 2ase pretreatment. Therefore it was concluded the 3-*O*-[^{35}S]sulfo group was not present on residue 2.

In order to prove whether the 3-*O*-[^{35}S]sulfo group was on residue 4, the 3-*O*-[^{35}S]sulfated HP octasaccharide needed to be converted to [^{35}S] tetrasaccharide. This

experiment was not conducted, as the result from reducing end analysis suggested that the 3-*O*-[^{35}S]sulfo group was present on the reducing end.

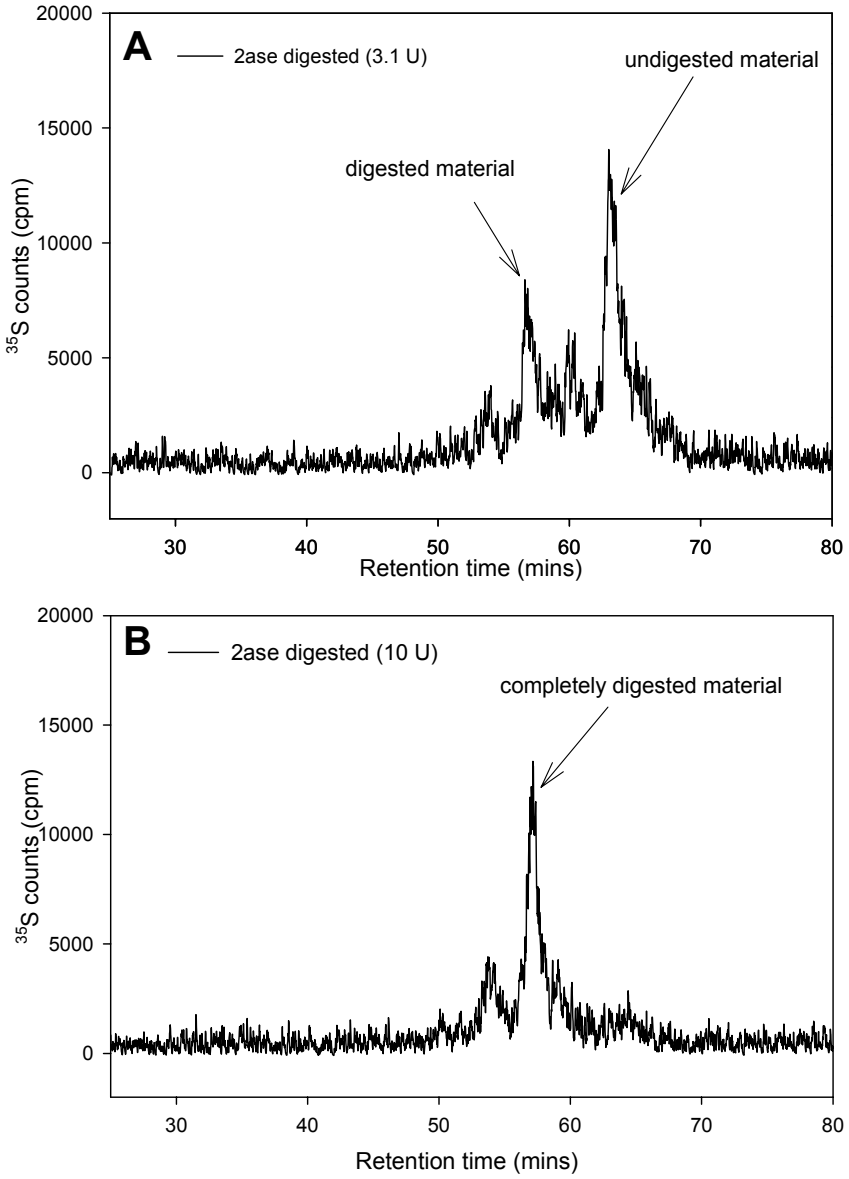

Figure 38. HPLC-DEAE-NPR chromatograms observing 2ase digestion of the 3-*O*-[^{35}S]sulfated HP octasaccharide. The 3-*O*-[^{35}S]sulfated HP octasaccharide was digested with different amounts of 2ase. *Panel A*, shows the partial digestion of the 3-*O*-[^{35}S]sulfated HP octasaccharide resulting from the addition 3.1 U of 2ase. As a result of partial digestion, the material from *panel A*, was further digested with 10 U of 2ase and its elution profile is shown in *panel B*.

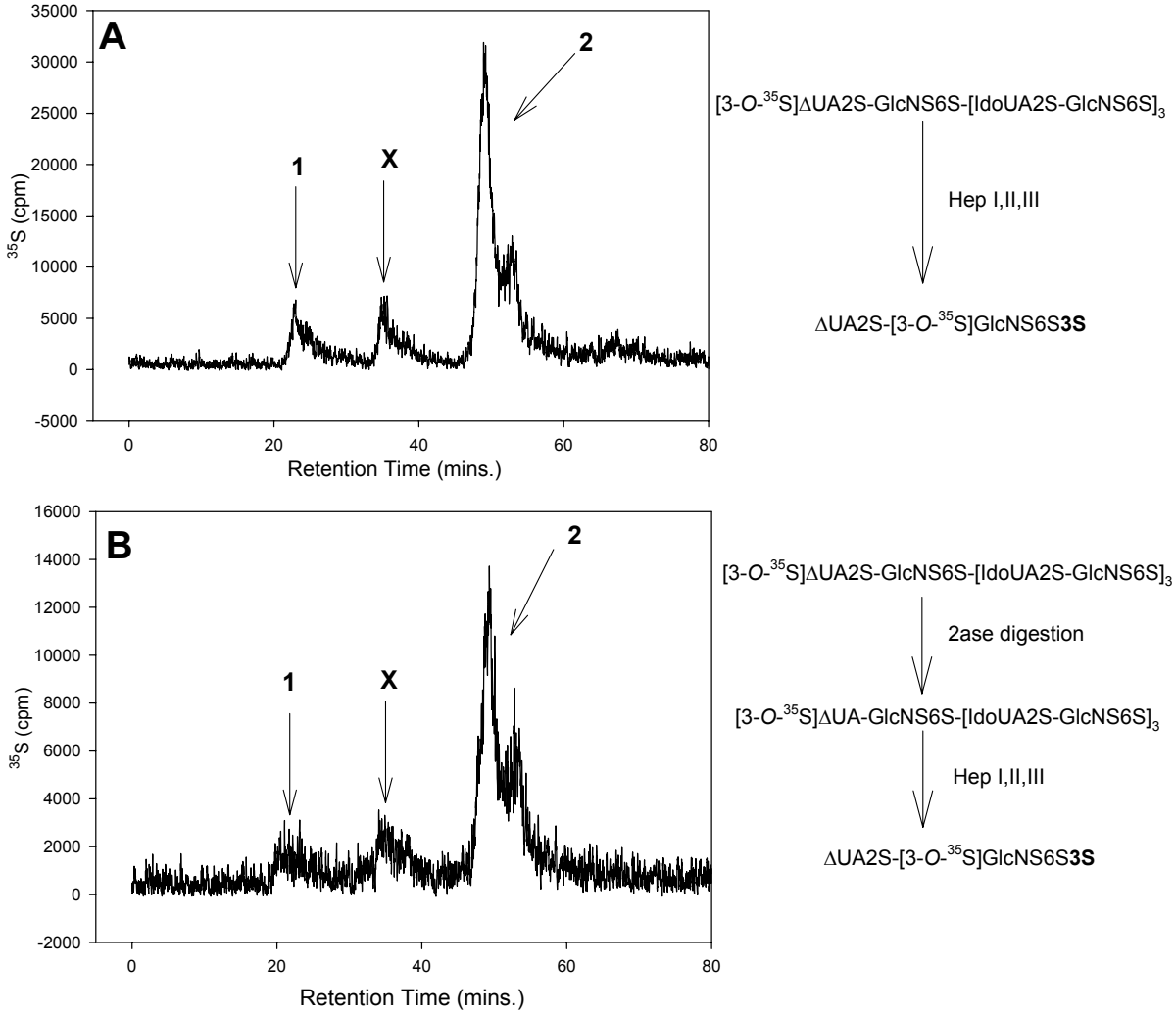

Figure 39. HPLC-PAMN chromatograms of 2ase digested and undigested 3-*O*-[^{35}S]sulfated HP octasaccharide. *Panels A* and *B* show the elution profiles of the 3-*O*-[^{35}S]sulfated HP octasaccharide digested with heparin lyases without or with pretreatment of 2ase, respectively. Elution condition is described in "methods" section. The enzymatic digestions are presented to the right the chromatograms. The anion exchange HPLC-PAMN elution conditions are presented in the "methods" section. *Arrow 1*, elution position of [^{35}S] free sulfate; *arrow 2*, elution position of ΔUA2S-[3-*O*-^{35}S]GlcNS6S3S; "*X*" elution position of an undetermined material.

Reducing end analysis

Reducing end analysis takes advantage of the presence of a chemically reactive hemiacetal group at the reducing end of the 3-*O*-[^{35}S]sulfated HP octasaccharide. A common method used to exploit the chemically reactive reducing end is to use reductive amination chemistry through the formation of a Schiff base (198). Subjecting the 3-*O*-[^{35}S]sulfated HP octasaccharide to heparin lyases digestion with or without prior reducing end modification permitted the determination of whether the 3-*O*-[^{35}S]sulfo group was on residue 6 or 8. The hypothesis was that 3-OST-3 transferred a sulfo group to the 3-OH position of the glucosamine residue on the reducing end of the HP octasaccharide (figure 36, residue 8). To investigate this possibility, the reducing end was chemically modified with 2-aminobenzmide (2-AB). It was decided that a [2-AB] tag would be used as [2-AB] labeled glycans can be resolved using HPLC (189). The reducing end modification with [2-AB] is shown in figure 40.

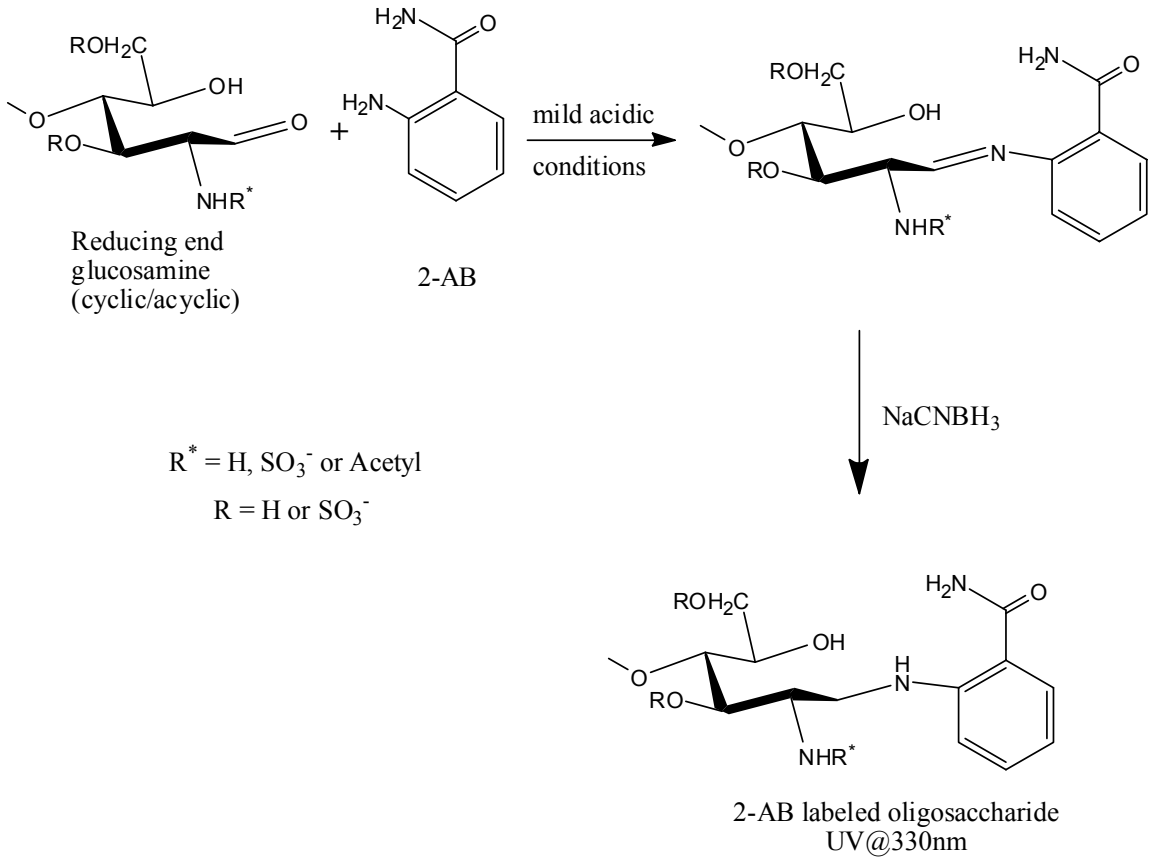

Figure 40. Reaction for 2-AB reducing end labeling of oligosaccharides. The reducing end glucosamine is shown in its ring opened form.

The [2-AB] labeling reaction involves a 2-step process as shown in figure 40. First, there is a Schiff base formation. The reducing end unit is in equilibrium between ring closed (cyclic) and ring open (acyclic) conformations. The primary amine group of [2-AB] is able to perform a nucleophilic attack on the carbonyl carbon of the reducing end sugar in its acyclic conformation. The result is the formation of a metastable Schiff base that is facilitated by mild acidic conditions. Secondly, the Schiff base is chemically reduced by sodium cynaoborohydride to yield the stable [2-AB] labeled glycan. The [2-AB] glycan will have characteristic UV absorbance at 330 nm.

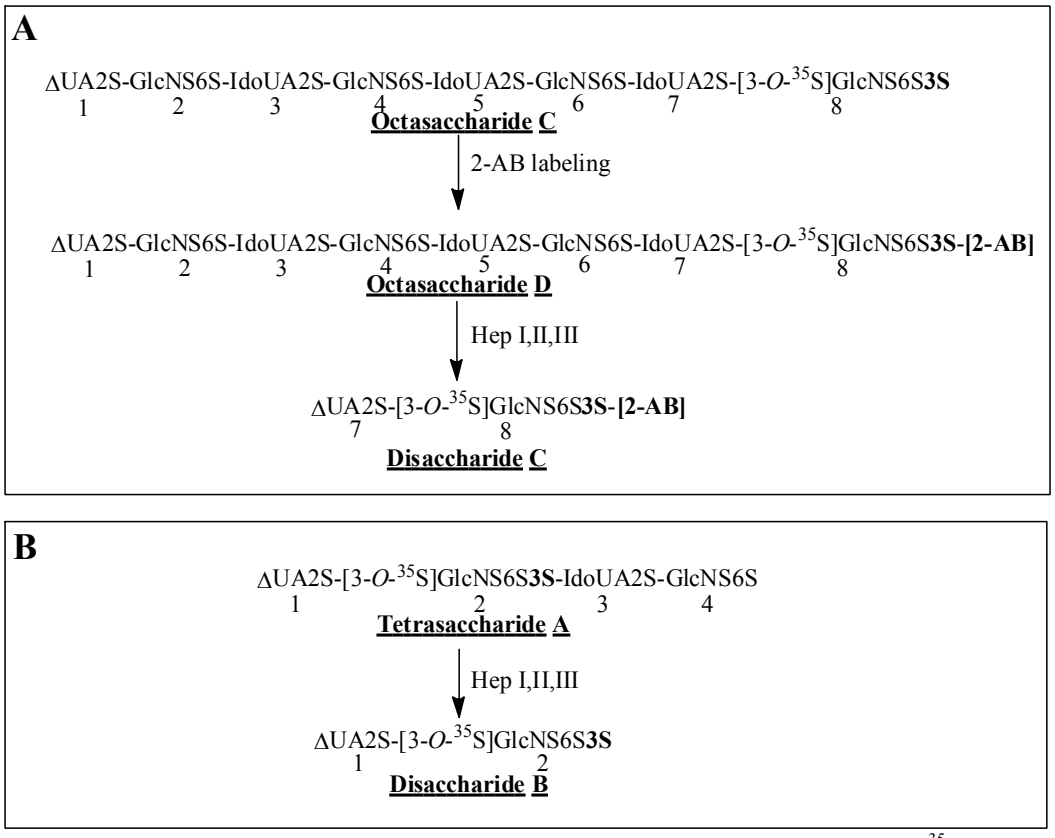

Figure 41. Strategy for the determination of reside 8 as the 3-*O*-sulfation site. The 3-*O*-[^{35}S]sulfated HP octasaccharide (octasaccharide C, panel A) is labeled with [2-AB] resulting in octasaccharide D (panel A). Octasaccharide D is digested with a mixture of heparin lyases to yield disaccharide C (panel A). Disaccharide B standard (panel B) is generated by the heparin lyases digestion of tetrasaccharide A (panel B). If disaccharides B and C co-elute, then residue 8 would carry the 3-*O*-[^{35}S]sulfo group.

The strategy for the determination of whether residue 8 contains the 3-*O*-[^{35}S]sulfo group is described in figure 41. The digestion of the 3-*O*-[^{35}S]sulfated HP tetrasaccharide with a mixture of heparin lyases will yield a [^{35}S] labeled disaccharide with a structure of ΔUA2S-[3-*O*-^{35}S]GlcNS6S3S (figure 41, panel B, disaccharide B). Subjecting the 3-*O*-[^{35}S]sulfated HP octasaccharide to reducing end labeling with [2-AB] would yield an octasaccharide that displays a [2-AB] label on the reducing end glucosamine (figure 41, panel A, octasaccharide D). Subjecting octasaccharide D to a mixture of heparin lyases would yield a [^{35}S] labeled disaccharide with a structure of ΔUA2S-[3-*O*-^{35}S]GlcNS6S3S-[2-AB] (figure 41, panel A, disaccharide C). The identities of disaccharides B and C would be determined by co-elution with standards on HPLC. As a result, the preparation of the

ΔUA2S-[3-*O*-^{35}S]GlcNS6S3S-[2-AB] standard was essential and is described below. To determine whether residue 6 contained the 3-*O*-[^{35}S]sulfo group, the 3-*O*-[^{35}S]sulfated HP octasaccharide-[2-AB] would be converted to tetrasaccharides by partial digestion with a mixture of heparin lyases (strategy not shown).

Preparation of the ΔUA2S-[3-O-^{35}S]GlcNS6S3S-[2-AB] standard

The preparation of the 3-*O*-[^{35}S]sulfated disaccharide-[2-AB] labeled standard was achieved from a heparin lyases-digested 3-*O*-[^{35}S]sulfated tetrasaccharide followed by [2-AB] labeling. The characterized 3-*O*-[^{35}S]sulfated HP tetrasaccharide was generated as previously described by incubating the HP tetrasaccharide with purified 3-OST-3 enzyme in the presence of [^{35}S]PAPS (figure 42, tetrasaccharide A) (121) . Digestion of tetrasaccharide A with a mixture of heparin lyases yields a [^{35}S] labeled disaccharide with a structure of ΔUA2S-[3-*O*-^{35}S]GlcNS6S3S (figure 42, disaccharide B). Subjecting this [^{35}S] labeled disaccharide to [2-AB] reducing end labeling would result in a [^{35}S] labeled disaccharide with a structure of ΔUA2S-[3-*O*-^{35}S]GlcNS6S3S-[2-AB] (figure 42, disaccharide C). Disaccharides B and C can be then analyzed on HPLC to observe their elution profiles.

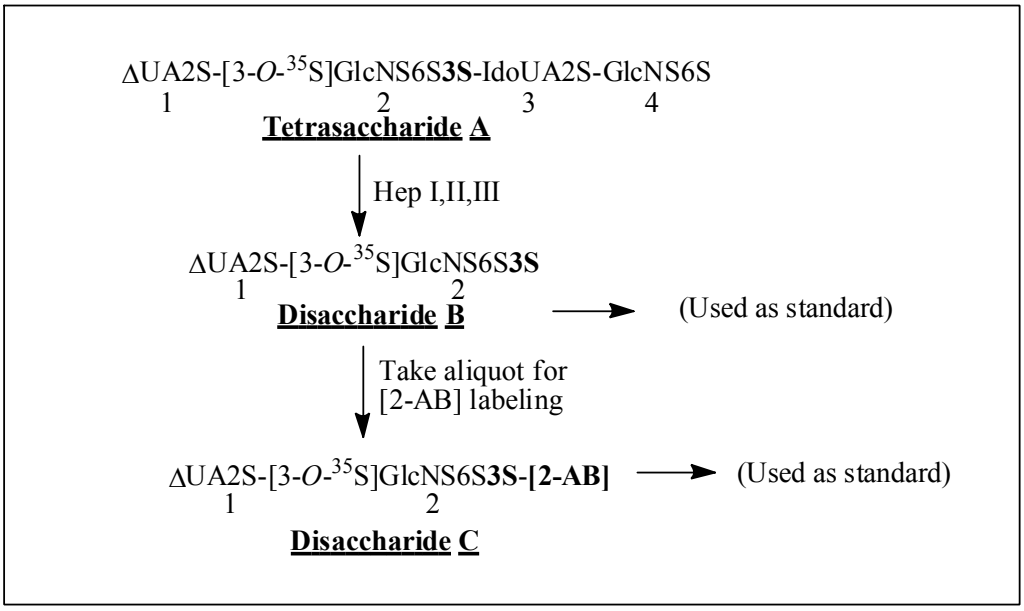

Figure 42. Strategy for generating [^{35}S] labeled disaccharide standards labeled with [2-AB]. The 3-*O*-[^{35}S]sulfated HP tetrasaccharide (tetrasaccharide A) is cleaved into its disaccharide components by heparin lyases resulting in disaccharide B. Disaccharide B is further modified by [2-AB] labeling, yielding another [^{35}S] labeled disaccharide standard (disaccharide C).

The strategy to generate the [2-AB] disaccharide standard as presented in figure 42 was carried out, and [^{35}S] labeled disaccharides B and C were analyzed by PAMN to observe their elution profiles. Tetrasaccharide A was digested with a mixture of heparin lyases and the resultant [^{35}S] labeled disaccharide with a structure of ΔUA2S-[3-*O*-^{35}S]GlcNS6S3S was resolved on PAMN (figure 43, panel A). As shown in figure 43 panel A, two major [^{35}S] labeled peaks were observed that had elution times of 30 mins. and 54 mins. Peak 1 at 30 mins. was free [^{35}S]sulfate, a result of de-sulfation of 3-*O*-[^{35}S]sulfated HP tetrasaccharide during the heparin lyases digestion. Peak 2 at 54 mins. was the elution position of the ΔUA2S-[3-*O*-^{35}S]GlcNS6S3S standard. An aliquot of this material was then subjected to [2-AB] reducing end labeling and the resultant was resolved on PAMN (figure 43, panel B). As shown in figure 43, panel B, two major [^{35}S] labeled peaks were also observed that had elution times of 30 mins. and 50 mins. Peak 1 was concluded to be [^{35}S]sulfate as it had a similar elution time as shown in figure 43, panel A, while peak 3 with an elution time of 50

mins. was believed to be the ΔUA2S-[3-*O*-^{35}S]GlcNS6S3S-[2-AB] standard. These observations suggest that we can generated the [2-AB] labeled disaccharide standard and separate it from its non-labeled precursor.

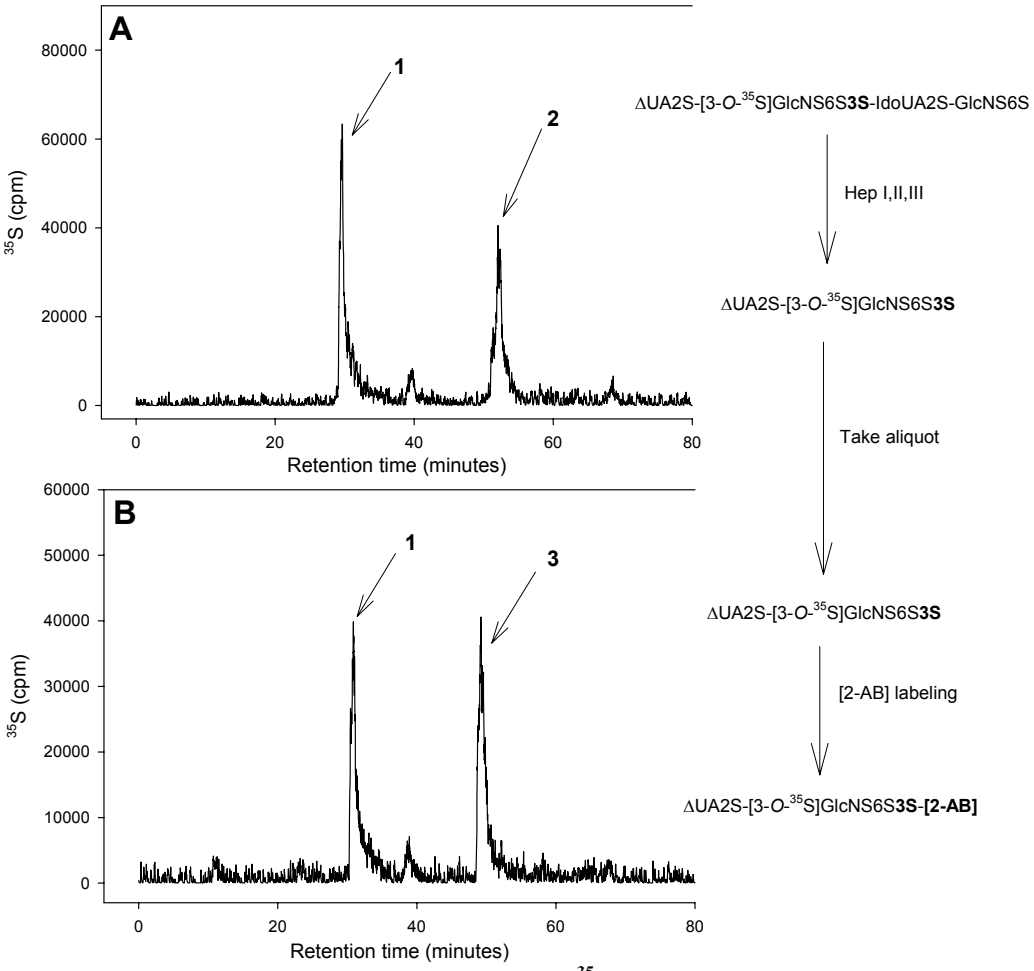

Figure 43. HPLC-PAMN chromatograms of ΔUA2S-[3-*O*-^{35}S]GlcNS6S3S and ΔUA2S-[3-*O*-^{35}S]GlcNS6S3S-[2-AB] standards. *Panel A*, the elution profile of the ΔUA2S-[3-*O*-^{35}S]GlcNS6S3S standard, which was generated by digesting the 3-*O*-[^{35}S]sulfated HP tetrasaccharide with a mixture of heparin lyases. *Panel B*, the elution profile of the ΔUA2S-[3-*O*-^{35}S]GlcNS6S3S-[2-AB] standard, which was generated by subjecting an aliquot of the resultant from *panel A* to [2-AB] reducing end labeling. *Arrow 1*, elution position of [^{35}S] free sulfate; *arrow 2*, elution position of ΔUA2S-[3-*O*-^{35}S]GlcNS6S3S; and *arrow 3*, elution position of ΔUA2S-[3-*O*-^{35}S]GlcNS6S3S-[2-AB]. The enzymatic and chemical modifications are shown next to the chromatograms.

Given the similarities observed in the retention times of peak 2 (figure 43, panel A) and peak 3 (figure 43, panel B), we chose to co-inject both standards (disaccharide B and C) to strengthen our hypothesis that the [2-AB] labeled disaccharide could be resolved from its

non-labeled precursor. The chromatograms are shown in figure 44. When equal amounts of the two [^{35}S] labeled disaccharide standards were co-injected onto the HPLC, we observed the presence of three major [^{35}S] labeled peaks (figure 44, panel A). Peak 1 is free [^{35}S]sulfate, a result of de-sulfation of the 3-*O*-[^{35}S]sulfated HP tetrasaccharide during the heparin lyases digestion, while peak 2 (48 mins.) was believed to be the unlabeled disaccharide, and peak 3 (44.5 mins.) was believed to be the [2-AB] labeled disaccharide. Due to the fact that peak 2 and peak 3 were eluted very close to each other, an additional experiment was necessary to further prove the conclusions.

To this end, the identity of peak 3 was further proven by co-injecting the two [^{35}S] labeled disaccharides at a different ratio on the HPLC. The chromatogram is shown in figure 44, panel B. When the two disaccharides were mixed at a ratio of 4:1, the relative intensities of peak 2 and peak 3 decreased and increased proportionately. The same three major [^{35}S] labeled peaks were observed, however it was clearly observed that the peak at 44.5 mins. was substantially lower in its intensity than the peak at 48 mins. This observation suggested that ΔUA2S-[3-*O*-^{35}S]GlcNS6S3S-[2-AB] and ΔUA2S-[3-*O*-^{35}S]GlcNS6S3S had elution positions of 44.5 mins. and 48 mins. respectively. Taken together, results here demonstrated that the two [^{35}S] labeled disaccharide standards (ΔUA2S-[3-*O*-^{35}S]GlcNS6S3S and ΔUA2S-[3-*O*-^{35}S]GlcNS6S3S-[2-AB]) could be generated and resolved using HPLC. Additionally, the results demonstrated that the [2-AB] reducing end labeling was successful with high coupling efficiency as evident by only a single [^{35}S] labeled peak in figure 43, panel B.

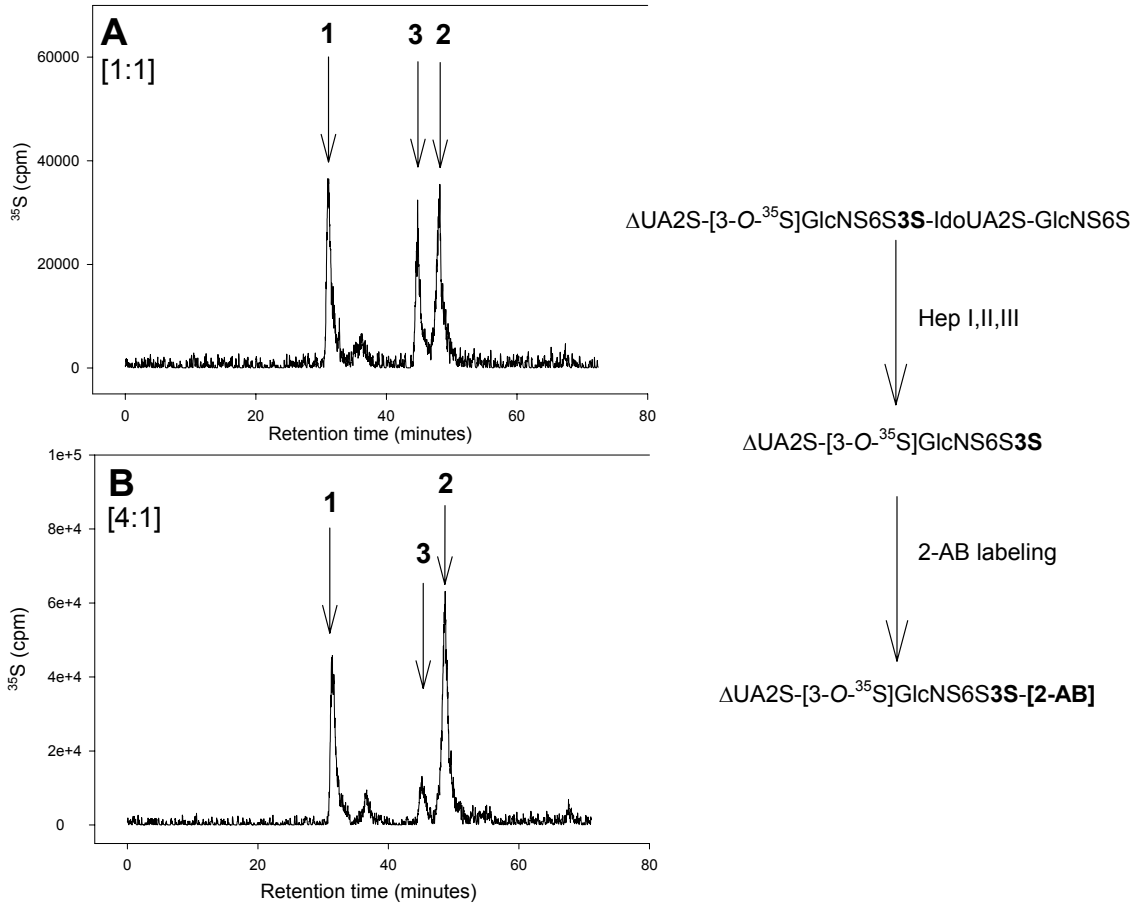

Figure 44. HPLC-PAMN chromatograms of ΔUA2S-[3-*O*-^{35}S]GlcNS6S3S and ΔUA2S-[3-*O*-^{35}S]GlcNS6S3S-[2-AB] standards (co-injected). Panels A and B show the chromatograms of ΔUA2S-[3-*O*-^{35}S]GlcNS6S3S vs. ΔUA2S-[3-*O*-^{35}S]GlcNS6S3S-[2-AB] at different ratios. *A* shows a 1:1 ratio respectively, while *B* shows a 4:1 ratio of the disaccharide standards respectively. HPLC-PAMN chromatography was performed as stated in "methods section". *Arrow 1*, elution position of [^{35}S] free sulfate; *arrow 2*, elution position of ΔUA2S-[3-*O*-^{35}S]GlcNS6S3S; *arrow 3*, elution position of ΔUA2S-[3-*O*-^{35}S]GlcNS6S3S-[2-AB]. The enzymatic and chemical modification reactions are illustrated to the right of the PAMN chromatograms.

Determination of whether residue 8 is the 3-O-sulfation site

To determine whether the 3-*O*-[^{35}S]sulfo group was present on residue 8, the approach as described in figure 41 was carried out. The 3-*O*-[^{35}S]sulfated HP octasaccharide was subjected to [2-AB] reducing end labeling. It is important to note here that the [2-AB] labeling of HP disaccharides (shown above) and of the HP tetrasaccharide (data not shown) proceeded with high coupling efficiency. This provided sufficient evidence to suggest that the [2-AB] labeling of the 3-*O*-[^{35}S]sulfated HP octasaccharide would proceed with the same

effectiveness. The [2-AB] labeled 3-*O*-[^{35}S]sulfated HP octasaccharide was then subjected to a mixture of heparin lyases and the resultant materials were subjected to disaccharide analysis on HPLC with the elution profile shown in figure 45. There were four categories of [^{35}S] labeled peaks observed. Peak 1 eluted at 30 mins. was concluded to be free [^{35}S]sulfate which was a result of de-sulfation of the 3-*O*-[^{35}S]sulfated HP octasaccharide-[2-AB] during the heparin lyases digestion. Peak 2 eluted at 57 mins. was hypothesized to be ΔUA2S-[3-*O*-^{35}S]GlcNS6S3S. The cluster of peaks labeled peak 3 eluted from 69 mins. to 73 mins. was determined to be unknown as no standards were demonstrated to have a similar elution position. Peak 4 eluted at 85 mins. was hypothesized to be a [^{35}S]sulfated HP tetrasaccharide that was less susceptible to heparin lyases digestion. The identity of peak 4 was investigated and described in the following section. However, at this point our concern was the correct identification of the [^{35}S] labeled disaccharide product (peak 2). Given the observation that the [2-AB] disaccharide eluted very close to the unlabeled disaccharide as shown in figure 44, an additional experiment was needed to increase our confidence in the assessment that peak 2 was ΔUA2S-[3-*O*-^{35}S]GlcNS6S3S.

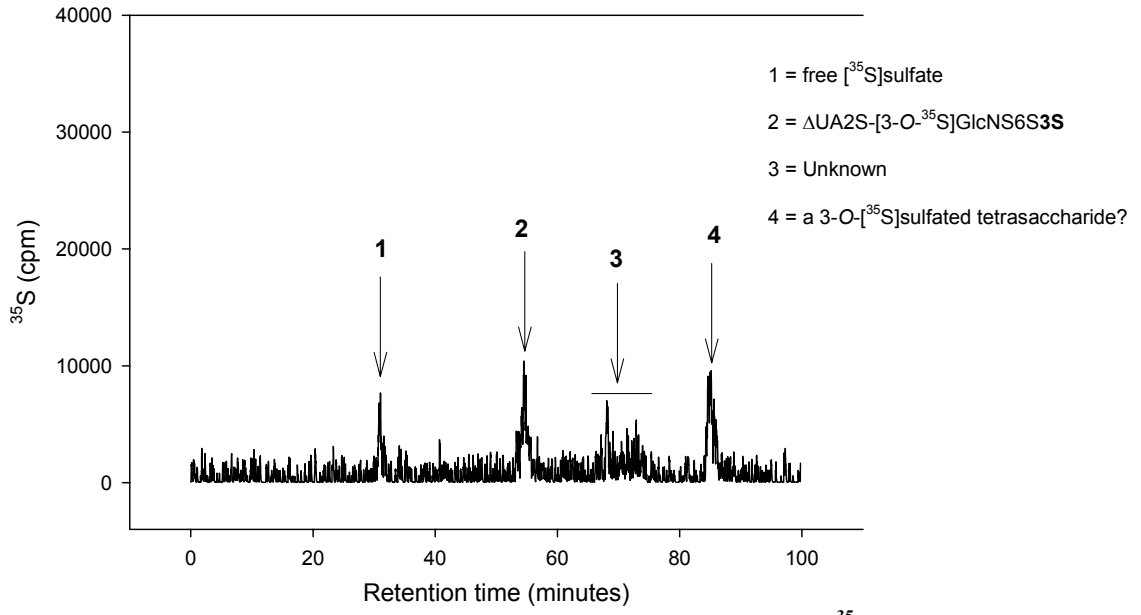

Figure 45. HPLC-PAMN chromatogram of heparin lyases digested 3-*O*-[^{35}S]sulfated HP octasaccharide-[2-AB]. The 3-*O*-[^{35}S]sulfated HP octasaccharide-[2-AB] was digested with a mixture of heparin lyases. The resultant material was subjected to analysis on the PAMN column. The elution conditions are described in the "methods" section. *Arrow 1*, elution position of [^{35}S] free sulfate; *arrow 2*, elution position of ΔUA2S-[3-*O*-^{35}S]GlcNS6S3S; *arrow 3*, elution position of unknown material; and *arrow 4*, elution position of a 3-*O*-[^{35}S]sulfated tetrasaccharide?

As a result, an identical amount of the digestion was co-injected with the ΔUA2S-[3-*O*-^{35}S]GlcNS6S3S standard and the HPLC elution profile is shown in figure 46. It was observed that the peak at 55 mins. (figure 46, peak 2) greatly increased in its intensity with the addition of the ΔUA2S-[3-*O*-^{35}S]GlcNS6S3S standard, while the intensities of peak 3 (cluster of peaks from 69 mins. to 73 mins.) and 4 (85 mins.) remained constant. The co-elution of the ΔUA2S-[3-*O*-^{35}S]GlcNS6S3S standard with peak 2 (figure 46) suggested that this peak has the same structure and is not [2-AB] labeled. These observations suggested that the [^{35}S] labeled disaccharide product that was released upon heparin lyases digestion of the 3-*O*-[^{35}S]sulfated HP octasaccharide-[2-AB] did not originate from the reducing end. These results suggest that the reducing end glucosamine (residue 8) does not carry a 3-*O*-[^{35}S]sulfo group.

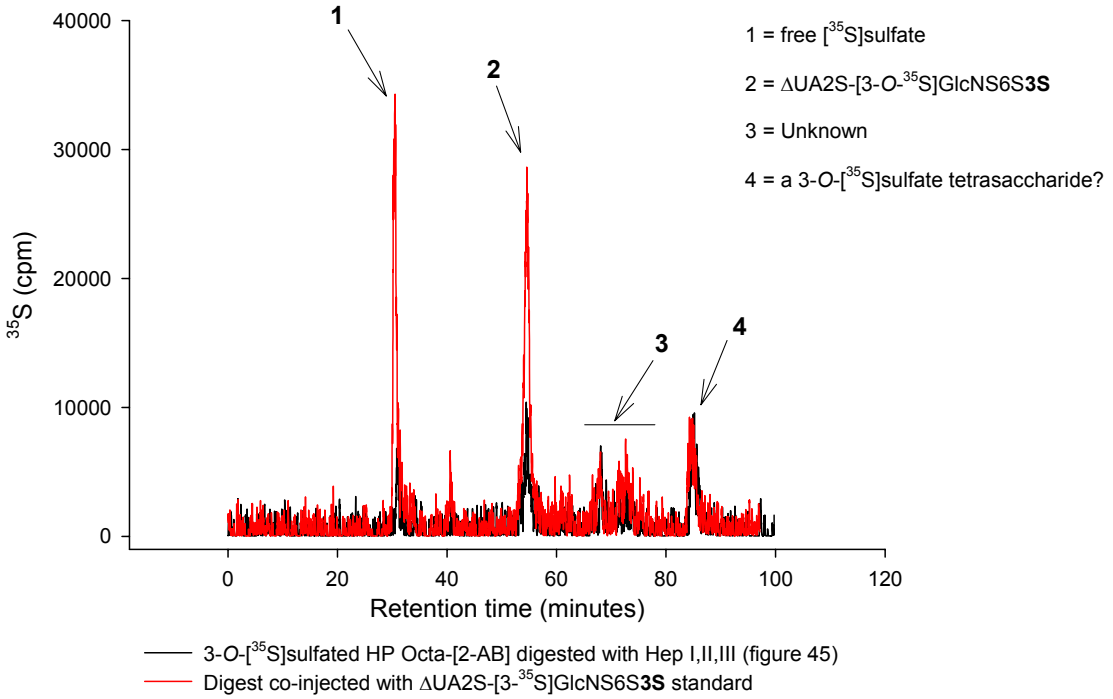

Figure 46. HPLC-PAMN chromatogram of heparin lyases digested 3-*O*-[^{35}S]sulfated HP octasaccharide-[2-AB] spiked with ΔUA2S-[3-*O*-^{35}S]GlcNS6S3S standard. Digested material from figure 45 was spiked with the ΔUA2S-[3-*O*-^{35}S]GlcNS6S3S standard (*red line*). The elution conditions are described in "methods" section. Data from figure 45 is overlaid (*black line*). *Arrow 1*, elution position of [^{35}S] free sulfate; *arrow 2*, elution position of ΔUA2S-[3-*O*-^{35}S]GlcNS6S3S; *arrow 3*, elution position of unknown material; and *arrow 4*, elution position of a 3-*O*-[^{35}S]sulfated tetrasaccharide?

Internal analysis

The results obtained from non-reducing and reducing end analysis of the 3-*O*-[^{35}S]sulfated HP octasaccharide as described above demonstrated that the 3-*O*-[^{35}S]sulfo group was not on the glucosamine located at residue 2 or residue 8. We decided to determine if the 3-*O*-[^{35}S]sulfo group was on residue 6 by converting the 3-*O*-sulfated HP octasaccharide-[2-AB] to a tetrasaccharide. The result from the heparin lyases digestion of the 3-*O*-[^{35}S]sulfated HP octasaccharide-[2-AB] suggested that the identification of residue 6 as the 3-*O*-sulfation site was feasible because the digestion yielded a tetrasaccharide as shown in figure 45.

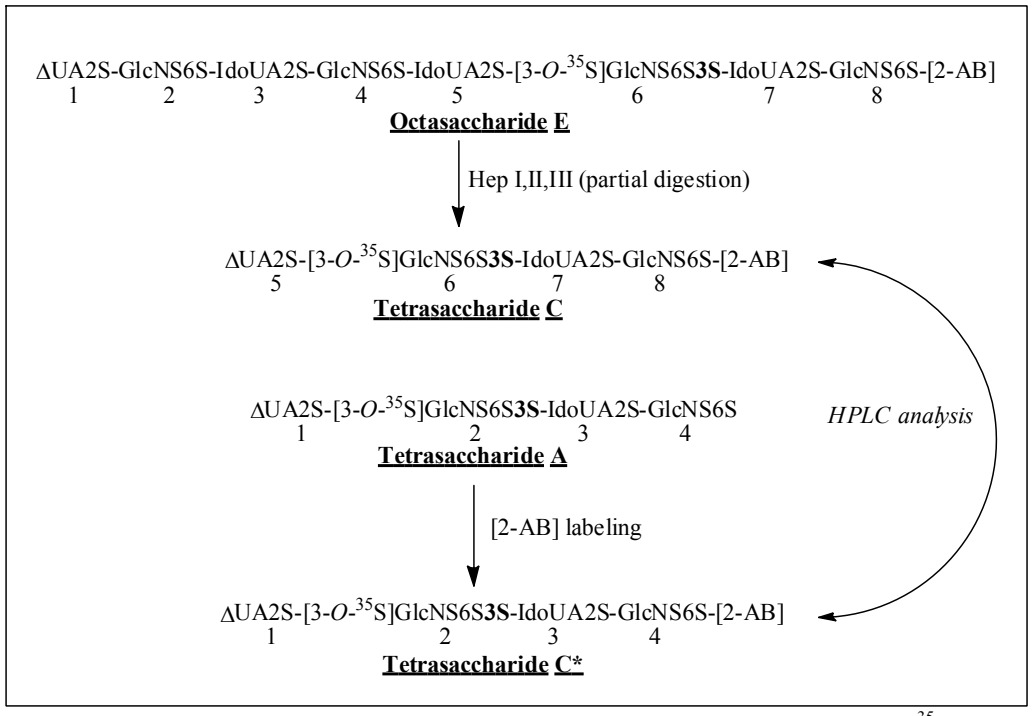

Figure 47. Strategy for the determination of reside 6 as the 3-*O*-sulfation site. The 3-*O*-[^{35}S]sulfated HP octasaccharide-[2-AB] (octasaccharide E) is converted into tetrasaccharide C by partial digestion from incubation with a mixture of heparin lyases. Tetrasaccharide C* standard is generated by 2-AB reducing end labeling of tetrasaccharide A. If tetrasaccharides C and C* co-elute, then residue 6 would carry the 3-*O*-[^{35}S]sulfo group.

Figure 47 describes the steps necessary to determine whether residue 6 carries the 3-*O*-[^{35}S]sulfo group. First, the [2-AB] labeled octasaccharide (figure 47, octasaccharide E) is converted to a [2-AB] labeled tetrasaccharide (figure 47, tetrasaccharide C) by partial digestion with a mixture of heparin lyases. Second, a [2-AB] labeled 3-*O*-[^{35}S]sulfated tetrasaccharide standard (figure 47, tetrasaccharide C*) is generated by [2-AB] labeling tetrasaccharide A. If tetrasaccharides C and C* co-elute on the PAMN column it would suggest that they are structurally identical, considering the fact that the 3-*O*-[^{35}S]sulfo group is not present on residue 8. This would suggest that residue 6 carries the 3-*O*-[^{35}S]sulfo group. To this end, tetrasaccharide C* was generated and determined whether it could be resolved from tetrasaccharide A using PAMN chromatography.

Preparation of the 3-O-[^{35}S]sulfated HP tetrasaccharide-[2-AB] standard

Tetrasaccharide A standard was prepared by incubating the HP tetrasaccharide substrate with purified 3-OST-3 in the presence of [^{35}S]PAPS. Under this condition a tetrasaccharide with a structure of ΔUA2S-[3-*O*-^{35}S]GlcNS6S3S-IdoUA2S-GlcNS6S will be generated (121). As expected, tetrasaccharide A was observed to migrate as a single [^{35}S] labeled peak at 86 mins. as shown in figure 48, panel A. This suggested that tetrasaccharide A was radioactively pure.

To prepare the tetrasaccharide C* standard, tetrasaccharide A was incubated with 2-aminobenzamide and reduced with sodium cyanoborohydride. The product was analyzed by PAMN chromatography (figure 48, panel B). A [^{35}S] labeled peak was observed at 89 mins. which was believed to be tetrasaccharide C*, and a minor [^{35}S] labeled peak that eluted at 74 mins. was observed of which the identity was unknown. Due to their close elution times, we could not confidently conclude that tetrasaccharides A and C* were separated by this method. As a result, tetrasaccharides A and C* were co-injected on the PAMN column and the chromatogram is shown in figure 48, panel C. This revealed two [^{35}S] labeled peaks at 82 mins. and 85 mins. that correlated to tetrasaccharides A and C* respectively, while the cluster of [^{35}S] labeled peaks from 71 mins to 74 mins was unknown but thought to be due to some de-sulfation during the [2-AB] labeling process. These observations suggested that both tetrasaccharides A and C* could be resolved using PAMN chromatography, which was later used to prove that 3-*O*-[^{35}S]sulfo group was indeed on residue 6.

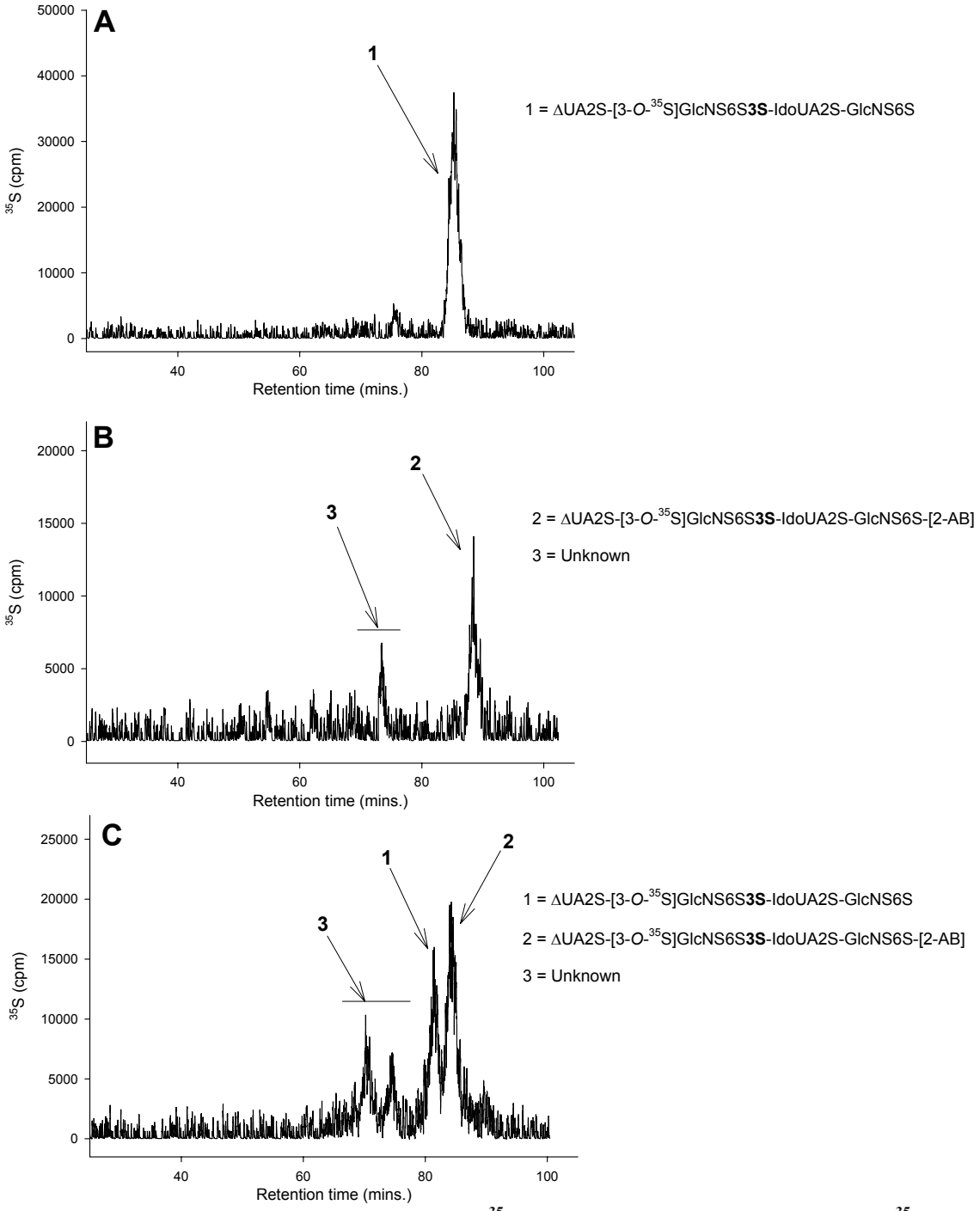

Figure 48. HPLC-PAMN chromatograms of 3-*O*-[^{35}S]sulfated HP tetrasaccharide and 3-*O*-[^{35}S]sulfated HP tetrasaccharide-[2-AB] standards. The [^{35}S] labeled material was eluted using a linear KH_2PO_4 gradient. The elution conditions are presented in the "methods" section. *Panel A* shows the elution profile of the 3-*O*-[^{35}S]sulfated HP tetrasaccharide standard (15,000 cpm), while *panel B* shows the elution profile of 3-*O*-[^{35}S]sulfated HP tetrasaccharide-[2-AB] standard (10,000 cpm). Panel C shows the elution profile of the 3-*O*-[^{35}S]sulfated HP tetrasaccharide-[2-AB] (15,000 cpm) spiked with the non-[2-AB] labeled precursor (5,000 cpm). *Arrow 1*, represents ΔUA2S-[3-*O*-^{35}S]GlcNS6S3S-IdoUA2S-GlcNS6S; *arrow 2*, represents ΔUA2S-[3-*O*-^{35}S]GlcNS6S3S-IdoUA2S-GlcNS6S-[2-AB]; and *arrow 3*, represents an undetermined species.

Determination of residue 6 as the 3-O-sulfation site

To determine whether peak 4 (figure 45) had a structure that was identical to tetrasaccharide C*, octasaccharide E (figure 47) was partially digested with a mixture of heparan lyases. The digested material was analyzed on the PAMN column (figure 49). A partial digest was observed as evident by the present of four [^{35}S] labeled peaks. The chromatogram that resulted was identical to what is shown in figure 45. Here the idea was to determine whether peak 4 was structurally similar to either tetrasaccharide A or C* shown in figure 47.

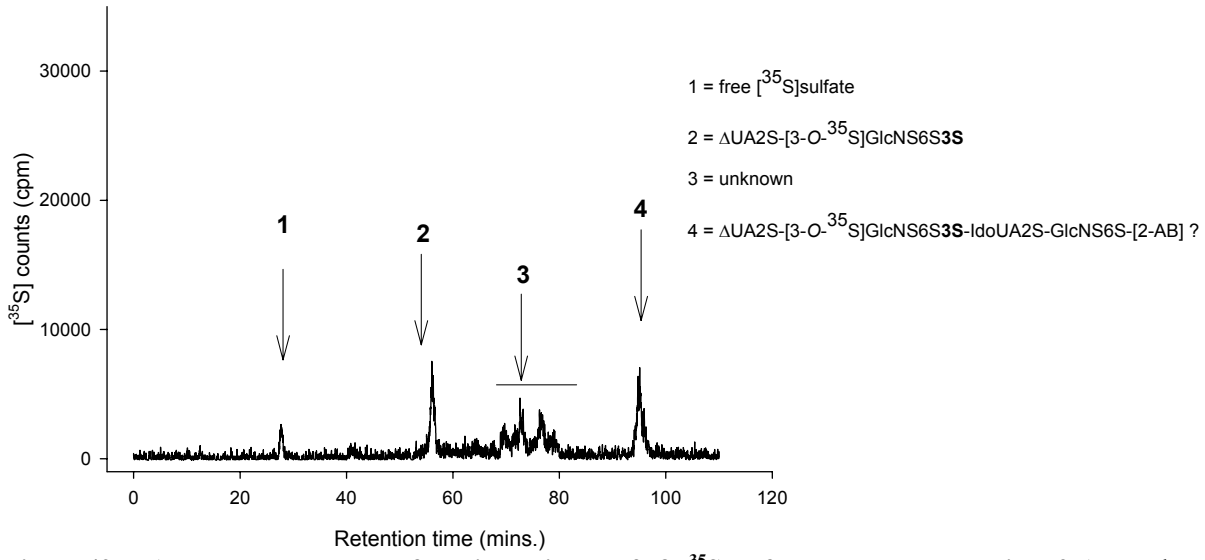

Figure 49. PAMN chromatogram of partially digested 3-*O*-[^{35}S]sulfated HP octasaccharide-[2-AB]. The [^{35}] labeled material was eluted using a linear KH_2PO_4 gradient. The elution conditions are presented in the "methods" section. Approximately 15,000 cpm of the partially digested 3-*O*-[^{35}S]sulfated HP octasaccharide-[2-AB] was subjected to PAMN chromatography. *Arrow 1*, represents free [^{35}S]sulfate; *arrow 2*, represents UA2S-[3-*O*-^{35}S]GlcNS6S3S; *arrow 3*, represents an undetermined species; and *arrow 4*, represents 3-*O*-[^{35}S]sulfated HP tetrasaccharide-[2-AB].

To determine whether peak 4, which resulted from the partial heparin lyase digestion of octasaccharide E, had a similar structure as either tetrasaccharide A or C* a co-injection was conducted. An identical amount of the digest (from figure 49) was co-injected on the PAMN column with the tetrasaccharide A standard. The chromatogram is shown in figure

50 (blue line, panel A). The same four [^{35}S] labeled peaks were observed as in figure 49. However, as a result of the co-injection of the tetrasaccharide A standard, one additional [^{35}S] labeled peak was observed that had an elution time of 90 mins. (figure 50, peak 5). This was concluded to be the elution time of tetrasaccharide A. The observance of this additional [^{35}S] labeled peak suggested that what resulted from the partial digestion of octasaccharide E (peak 4) is not structurally similar to tetrasaccharide A. In a similar manner, tetrasaccharide C* was co-injected on the PAMN column with an identical amount of the partially digested octasaccharide E. The chromatogram is shown in figure 50 (red line, panel B). The chromatogram showed the presence of four [^{35}S] labeled peaks. A noticeable increase was observed in the intensity and area of peak 4 (97 mins.). This observation along with the absence of any additional [^{35}S] labeled peaks suggested that the tetrasaccharide C* (see figure 47) had an elution time similar to that of peak 4. As a result, peak 4 was considered structurally identical to tetrasaccharide C*. Additionally, it is important to note here that peak 4 that resulted from the partial digestion of octasaccharide E, shown in figure 49, eluted at a similar position as tetrasaccharide C* on a P-10 size exclusion column (data not shown) which further suggested that it was indeed a 3-*O*-[^{35}S]sulfated tetrasaccharide that carried the [2-AB] label.

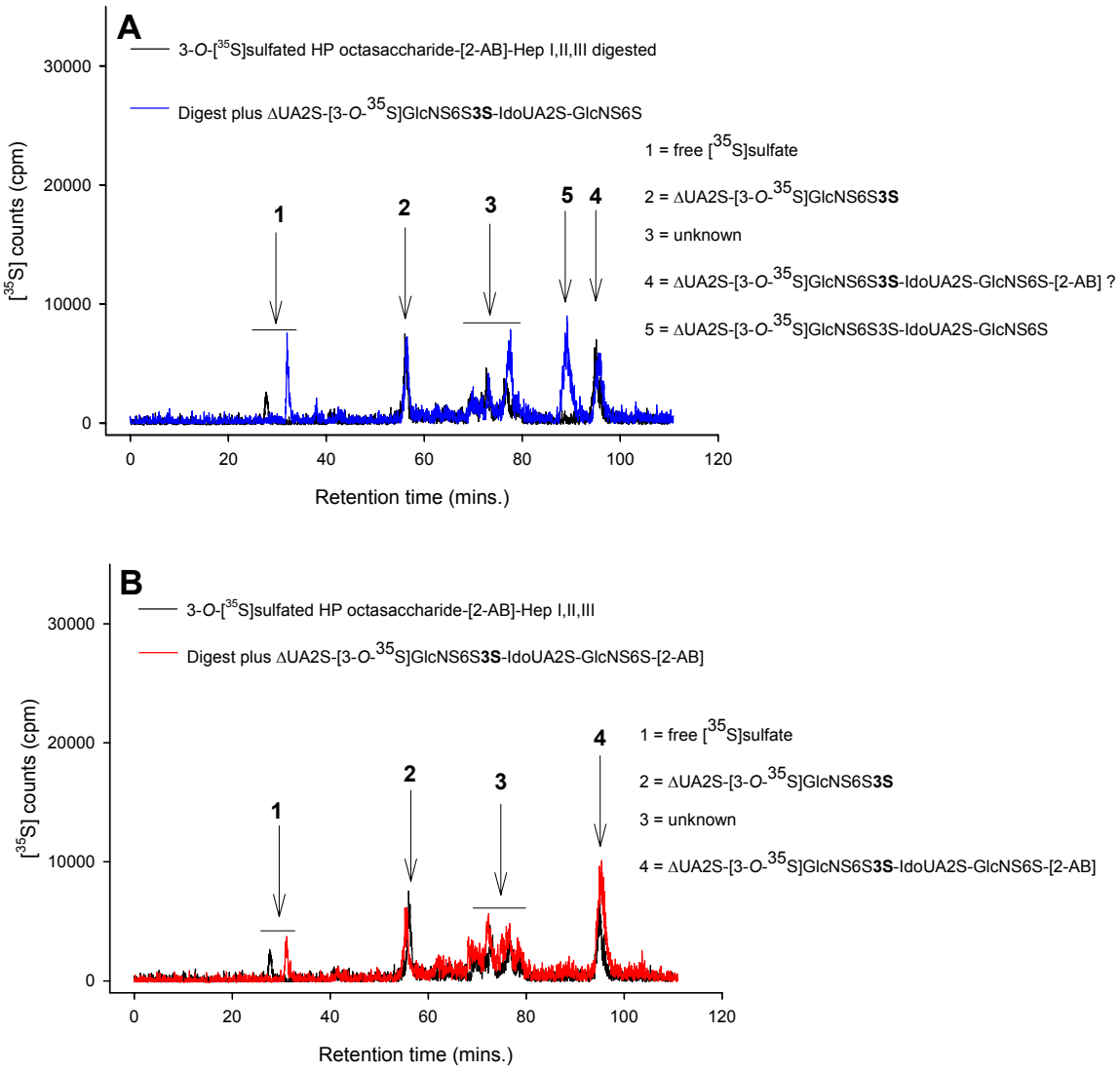

Figure 50. PAMN chromatogram of partially digested 3-*O*-[^{35}S]sulfated HP octasaccharide-[2-AB] spiked with [^{35}S]sulfated HP tetrasaccharide standards. The [^{35}] labeled material was eluted using a linear KH_2PO_4 gradient. The elution conditions are presented in the "methods" section. *Panel A* shows the chromatogram that resulted from co-injection with 3-*O*-sulfated HP tetrasaccharide standard (15,000 cpm) (*blue line*). P*anel B* shows shows the chromatogram that resulted from co-injection with 3-*O*-sulfated HP tetrasaccharide-[2-AB] standard (30,000 cpm) (*red line*). *Arrow 1*, represents free [^{35}S]sulfate, *arrow 2*, represents ΔUA2S-[3-*O*-^{35}S]GlcNS6S3S, *arrow 3,* represent unknown species, *arrow 4,* represents ΔUA2S-[3-*O*-^{35}S]GlcNS6S3S-IdoUA2S-GlcNS6S-[2-AB], and *arrow 5*, represents ΔUA2S-[3-*O*-^{35}S]GlcNS6S3S-IdoUA2S-GlcNS6S. The *black line* in each panel shows the elution profile as shown in figure 49.

These observations suggests that the parital digestion of octasaccharide E results in a 3-*O*-[^{35}S]sulfated tetrasaccharide that carries a [2-AB] label. The presence of the [2-AB] suggested that it originated from the reducing end of the octasaccharide. As a result, these

observations demonstrate that the glucosamine at position 6 carried the 3-*O*-[^{35}S]sulfo group, considering position 8 had been previously excluded. This results in an octasaccharide sequence of ΔUA2S-GlcNS6S-IdoUA2S-GlcNS6S-IdoUA2S-[3-*O*-^{35}S]GlcNS6S3S-IdoUA2S-GlcNS6S. The confirmation of residue 6 excluded residue 4 as being the site for 3-*O*-sulfation. If residue 4 did carry the 3-*O*-[^{35}S]sulfo group, partial heparin lyases digestion of the 3-*O*-[^{35}S]sulfated HP octasaccharide-[2-AB] would have resulted in a hexasaccharide carrying both [^{35}S]sulfo and [2-AB] labels. This would have a very different retention time on the HPLC from that of tetrasaccharide C*.

In summary, we conducted non-reducing, reducing end, and internal sequence analysis to prove the structure of the 3-*O*-[^{35}S]sulfated HP octasaccharide. The results obtained from non-reducing end analysis demonstrated that residue 2 did not carry the 3-*O*-[^{35}S]sulfo group. Likewise the results obtained from reducing end analysis demonstrated that residue 8 did not carry the 3-*O*-[^{35}S]sulfo group. The internal analysis of the 3-*O*-[^{35}S]sulfated HP octasaccharide-[2-AB] suggested that residue 6 did carry the 3-*O*-[^{35}S]sulfo group. Because this 3-*O*-sulfated HP octasaccharide can be prepared with by one step 3-OST-3 modification of a HP octasaccharide substrate we could synthesize relatively large amounts of material to test its antiviral activity in a cell based assay. The next section describes the procedure for the synthesis of several hundred micrograms of this 3-*O*-sulfated HP octasaccharide.

Scale up preparation of the gD binding 3-O-sulfated HP octasaccharide

The key step for the synthesis of hundreds of micrograms of the 3-*O*-sulfated HP octasaccharide was the coupling of the 3-OST-3 modification with a PAPS regeneration

system. The advantage of using the PAPS regeneration system in this study was to utilize 3-OST-3 more effectively by continuously removing PAP which is a product inhibitor of 3-OST-3. Additionally, the expense of the synthesis would be significantly reduced because a low cost sulfo donor was used. Although the latter consideration would be beneficial for commercial scale synthesis, it is beyond the scope of this thesis.

The PAPS regeneration system, discovered by Professor Chi-Huey Wong, was initially coupled with *Rhizobium* Nod factor sulfotransferase (NodST) for the enzymatic synthesis of *N*,*N*'-diacetylchitobiose 6-sulfate (199). In this study, the coupling of the PAPS regeneration system with 3-OST-3 modification requires two enzymes: aryl sulfotransferase-IV (AST-IV) and 3-OST-3 as shown in figure 51. This system can be considered a two-step process that continues for multiple rounds. Step one utilizes the reverse activity of AST-IV. Namely, AST-IV transfers the sulfo group from *p*-nitrophenyl sulfate (PNPS) to PAP, to generate PAPS (200). Step two is the 3-OST-3 modification. The 3-OST-3 enzyme transfers the sulfo group from PAPS that is generated by AST-IV to the HP octasaccharide substrate. During the 3-OST-3 modification, PAP is formed which could inhibit the activity of 3-OST-3. However this is not a concern in this system because PAP is converted back to PAPS by AST-IV. Therefore, the overall net reaction was the transfer of the sulfo group from PNPS to the HP octasaccharide to form the 3-*O*-sulfated HP octasaccharide.

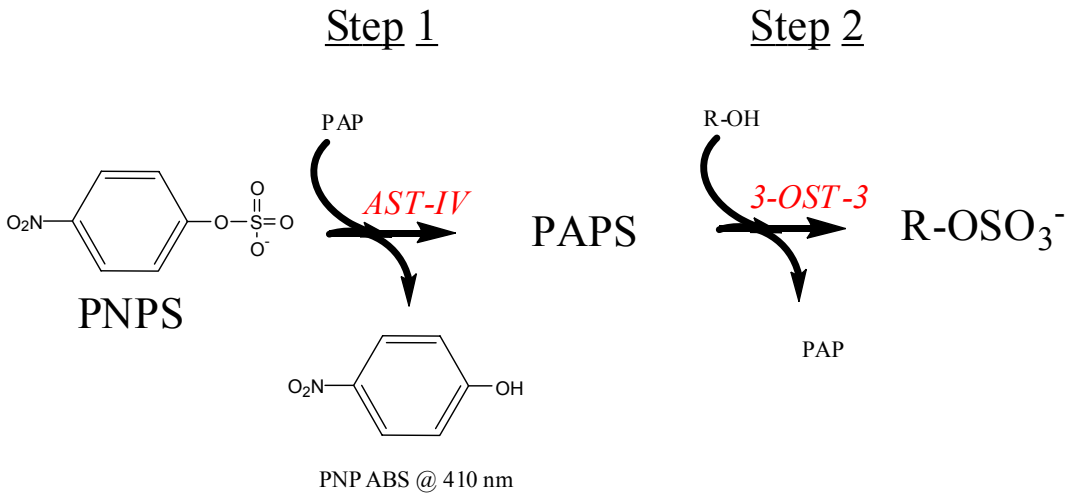

Figure 51. PAPS regeneration system with *p*-nitrophenyl sulfate (PNPS), aryl sulfotransferase (AST-IV) and 3-OST-3 to generate 3-*O*-sulfated HP octasaccharide. Step 1: AST IV transfers the sulfo from PNPS (in excess) to PAP to generate PAPS and the release of PNP (*p*-nitrophenol). Step 2: 3-OST-3 then transfers the sulfo group from PAPS to the 3-OH position of the waiting HP octasaccharide (R-OH), to generate 3-*O*-sulfated HP octasaccharide ($R\text{-}OSO_3^-$). The PAP generated in step 2 is processed again by AST-IV, and PAPS is regenerated to allow for subsequent cycles to occur.

To monitor whether the 3-OST-3 modification coupled with the PAPS regeneration system, the amount PNP generated from the reaction was monitored. This was done by measuring the concentration of PNP at 410 nm. The reaction was initiated by incubating AST-IV, 3-OST-3, PAP, and PNPS at room temperature (without HP octasaccharide substrate). The O.D. value (410 nm) reached a plateau after 15 minutes suggesting that the conversion of PNPS to PNP that is catalyzed by AST-IV reached equilibrium. At this point the HP octasaccharide substrate was added and the continued increase of the value of O.D. (410 nm) was observed (data not shown). This suggests that the transfer of the sulfo group to the HP octasaccharide pulled the equilibrium to PNP production. After overnight incubation, the 3-*O*-sulfated HP octasaccharide was purified by DEAE chromatography. The products were analyzed HPLC as described below.

Approximately 200 µg of HP octasaccharide substrate was processed using this reaction system. The purity of the resultant 3-*O*-sulfated HP octasaccharide was determined by monitoring the absorbance at 232 nm. The elution position of the product was determine

by using 3-*O*-[^{35}S]sulfated HP octasaccharide prepared as describe above. The HPLC profile is shown in figure 52.

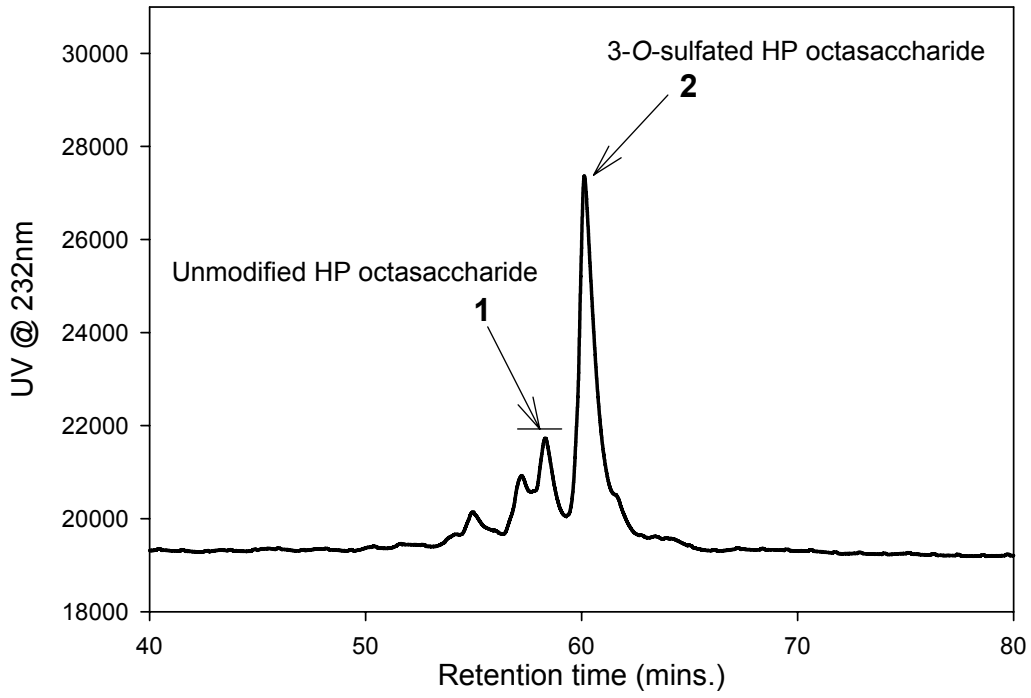

Figure 52. DEAE-NPR chromatography analysis of the 3-*O*-sulfated HP octasaccharide. An aliquot from the PAPS regeneration product was subjected to HPLC, with elution conditions described in "methods" section. *Peak 1* represents the unmodified HP octasaccharide, and *peak 2* represent the 3-*O*-sulfated HP octasaccharide.

The UV peak that was eluted at 61 mins. (peak 2) co-migrated with the 3-*O*-[^{35}S]sulfated HP octasaccharide suggesting the it has the structure of ΔUA2S-GlcNS6S-IdoUA2S-GlcNS6S-IdoUA2S-GlcNS6S3S-IdoUA2S-GlcNS6S. The UV peak that eluted at 57 mins. (peak 1) co-eluted with the unmodified HP octasaccharide suggesting this is the starting material due the incomplete modification. Based on relative peak areas, it was estimated that the 3-*O*-sulfated HP octasaccharide was 80% pure. To estimate the amount of the product, a quantitative HPLC analysis was conducted using the starting material as a standard. It was estimated that approximately 130 μg of the 3-*O*-sulfated HP octasaccharide was generated and recovered. This material has been given to Dr. Shukla (UIC), whom is

currently conducting cell based assays to investigate its efficacy an inhibiting viral fusion. Results obtained will determine whether disrupting gD binding to its polysaccharide cellular receptor is a viable approach to inhibit HSV infections.

Mass Spectrometry analysis of Arixtra®

We next determined the molecular mass of the standard compound Arixtra® using electrospray ionization mass spectrometry (ESI-MS). This experiment was conducted primarily to optimize the mass spectrometry conditions. A high degree of de-sulfation of the sample was observed when high voltage and temperature was used during analysis (data not shown). During optimization, it was observed that the degree of de-sulfation of the sample could be decreased by substantially lowering the voltage and temperature. Eventhough the presence of some de-sulfation was observed at the optimized conditions, data obtained allowed for the correct determination of the sample as shown in figure 53. The sample showed four prominent molecular ion peaks. These were $[M-3H]^{3-}$ at 501.3 m/z (M_r = 1506.9 Da), $[M-6H+3Na]^{3-}$ at 523.9 m/z (M_r = 1508.7 Da), $[M-5H+3Na]^{2-}$ at 786.4 m/z (M_r = 1505.8 Da), and $[M-2H]^{2-}$ at 752.4 m/z (M_r = 1506.8 Da). From this data the molecular weight of the standard compound Arixtra®, was determined to be 1507.1 ± 1.0 Da which is close to the known molecular mass of Arixtra® which is 1506.9 Da. As a result of this data, it was hypothesized that under the optimized conditions the determination of the molecular masses of the unmodified HP octasaccharide and the 3-*O*-sulfated HP octasaccharide were possible.

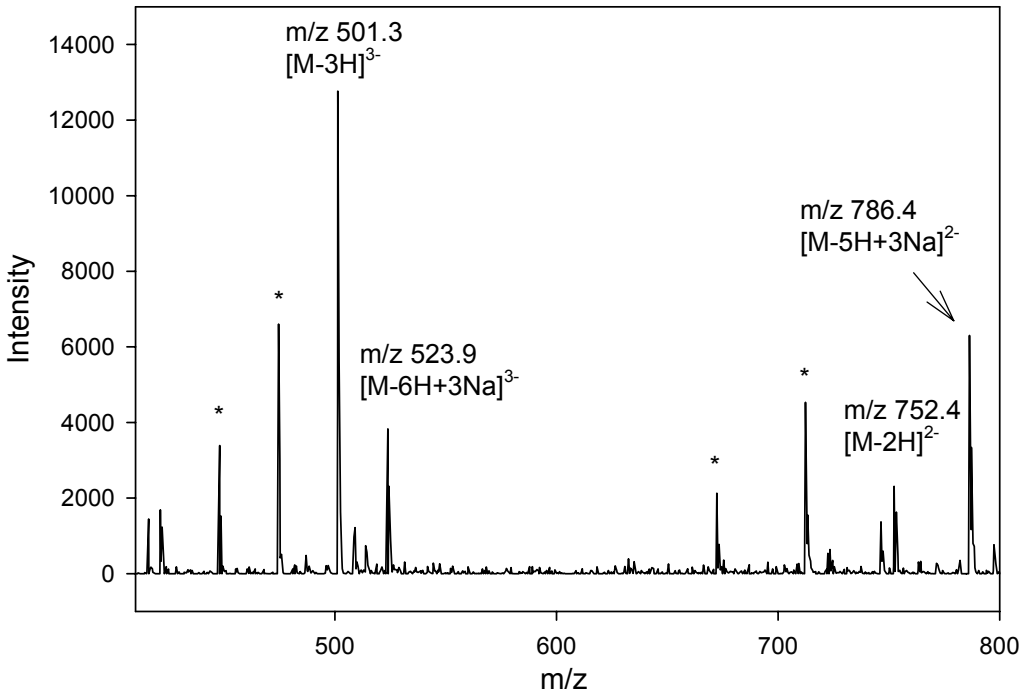

Figure 53. Electrospray ionization mass spectrum of Arixtra®. Arixtra (100 μM) contained in 70% acetonitrile and 10 μM imidazole was introduced by direct infusion (10 μl/min) into the mass spectrometer. The expected ions are indicated, where "Na" represents a sodium adduct. Asterisk (*) represents signals that result from de-sulfation of Arixtra®.

Mass Spectrometry analysis of the unmodified HP octasaccharide

The unmodified HP octasaccharide had its mass determined using ESI-MS under the optimized conditions and the resulting spectrum is shown in figure 54. The sample showed two prominent molecular ion peaks. These were $[M-7H+2Na]^{5-}$ at 469.3 m/z (M_r = 2307.5 Da) and $[M-5H+Na]^{4-}$ at 580.3 m/z (M_r = 2303.2 Da). From this data the molecular mass of the unmodified HP octasaccharide was determined to be 2305.4 ± 2.15 Da which is close to the anticipated molecular mass of the unmodified HP octasaccharide (M_r = 2306.9 Da) with a structure as shown in figure 29, panel C. At this point the number of 3-*O*-sulfo groups transferred to the unmodified HP octasaccharide substrate is unknown. However by comparing the mass spectrums of the

unmodified HP octasaccharide and the 3-*O*-sulfated HP octasaccharide the number of 3-*O*-sulfo groups can be determined. To the end, the 3-*O*-sulfated HP octasaccharide had its molecular mass determined using ESI-MS.

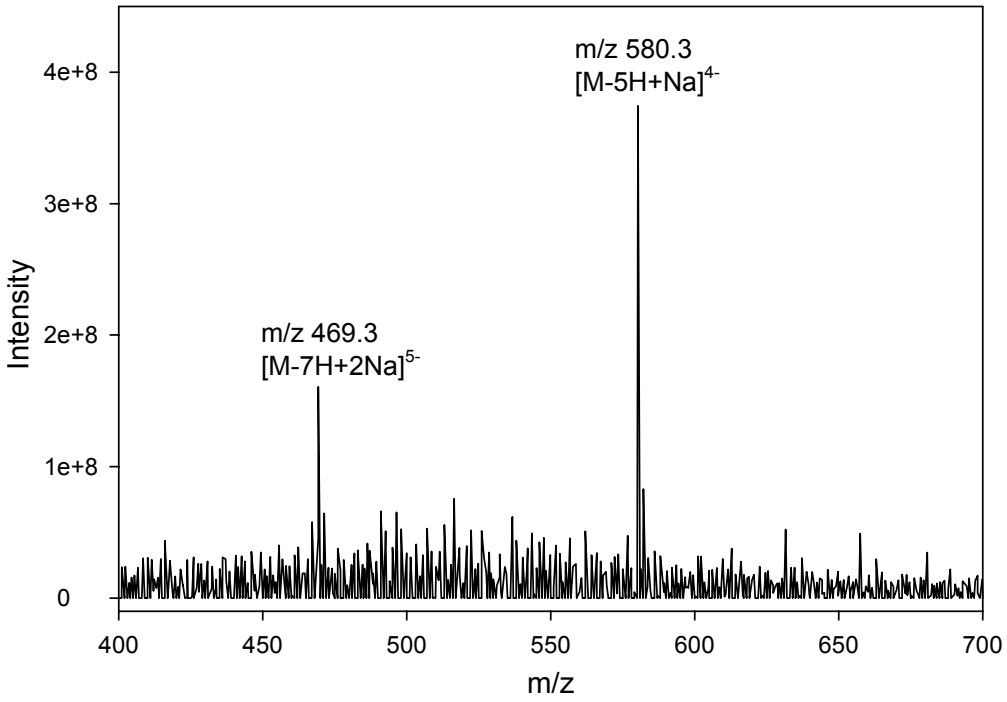

Figure 54. Electrospray ionization mass spectrum of the unmodified HP octasaccharide. The unmodified HP octasaccharide (10 μM) contained in 70% acetonitrile and 10 μM imidazole was introduced by direct infusion (10 μl/min) into the mass spectrometer. The expected ions are indicated, where "Na" represents a sodium adduct.

Mass Spectrometry analysis of the 3-O-sulfated HP octasaccharide

Results obtained from structural characterization experiments presented above, suggest that 3-OST-3 transfers one 3-*O*-sulfo group to the unmodified HP octasaccharide substrate. This result was further strengthen as the purified 3-*O*-sulfated HP octasaccharide had its molecular mass determined using ESI-MS. The mass spectrum of the 3-*O*-sulfated HP octasaccharide is shown in figure 55. The sample showed three prominent molecular ion peaks. These were $[M-8H]^{8-}$ at 297 m/z (M_r = 2384.0 Da), $[M-13H+5Na]^{8-}$ at 311 m/z (M_r =

2386.1 Da), and $[M-16H+7Na+Imid]^{8-}$ at 325.1 m/z (M_r = 2387.9 Da). From this data the molecular weight of the 3-*O*-sulfated HP octasaccharide was determined to be 2386.0 ± 1.6 Da which is close to the anticipated molecular mass of a HP octasaccharide that carries one 3-*O*-sulfo group (2386.8 Da)

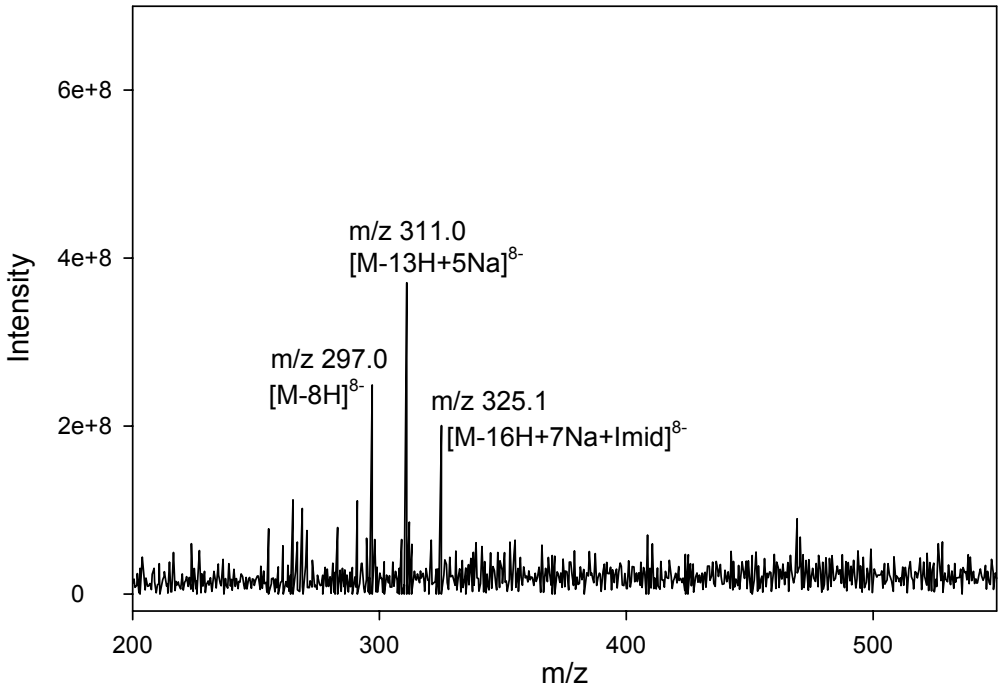

Figure 55. Electrospray ionization mass spectrum of the 3-*O*-sulfated HP octasaccharide. The 3-*O*-sulfated HP octasaccharide (20 μM) contained in 70% acetonitrile and 10 μM imidazole was introduced by direct infusion (10 μl/min) into the mass spectrometer. The expected ions are indicated. "Na" and "Imid" represents sodium and imidazole adducts respectively.

Conclusions

HS has been implicated in the infection mechanism of numerous viruses that affect humans (3, 162-165). Specifically, HS has been shown to assist in the viral infection mechanism for HSV-1, at both the viral attachment and viral fusion stages of infection via interactions for viral envelope glycoproteins (130, 175, 201). Due to the structural diversity contained with HS sequences, the functional relationships between specific saccharide

sequences and their ability to promote HSV infections remain largely unknown, as it is extremely difficult to obtain sufficient quantities of a homogenous HS sequence.

In the present chapter, we determined that incubating the HP octasaccharide with purified 3-OST-3 in the presence of [^{35}S]PAPS resulted in a gD binding 3-*O*-[^{35}S]sulfated HP octasaccharide that was 80% pure in terms of radioactivity. This was found to be sufficient enough to complete is structural characterization as we set to determine which glucosamine residue that carried the 3-*O*-[^{35}S]sulfo group. Results obtained from non-reducing end analysis demonstrated that residue 2 did not carry of the 3-*O*-[^{35}S]sulfo group. Results obtained from reducing end analysis revealed that residue 8 did not carry the 3-*O*-[^{35}S]sulfo group. Internal sequencing analysis demonstrated that 3-OST-3 transfers a 3-*O*-[^{35}S]sulfo group to the glucosamine located at residue 6 within the unmodified HP octasaccharide, resulting in a sequence of ΔUA2S-GlcNS6S-IdoUA2S-GlcNS6S-IdoUA2S-GlcNS6S<u>3S</u>-IdoUA2S-GlcNS6S (3-*O*-sulfation is underlined). To our knowledge, the elucidation of this gD binding sequence has not be reported before and is only the second sequence that has been characterized and demonstrated to provide binding sites for gD. The characterization of the 3-*O*-sulfated HP octasaccharide provides a novel gD structure that provides additional structural information about heparan sulfate assisted viral entry. Using a PAPS regeneration system coupled with 3-OST-3 modification, we were able to generate and purify sufficient amounts of the characterized gD binding 3-*O*-sulfated HP octasaccharide warranted for cell based assays. When cell based assays are completed, it will represent the first attempt to inhibit HSV viral infection by exploiting a structurally defined oligosaccharide's ability to bind to gD. Finally, utilizing electrospray mass spectrometry our results were confirmed in that 3-OST-3 transfers only one 3-*O*-sulfo group to the HP octasaccharide substrate.

CHAPTER V

PURIFICATION OF HEPARAN SULFATE FROM BOVINE KIDNEY

Introduction

HS is a highly sulfated polysaccharide that is presented in abundant quantities on the cell surface, thereby making it an ideal target for the modulation of many biological processes through its interactions with various biologically important proteins. HS has been found to play a role in the HSV infection mechanism through its interactions with HSV gD. If the minimal required sequence for this interaction is determined, it may be possible to inhibit HSV infections by mimicking it polysaccharide based receptors. As a consequence in Chapter III, a 3-*O*-sulfated HP octasaccharide was determined to be of the minimum size required for gD binding. In Chapter IV, characterization of this 3-*O*-sulfated HP octasaccharide was completed. Results obtained do provide additional structural information regarding the HS assisted HSV entry mechanism. However, only when a diverse library of structurally defined sequences that possesses binding affinity for gD becomes available, can one begin to uncover the structure-activity relationships of HS.

To this end, we describe the isolation and purification of large quantities of HS from bovine kidney by modifying and optimizing a previously published method (185). Once purified, the HS was subjected to partial digestion by heparin lyases to generate an HS oligosaccharide library of various sizes. Milligram amounts of the HS octasaccharide library were modified with 3-OST-3 with hopes that a novel gD binding sequence could be

generated in sufficient amounts to complete structural characterization. This would again provide new insights to the currently unknown structure-activity relationship between HS and gD.

Purification of HS from bovine kidney acetone powder

Since the HS that was commercially available, utilized bovine kidney as the starting material, we attempted to use the same and process it through an identical purification procedure (185). This initial attempt was abandoned because it was estimated that ~600 L of chloroform/methanol and ether would be needed to defat and dry the tissue to produce the starting material required for large scale production. Because of this a different starting material needed to be selected. As described in the previous publication (185), the goal of the high amounts of chloroform/methanol and ether was to remove fat and to completely dry the resulting tissue into its powder form. Fortunately, bovine kidney acetone powder was found to be commercially available. Since this material has already been defated and completely dried no chloroform/methanol and ether was needed to process this material. As a result, the bovine kidney acetone powder was used as the starting material for the isolation and purification of large quantities of HS.

The purification procedure can be separated into eight steps as described below (figure 56). It is important to note here that the recovery yield from each step was monitored to ensure the highest recovery yield possible. This was done by taking an aliquot after the completion of one step and spiking it with [^{35}S] labeled HS, and then this material was subjected to the next step. The recovery yield was observed by the amount of [^{35}S] labeled HS that was recovered.

Step one: Homogenization and protein denaturation

Each round of purification begins with the homogenization of the 200 g of bovine kidney acetone powder. The acetone powder is homogenized in 4 L of distilled water. The resulting homogenate is then heated at 100°C for 1 hr to denature proteins and to destroy the presence of any bacteria. Due to high volumes that were to be heated along with the size limitations of our water bath, we decided to autoclave the homogenate for 1 hr. This provided a simple, yet efficient way to denature proteins that were contained in the large volumes of the homogenate.

Step two: Protease Digestions (2 rounds)

Denaturing the proteins serves to increase their susceptibility to be degraded during protease digestion. The amount of protein associated with the homogenate was considered to be high, thus two rounds of protease digestion were carried out.

Step three: Trichloroacetic acid (TCA) precipitation

After proteins had been degraded, they were subsequently precipitated by the addition of trichloroacetic acid (TCA). The supernatant which contains the HS was collected and processed in subsequent steps.

Step four: Ethanol precipitation

The HS is then precipitated using cold ethanol. It is important to note that after TCA precipitation, the pH of the supernatant was not surprisingly found to be extremely acidic pH between 0.5-1.0. During procedure optimization, it was discovered that ethanol

precipitations of HS was required to be carried out at more of a neutral pH (~7.85) for maximum recovery yield of 90-95%. If the HS precipitation was carried out at very acidic or low pH, the recovery yield from this step alone decreased to approximately 40%. The most efficient approach to neutralize the TCA supernatant was to use NaOH pellets. We used NaOH pellets so that the volume would be as small as possible. Minimizing the volume was a huge concern because at this point approximately 15 L of material was generated. After the ethanol precipitation the volume was reduced significantly to approximately 1 L which was more manageable.

Step five: Beta-elimination

After ethanol precipitation, the HS was considered to be in its proteoglycan form. In this form, HS is considered to be linked to its core protein at specific serine residues. Beta-elimination by the addition of NaOH and $NaBH_4$, serves to break this linkage and stabilize the HS polysaccharide so that further degradation does not occur.

Step six: Ethanol precipitation

After beta-elimination the HS (free from its core protein), is precipitated as before using cold ethanol. HS precipitation here serves to decrease the volume and to increase the concentration of HS for subsequent steps.

Step seven: Chondrotinase digestion

At this point, it is possible that the material contains some amount of chondroitin sulfate (CS). The CS needed to be removed as the final step in the purification procedure

utilizes anion exchange chromatography. CS, like HS, is a long polysaccharide that carries numerous negative charges. As a result, it would be difficult to separate CS from HS using this method. Furthermore, the presence of CS would interfere with HS quantification as a positively charged based alcian blue assay will be used as described later.

Step eight: Anion exchange chromatography

The resultant material after CS digestion is subjected to anion exchange DEAE chromatography using the AKTA FPLC system. This is the final step in the purification procedure which serves to separate HS from any residual protein contaminants that may have survived. The HS is separated from protein and eluted using a NaCl gradient. A representative DEAE elution profile is shown in figure 57.

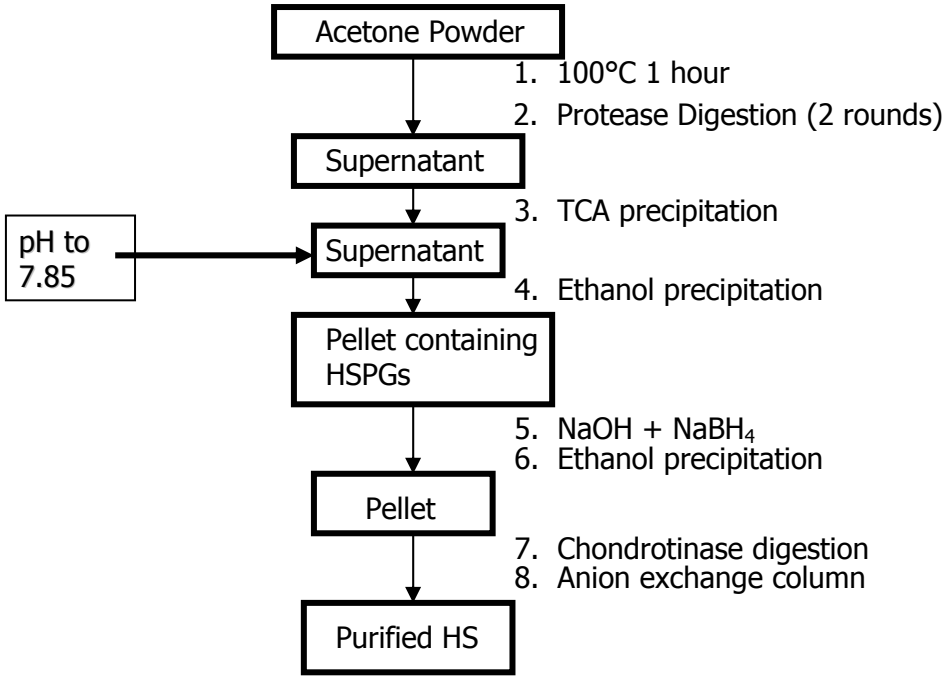

Figure 56. Optimized scheme for HS purification from bovine kidney acetone powder. The purification procedure consists of eight separate steps. Each step is described in greater detail in the text.

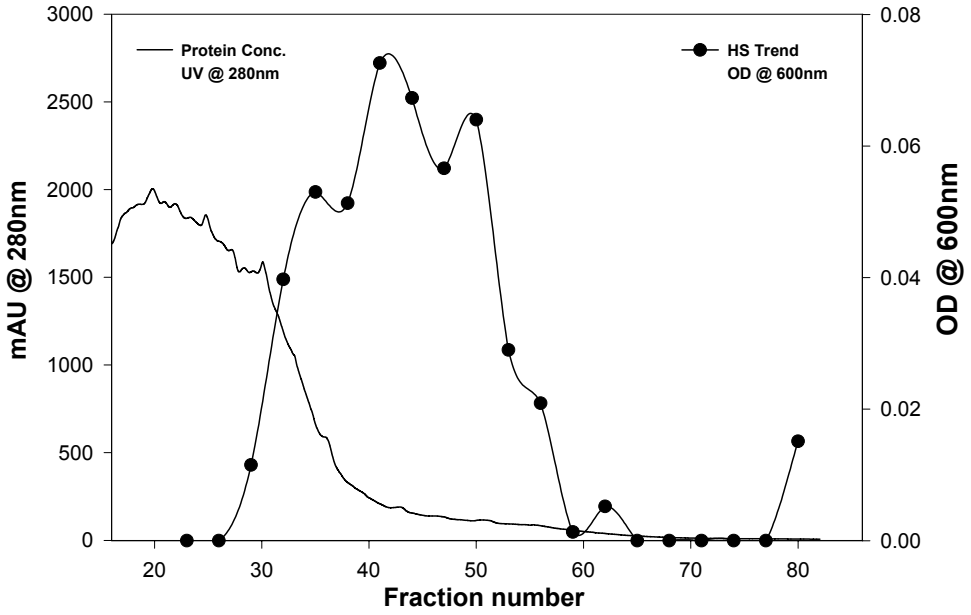

Figure 57. FPLC anion exchange profile of the purification of HS. Column size: (1 × 20 cm). The column was equilibrated with a solution of 50 mM NaAc, 250 mM NaCl pH 5. HS was eluted using with a 400 ml gradient of 1 M NaCl in 50 mM NaAc, pH 5 at a flow rate of 4 ml/min. Protein concentration was monitored by online absorbance detection at 280 nm. HS was monitored using the alcian blue assay on every third fraction.

In figure 57, the protein concentration was monitored using an online UV detector while the HS elution trend was monitored using the alcian blue assay on every third fraction. It was observed that there was some degree of overlap between the protein and HS elution patterns. However, the majority of the protein seemed to be eluted prior to fraction 38. As a result, all fractions after this point were collected, dialyzed and deemed to be purified HS. Furthermore, the chromatogram suggested that the majority of the protein could be separated from HS using this method as the majority of the protein did not bind to the column.

Quantification and purity of HS

The amount of HS that was ultimately purified was quantified using an alcian blue assay as described in the "methods" section. This assay has been developed, optimized, and reported in a previous publication (186). This assay takes advantage of HS ability to interact

with the positively charged dye through its negative charged groups. As a result, HS binds to the dye in a concentration dependent fashion as shown in figure 58.

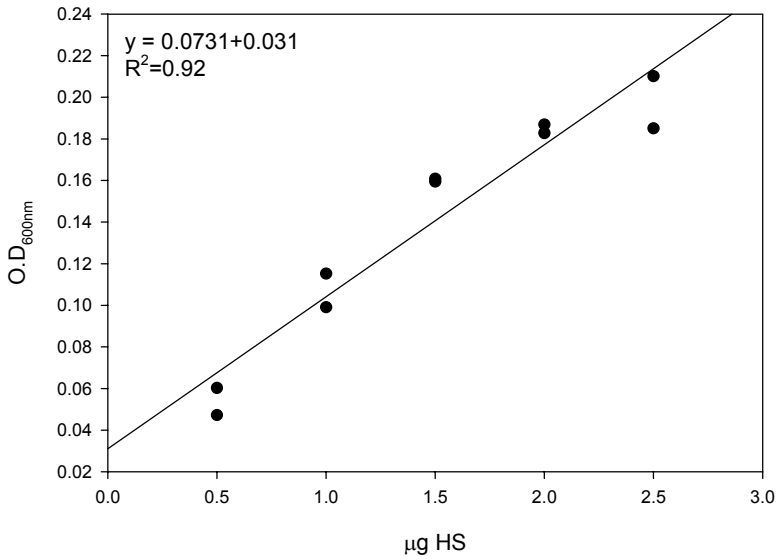

Figure 58. Alcian blue assay for the quantification of HS. The standard curve was prepared in duplicate with HS (ICN) samples from 0-2.5 μg. The assay was preformed as explained in "methods" section, with analysis at 600 nm. The linear regression and R^2 value is present in the graph. The purified HS were prepared in duplicated at various concentrations to fall on the standard curve.

Figure 58, shows a representative standard curve using the alcian blue assay with HS (ICN), in order to observe whether this method could be used to quantify the amount of HS that was purified. It was clearly observed that there is a linear correlation between the amount of HS (ICN) and the $O.D_{600nm}$. Specifically, it was observed that the standard curve maintained its linearity up to approximately 2-2.5 μg HS (ICN). It is important to note that once the concentration of the purified HS was determined, it was possible to generate a standard curve using it with results similar to what is shown in figure 56. This observation suggested that this assay could be used to directly quantify the amount of HS that was purified, assuming the dilutions would be fixed so as they would fall within this linear range.

The purity of the final HS sample was evaluated using the well established Bradford assay for the quantification of proteins. Based on the FPLC profile at 280 nm, it was believed that the protein present was low (figure 57). Results obtained from the Bradford assay, using bovine serum albumin (BSA) as a standard, suggested that very little protein remained in the sample. This was evident as the protein concentration was determined to be less than 5 μg/ml, which was the detectable limit of the assay (data not shown). Consequently, the relative purity of the HS was deemed acceptable when the ratio between HS to protein was considered. The purity was further investigated by HS ability to be modified by HS sulfotransferases when compared to that of HS (ICN). Any contamination (i.e. proteins) would have adverse effects on these modification reactions. Results suggested that the sulfotransferases where able to transfer a [^{35}S]sulfo group with comparable efficiency to both purified HS and HS (ICN) (data not shown). This was extremely important as the HS oligosaccharide library would need to be modified by 3-OST-3 to generate potential gD binding oligosaccharides.

The above optimized HS purification procedure was carried out seven times, each processing 200 g of bovine kidney acetone powder. Each round of purification took approximately 14 days to complete. The major challenge included designing a method with appropriate instrumentation that could accommodate the large volumes that were generated, which were in excess of 15 L prior to step 4, during each round of purification. Each round yielded on average approximately 120-130 mg of purified HS, with a final recovery yield greater than 60%. Considering the amount of steps and the high volumes that were generated and processed, a 60% recovery yield was deemed satisfactory. A total of 1600 g of bovine kidney acetone powder was ultimately processed which has yielded over 770 mg of purified

HS that has an estimated commercial value of greater than $46,000. This material was later used to generate a HS oligosaccharide library from its partial digestion by heparin lyases.

Generation and isolation of gD binding HS oligosaccharide

The purification of large amounts of HS allowed for the generation of milligram amounts of various sized HS oligosaccharides. The HS was partially digested by heparin lyase III (Hep III). The Hep III digestion was optimized to give the most octasaccharide and hexasaccharide pools upon resolving on a P-6 size exclusion column. Results from optimization suggested that digesting 5 mg of HS with 6.1 mU of Hep III was necessary to achieve this goal. To this end, twenty reactions (5 mg HS/reaction) was each digested with 6.1 mU of Hep III and subjected to size exclusion chromatography. The P-6 elution profile is shown in figure 59.

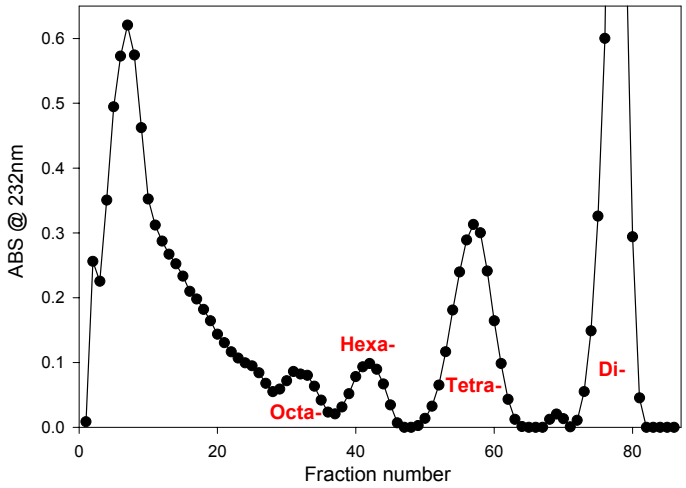

Figure 59. HS oligosaccharide library production. Profile of ~100mg of purified HS digested with Hep III. Twenty separate digestions (~5 mg of HS/digestion) were incubated with 6.1mU Hep III/digestion. Each digestion mixture ~1 ml consisted of HS, 50 mM NaH_2PO_4 and 100 ug/ml BSA, pH 7 incubated at 37°C for 24 hrs. Digestions were terminated by heating at 100°C for 15 mins. All mixtures are loaded on a Bio-Gel P- 6 size exclusion column (2.5 x 200 cm) equilibrated with 0.5 M ammonium bicarbonate at a flow rate of 0.5 ml/min and 4.5 ml fractions were collected.

Based on the elution profile shown in figure 59, it was observed that we were able to sufficiently resolve from octasaccharides down to disaccharides using this method. Based on their absorbance at 232 nm, we could estimate that amount of material contained within each oligosaccharide pool. In the previous publication by our laboratory, approximately 400 ng of a 3-*O*-sulfated gD binding HS octasaccharide was isolated by processing 40 mg of HS. Therefore, we hypothesized that processing 300 mg of HS would result in a sufficient amount of a gD binding oligosaccharide to complete its characterization.

It was observed that processing 300 mg of HS through the optimized Hep III partial digestion yielded approximately 10 mg of HS hexasaccharide library. This library was demonstrated to contain a gD binding octasaccharide as described in a previous publication (181). The HS hexasaccharide library was then incubated with purified 3-OST-3 enzyme in the presence of [^{35}S]PAPS to generate a 3-*O*-[^{35}S]sulfated HS library. We attempted to use two forms anion exchange chromatography, as did the previous report, to purify a gD binding 3-*O*-sulfated HS octasaccharide from the library. However, after processing the material it was observed that only 5 µg of a gD binding 3-*O*-sulfated HS octasaccharide was isolated. This was much lower than was previously expected. Based on this recovery, it was estimated that 5-10 g of HS needed to be processed to complete characterization and cell-based assays. As it was not plausible for us to attempt this, the isolation of a gD binding HS oligosaccharide from a HS library was abandoned.

Applications for purified HS

Eventhough we were not able to generate sufficient quantities of a gD binding 3-*O*-sulfated HS octasaccharide, the purification of large amounts of HS has greatly assisted our

continued study of HS and its biological functions. As the laboratory continues to study HS biosynthesis, recombinant proteins of the various HS biosynthetic enzymes have been expressed and purified using traditional molecular cloning techniques. Upon purification of these biosynthetic enzymes, their activities were able to be investigated utilizing the purified HS as a substrate. Additionally, given that many of the HS biosynthetic enzymes are present in multiple isoforms, the substrate specificities of these isoforms were also able to be investigated using the diverse sequences contained with the purified HS polysaccharide.

The structural study of biologically important HS sequences at the polysaccharide level is a daunting task due to its structural diversity and technological limitations. However, it is much easier to study HS sequences at their oligosaccharide to disaccharide levels. The laboratory also has expressed and purified three HS degrading enzymes, endoglycosidases, heparin lyase I, II, and III. After purification of these enzymes, their activities were also investigated utilizing the purified HS as a substrate. Heparin lyases serve to degrade the HS polysaccharide into its disaccharide and/or oligosaccharide components, by cleaving glycosidic bonds depending on various sulfations patterns within the polysaccharide. Additionally, various sized oligosaccharide standards and libraries were generated by partial digestion by heparin lyases and the resulting sized oligosaccharides were separated and resolved by size exclusion chromatography as shown in figure 59.

Conclusions

We were able to efficiently isolate and purify HS from bovine kidney acetone powder, using an eight step optimized procedure. By using commercially available bovine kidney acetone powder, we were able to avoid the use of the harmful amounts of

chloroform/methanol and ether estimated for large scale production. It was observed that processing 200 g of acetone powder resulted in approximately 120-130 mg of purified HS with a recovery yield of 60%. We were able to process 1600 mg of acetone powder which yielded over 770 mg of purified HS.

The purified HS was used to generate milligram amounts of a HS oligosaccharide library by its partial digestion by heparin lyases. Specifically, processing 300 mg of HS yielded 10 mg of the HS hexasaccharide library. We subjected this library to 3-*O*-sulfation by incubation with purified 3-OST-3 in the presence of [^{35}S]PAPS. We attempted to isolate a gD binding 3-*O*-sulfated HS oligosaccharide from the library, however due to low recovery yields we were only able to obtain approximately 5 μg of a 3-*O*-sulfated HS oligosaccharide. As a result of low yields, we were not able to isolate sufficient amounts of a gD binding oligosaccharide from the library to complete its characterization.

HS is the central molecule of interest in our laboratory. HS is a highly sulfated polysaccharide that is presented in abundant quantities on the cell surface, thereby making it an ideal target for the modulation of many biological processes through its interactions with various biologically important proteins. The laboratory is interested in understanding the "non-template" driven biosynthesis of HS through investigations of HS biosynthetic enzymes. Moreover, the laboratory is interested studying the roles that HS play in assisting in HSV viral infections and its roles in regulating blood coagulation. As a result, the purification of large quantities of HS was a great success and is used frequently in the laboratory. Purified HS is a valuable reagent to have on hand to study HS biosynthesis, its structure and how they relate to its diverse function. Given the high commercial cost of HS

(ICN) along with it being abruptly discontinued, an efficient large scale purification procedure was essential.

Furthermore, we were able to send milligram amounts of purified HS to various collaborators to explore novel biological interactions that implicate HS. By generating microgram amounts of 3-*O*-sulfated HS (3-OST-1/3-OST-3), novel investigations and experimentations are forthcoming that may suggest specific 3-*O*-sulfated HS sequences have different and previously unknown biological properties.

CHAPTER VI

CONCLUSIONS

HS has been implicated in the infection mechanism of numerous viruses that affect humans (3, 162-165). Specifically, HS has been shown to assist in the viral infection mechanism for HSV-1, at both the viral attachment and viral fusion stages of infection via its interactions with various HSV-1 envelope glycoproteins (130, 175, 201). Due to the structural diversity contained with HS sequences, the functional relationship between specific saccharide sequences and their ability to promote HSV infections remain largely unknown, as it is extremely difficult to obtain sufficient quantities of a homogenous HS sequence.

In a previous study, it was demonstrated that HS modified by 3-OST-3, and not 3-OST-1, was able to bind to gD to initiate HSV-1 viral entry into target cells (130). As a result, it was hypothesized that if the specific HS sequence that allows for gD binding that subsequently promotes viral fusion is elucidated, then it could possibly serve as a lead compound for further development of HS based therapeutics. The development of HS based therapeutics may aid in the treatment of HSV infection by disrupting viral entry by targeting the virus interactions with its polysaccharide based cellular receptors. As a result, the goal of this dissertation was four fold. First, was to achieve high expression levels of gD that were needed to investigate its binding to various sized HP oligosaccharides (Chapter III). Second, using structurally defined HP oligosaccharide substrates, was to generate gD binding 3-*O*-sulfated HP oligosaccharides of various sizes and determine the minimal required length for

gD binding (Chapter III). Third, was to characterize the oligosaccharide that possessed the greatest binding for gD and generate sufficient quantities to conduct cell based assays (Chapter IV). Fourth, was to generate and isolate a novel gD binding sequence from a HS derived oligosaccharide library (Chapter V).

In Chapter III, the expression of the ectodomain of gD (Lys_{26}-His_{332}) in large quantities from *E. coli*. was described. The successful expression of gD (5 mg/L culture) was achieved by co-expressing the bacteria chaperone proteins GroEL and GroES. To our knowledge, using a bacteria expression system to prepare gD or other HSV envelope proteins has not been reported. This represents a novel approach to express HSV envelope proteins that could be used to develop a vaccine against HSV infections. As a result, future investigations are forthcoming that will investigate other HSV envelope glycoproteins (gC and gB) that will require their expression in *E. coli*. Results presented in this chapter demonstrated that the HP oligosaccharides of various sizes had a high susceptibility to 3-*O*-sulfation by 3-OST-3 in a size dependent manner. gD binding investigations revealed that the 3-*O*-[^{35}S]sulfated HP oligosaccharides bound to purified gD in a size dependent manner with the 3-*O*-[^{35}S]sulfated HP octasaccharide having the minimum length required for detectable gD binding. The binding affinity of the 3-*O*-[^{35}S]sulfated HP octasaccharide to gD was determined to have a K_d value of 19 μM. Prior to this work, the minimal length required for gD binding had not be investigated.

In Chapter IV, the structural characterization of the gD binding 3-*O*-[^{35}S]sulfated HP octasaccharide was described. Specifically, the glucosamine residue that carried the 3-*O*-[^{35}S]sulfo group transferred by 3-OST-3 was determined using a combination of chemical and enzymatic modifications from both non-reducing and reducing ends. Results

demonstrated that 3-OST-3 transfers a 3-*O*-[^{35}S]sulfo group to the glucosamine located at residue 6 of the unmodified HP octasaccharide, resulting in a sequence of ΔUA2S-GlcNS6S-IdoUA2S-GlcNS6S-IdoUA2S-GlcNS6S3S-IdoUA2S-GlcNS6S (3-*O*-sulfation is underlined). To our knowledge, the elucidation of this gD binding sequence has not be reported before and is only the second sequence that has been characterized and demonstrated to provide binding sites for gD. Using a PAPS regeneration system coupled with 3-OST-3 modification we were able to generate nearly 130 μg of the characterized 3-*O*-sulfated HP octasaccharide. This will allow for the 3-*O*-sulfated HP octasaccharide to be tested in a cell based assay to determine if it could inhibit HSV viral fusion. These experiments are currently being conducted in Dr. Shukla's laboratory and results are forthcoming. To our knowledge this represents the initial experiment of this kind which will determine the feasibility of using structurally defined HS/HP sequence to inhibit HSV viral infections.

The 3-*O*-sulfated HP octasaccharide and the 3-*O*-sulfated HS octasaccharide are found to display 13 and 7 sulfate groups respectively (figure 60). Given that their binding affinities to gD were found to be nearly identical, suggests that the interactions between gD and HS/HP sequences are more than mere non-specific electrostatic interactions.

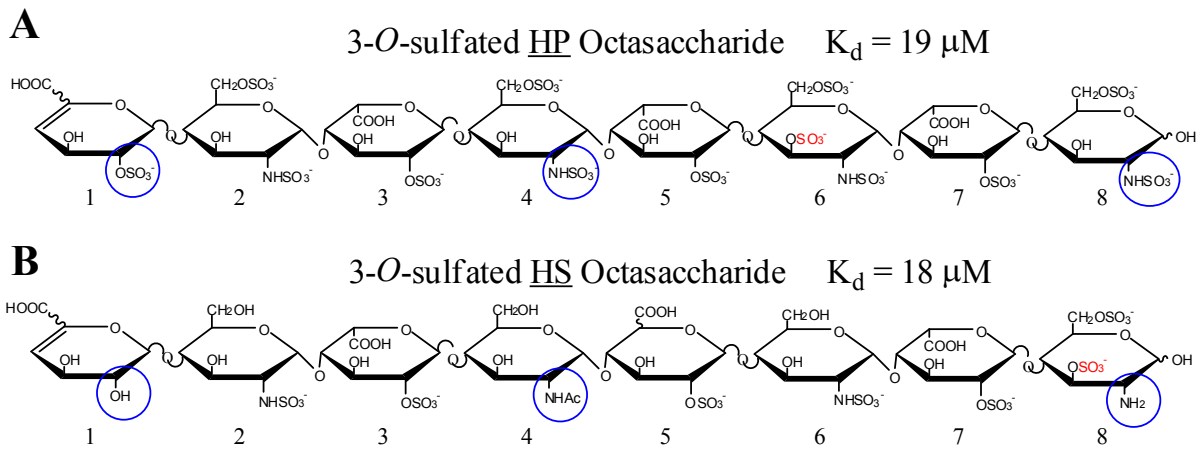

Figure 60. Known characterized gD binding structures. Shown in *panel A* is the 3-*O*-sulfated HP octasaccharide, shown in *panel B*, is the 3-*O*-sulfted HS octasaccharide. The binding affinities are presented as K_d values. The critical 3-*O*-sulfo group transferred by 3-OST-3 is illustrated in red. The noticeable differences beyond 6-*O*-sulfations are circled in blue.

When the two gD binding structures are further examined, there are a few noticeable differences beyond the number of sulfate groups and the presence of 6-*O*-sulfate groups. If the HS gD binding sequence is compared to the HP gD binding sequence the differences are as follows: 1) the absence of a 2-*O*-sulfate group on the non-reducing end uronic acid, 2) the presence of an *N*-acetyl group instead of a *N*-sulfate group on residue 4, and 3) the presence of an *N*-unsubstituted glucosamine instead of an *N*-sulfated glucosamine at the reducing end residue 8. As a result of the two characterized 3-*O*-sulfated octasaccharides (see figure 58) having similar binding affinities for gD, it suggests that the differences between the two may be located in regions or positions that have little to no affect on gD binding. However, only when a diverse library of structurally characterized sequences becomes available that demonstrate binding to gD, can the specific structural motifs that promote gD binding be uncovered. The characterization of the 3-*O*-sulfated HP octasaccharide provides a novel gD structure that along with the previously characterized 3-*O*-sulfated HS octasaccharide provides additional structural information about heparan sulfated assisted viral entry.

In Chapter V the large scale purification of HS from bovine kidney acetone powder was described. Using an eight step optimized procedure, we were able to purify 120-130 mg of HS from 200 g of bovine kidney acetone powder. Processing 1600 mg of acetone powder yielded over 770 mg of purified HS. To search for an additional gD binding structure, we partially digested 300 mg of HS using a mixture of heparin lyases. This resulted in approximately 10 mg of a HS hexasaccharide library. We subjected the library to 3-OST-3 modification in attempt to generate and isolate a novel gD binding oligosaccharide. However, results obtained suggested that the recovery yield was much lower than initially expected. It was estimated that approximately 5 μg of a 3-*O*-sulfated HS oligosaccharide was recovered. This amount was deemed insufficient to conduct the propose experiments. Eventhough we were not able to generate sufficient quantities of a gD binding 3-*O*-sulfated HS oligosaccharide, the purification of large amounts of HS has greatly assisted our continued study of HS and its biological functions. As the laboratory continues to investigate and understand HS biosynthesis, the purified HS is serving as a valuable tool for the determination of activities of recombinant HS biosynthetic enzymes.

Herpes viral infections are prevalent in humans. Unique HS/HP sequences play intimate roles during the infection process. Developing a HS/HP based antiviral drug could be a viable approach to treat HSV infection. Understanding the structural-activity relationship of HS/HP in promoting HSV infections is essential for achieving this goal. The work described above provides additional structural evidence of the HS/HP mediated HSV infection mechanism. Specifically, this work represents the first success in determining and an oligosaccharide's gD binding affinity, characterization of its structure, and the preparation

of sufficient quantities for cell based assays. Further development of this project could uncover a new way to treat diseases related to HSV infections.

Appendix 1:

Curriculum Vitae

Ronald Jarrod Copeland

Division of Medicinal Chemistry
& Natural Products, CB #7360
School of Pharmacy
University of North Carolina at Chapel Hill
Chapel Hill, NC 27599

Work: (919)-962-0065
Fax: (919)-843-5432
Email: copelanr@email.unc.edu
Hometown**:** Suffolk, Virginia

Education:

- University of North Carolina at Chapel Hill, 2001-present
  Ph.D. Candidate, Division of Medicinal Chemistry and Natural Products
  Graduation: December 2006

- Norfolk State University, 1997-2001
  B.S. in Chemistry (Honors)
  Summa Cum Laude
  Norfolk State University DNIMAS Graduate, 2001

Current Research Interests:

Molecular and Chemical Biology, Carbohydrate and Protein Biochemistry, Antiviral Drug design, Viral Inhibition: Protein/carbohydrate structural interactions; Heparin/heparan sulfate structure and biochemistry as they relate to viral infectivity

Publications:

- Tiwari, V., O'Donnell, C., Copeland, R.J., Scarlett, T., Liu, J., Shukla, D. Soluble 3-*O*-sulfated heparan sulfate allows herpes simplex virus type-1 entry and spread into resistant Chinese hamster ovary (CHO-K1) cells. (2006) *submitted* **J. Gen. Virol**.

- Liu, J., Shriver, Z., Pope, R.M., Thorp, S.C., Duncan, M.B., Copeland, R.J., Raska, C.S., Yoshida, K., Eisenberg, R.J., Cohen, G., Linhardt, R., Sasisekharan, R. Characterization of a heparan sulfate octasaccharide that binds to herpes simplex virus type 1 glycoprotein D. (2002) **J. Biol. Chem. 277**:33456-33467

Awards:

- *Scholar*, David and Lucille Packard Foundation, 2001-2006
  - An award to outstanding students from Historically Black Colleges and Universities engaged in graduate studies in the physical and life sciences.
  - $100,000 for graduate studies over 5 years

- *Scholar*, Dorozetz National Insitute for Minorities in Applied Sciences (DNIMAS) Program, Norfolk State University, 1997-2001
  - A 4-year full scholarship awarded to outstanding students to pursue their undergraduate science degree at Norfolk State University
  - Primary mission of the program is to address the severe shortage of minority scientists by producing graduates who are capable of successfully completing graduate studies in the basic and applied sciences.

- Distinguished Academic Honors, DNIMAS Program, 2001

- Top Senior Award, DNIMAS Program, 2001

Undergraduate Research Experience:

- *Participant*, Research Education Support (RES) Pre-Entry Program, UNC-CH, Chapel Hill NC, Summer 2001
  Program provides support for incoming graduate students to begin research in a laboratory the summer directly preceding enrollment
  - **Advisor:** Dr. Jian Liu (Medicinal Chemistry and Natural Products)
  - **Project:** Heparan Sulfate Library Preparation using Endoglycosidases

- *Participant*, Summer Pre-Graduate Research Experience (SPGRE), UNC-CH, Chapel Hill NC, Summer 2000
  - **Advisor**: Dr. Richard Superfine (Physics and Astronomy)
  - **Project:** DNA Nanotubes for Computing (Nanotechnology)

- *Participant*, Summer Research Internship Program (SRIP), University of Virginia, Charlottesville, VA, Summer 1999
  - **Advisors:** Dr. Lloyd Gray (Clinical Pathology) and Dr. Doris Haverstick (Pathology)
  - **Project:** Preliminary Testing of a Novel Antiproliferative Ca^{2+} Channel Blocker for Implications in treating cancer using Cytostatic Approaches

- *Student Research Assistant*, Norfolk State University, Norfolk, VA and Laboratory for the Study of Reproductive Biochemistry and Molecular Biology, Virginia Beach, VA, 1998-2000
  - **Mentor:** Dr. Joseph Hall, Chemistry Department
  - **Project:** Purification of *N*-Acetyl-Hexosamindase

Work Experience:

- *Graduate Research Assistant*, Division of Medicinal Chemistry, School of Pharmacy (SOP), University of North Carolina at Chapel Hill, 2001-current
    - **Thesis advisor:** Dr. Jian Liu, Assistant Professor
    - **Dissertation Title:** Preparation and Characterization of a Heparin-Derived Oligosaccharide that Binds to Herpes Simplex Virus Type 1 Glycoprotein D

- *Graduate Assistant*, Summer Pre-Graduate Research Experience (SPGRE) Program, Chapel Hill, NC, Summer 2005.
    - This 10 week program offers undergraduates the opportunity to perform research, take a GRE preparatory course, and network with a variety of scientists/scholars on the UNC-Chapel Hill campus. Served as a group leader, directing ten students through their summer long activities. Duties also included assisting in the organization of weekly seminars and a variety of administrative tasks.

- *Rotation Student Training*-- Assisted in the training of one rotating graduate student (Spring 2005) working in the laboratory.

Committees/Organizations:

- *Member,* UNC-School of Pharmacy Graduate Student Organization (GSO), 2001-present
- *Member,* E-Mentoring Program, Norfolk State University, 2005-present
- *Member,* American Association of the Advancement of Science (AAAS), 2004-present
- *Committee Member,* Boka W. Hadzija Distinguished Award Selection Committee, 2005
- *Member,* Alpha Kappa Mu National Honor Society, Norfolk State University Chapter, 1999-2001
- *Member*, Golden Key National Honor Society, Norfolk State University, 1999-2001

Skills/Techniques

- Molecular Biology
    - Agarose gel electrophoresis
    - Western Blotting
    - Exposure to molecular cloning- Primer design, plasmid amplification/purification, and DNA sequencing data analysis
    - Recombinant protein expression/purification-bacteria and insect cells

- Biochemical/Bio-Analytical
    - Affinity co-electrophoresis
    - Carbohydrate Purification
    - Carbohydrate Structural Analysis

- Radioactive isotope detection/Handing/Disposal/Safety Training
- SDS-PAGE
- Immunoprecipitation Assays
- HPLC-- Ion exchange, size exclusion, reverse phase ion pairing
- FPLC--Ion exchange, size exclusion, affinity
- Capillary electrophoresis--zone electrophoresis in normal and reverse polarity
- Chemical and enzymatic degradation of complex carbohydrates for structural analysis
- Chemical conjugation of complex glycans and glycoproteins
- UV Spectrophotometry--Quantitative Analysis of carbohydrates, nucleic acids, and proteins
- Mammalian cell culture--DNA transfection, radioactive metabolic labeling of proteoglycans

- Exposure to: Atomic Force Microscopy Imaging (AFM)-Summer 2000
  - Spectrofluorometer (SLM) techniques and ELISA, Summer 1999

REFERENCES

1. Rosenberg, R.D., Showrak, N.W., Liu, J., Schwartz, J.J., and Zhang, L. 1997. Heparan sulfate proteoglycans of the cardiovascular system: specific structures emerge but how is synthesis regulated? *J. Clin. Invest.* 99:2062-2070.

2. Bernfield, M., Gotte, M., Park, P.W., Reizes, O., Fitzgerald, M.L., Lincecum, J., and Zako, M. 1999. Functions of cell surface heparan sulfate proteoglycans. *Ann. Rev. Biochem.* 68:729-777.

3. Liu, J., and Thorp, S.C. 2002. Heparan sulfate and the roles in assisting viral infections. *Med. Res. Rev.* 22:1-25.

4. Alexander, C.M., Reichsman, F., Hinkes, M.T., Lincecum, J., Becker, K.A., Cumberledge, S., and Bernfield, M. 2000. Syndecan-1 is required for Wnt-1-induced mammary tumorigenesis in mice. *Nat. Genet.* 25:329-332.

5. Liu, D., Shriver, Z., Venkataraman, G., Shabrawi, Y.E., and Sasisekharan, R. 2002. Tumor cell surface heparan sulfate as cryptic promoters or inhibitors of tumor groth and metastasis. *Proc. Natl. Acad. Sci.* 99:568-573.

6. Reizes, O., Lincecum, J., Wang, Z., Goldberger, O., Huang, L., Kaksonen, M., Ahima, R., Hinkes, M.T., Barsh, G.S., Rauvala, H., et al. 2001. Transgenic Expression of Syndecan-1 Uncovers a Physiological Control of Feeding Behavior by Syndecan-3. *Cell* 106:105-116.

7. Hwang, H.-Y., Olson, S., Esko, J.D., and Horvitz, H.R. 2003. Caenorhabditis elegans early embryogenesis and vulval morphogenesis require chondroitin biosynthesis. *Nature* 423:439-443.

8. Mizuguchi, S., Uyama, T., Kitagawa, H., Nomura, K.H., Dejima, K., Gengyo-Ando, K., Mitani, S., and Sugahara, K. 2003. Chondroitin proteoglycans are involved in cell division of Caenorhabditis elegans. *Nature* 423:443-448.

9. Kelly, T., Miao, H.Q., Yang, Y., Navarro, E., Kussie, P., Huang, Y., MacLeod, V., Casciano, J., Joseph, L., Zhan, F., et al. 2003. High heparanase activity in multiple myeloma is associated with elevated microvessel density. *Cancer Res.* 63:8749-8756.

10. Fraser, J.L., T., Laurent, U. 1997. Hyaluronan: its nature, distribution, functions, and turnover. *Journal of Internal Medicine* 242:27-33.

11. Laurent, T., Fraser, JRE. 1992. Hyaluronan. *FASEB Journal* 6:2397-2404.

12. Liao, Y., Jones, SA., Forbes, B., Martin, GP., Brown, MB. 2005. Hyaluronan: pharmaceutical characterization and drug delivery. *Drug Delivery* 12:327-342.

13. Hascall VC, R.R. 1972. Characteristics of the protein-keratan sulfate core and of keratan sulfate prepared from bovine nasal cartilage proteoglycan. *J. Biol. Chem.* 247:4529-4538.

14. Lindahl, U., and Hook, M. 1978. Glycosaminoglycans and their binding to biological macromolecules. *Ann. Rev. Biochem.* 47:385-417.

15. Murata K, Y.Y. 1987. Dermatan sulfate isomers in human articular cartilage characterized by high-performance liquid chromatography. *Biochem. Int.* 15:87-94.

16. Funderburgh, J. 2000. Keratan sulfate: structure, biosynthesis, and function. *Glycobiology* 10:951-958.

17. Laabs, T., Carulli, D., Geller, H.M., and Fawcett, J.W. 2005. Chondroitin sulfate proteoglycans in neural development and regeneration. *Curr. Opin. Neurobiol.* 15:116.

18. Carulli D, L.T., Geller HM, Fawcett JW. 2005. Chondroitin sulfate proteoglycans in neural development and regeneration. *Curr. Opin. Neurobiol.* 15:116-120.

19. Mulloy B, F.M., Jones C, Davies DB. 1993. NMR and molecular-modelling studies of the solution conformation of heparin. *Biochem. J.* 293:849-858.

20. Coombe, D.R., and Kett, W.C. 2005. Heparan sulfate-protein interactions: therapeutic potential through structure-function insights. *Cellular and Molecular Life Sciences (CMLS)* 62:410.

21. Hileman, R.E., Fromm, J.R., Weiler, J.M., and Linhardt, R.J. 1998. Glycosaminoglycan-protein interactions: definition of consensus sites in glycosaminoglycan binding proteins. *BioEssays* 20:156-167.

22. Toida, T., Yoshida, H., Toyoda, H., Koshiishi, T., Imanari, T., Hileman, R.E., Fromm, J.R., and Linhardt, R.J. 1997. Structural differences and the presence of unsubstituted amino groups in heparan sulfates from different tissues and species. *Biochem. J.* 322:499-506.

23. Lindahl, U., Kusche-Gullberg, M., and Kjellen, L. 1998. Regulated diversity of heparan sulfate. *J. Biol. Chem.* 273:24979-24982.

24. Bernfield, M., Kokenyesi, R., Kato, M., Hinkes, M.T., Spring, J., Gallo, R.L., and Lose, E.L. 1992. Biology of the syndecans: A family of transmembrane heparan sulfate proteoglycans. *Ann. Rev. Cell Biol.* 8:365-393.

25. Couchman, J.R., Woods, A. 1996. Syndecans, signaling and cell adhesion. *J. Cell. Biochem.* 61:578-584.

26. Rapraeger, A.C. 2000. Syndecan-regulated receptor signaling. *J. Cell Biol.* 149:995-997.

27. Wight, T.N., Kinsella, M.G., Qwarnström, E.E. 1992. The role of proteoglycans in cell adhesion, migration and proliferation. *Curr. Opin. Cell Biol.* 4:793-801.

28. Esko, J.D., Zhang, L. 1996. Influence of core protein sequence on glycosaminoglycan assembly. *Curr. Opin. Struct. Biol.* 6:663-670.

29. Carey, D.J. 1997. Syndecans: multifunctional cell-surface coreceptors. *Biochem. J.* 307:1-16.

30. A.C. Rapraeger, V.L.O. 1998. Molecular interactions of the syndecan core proteins. *Curr. Opin. Cell Biol.* 10:620-628.

31. Gotte, M. 2003. Syndecans in inflammation. *FASEB Journal* 17:575-591.

32. Fransson, L., Edgren, G., Havsmark, B., Schmidtchen, A. 1995. Recycling of a glycosylphosphatidylinositol-anchored heparan sulphate proteoglycan (glypican) in skin fibroblasts. *Glycbiology* 5:407-415.

33. Yanagishita, M. 1992. Glycosylphosphatidylinositol-anchored and core protein-intercalated heparan sulfate proteoglycans in rat ovarian granulosa cells have distinct secretory, endocytic and intracellular degradative pathways. *J. Biol. Chem.* 267:9505-9511.

34. Hacker U, N.K., Perrimon N. 2005. Heparan sulphate proteoglycans: the sweet side of development. *Nat. Rev. Mol. Cell Biol.* 6:530-541.

35. Kleeff, J., T. Ishiwata, A. Kumbasar, H. Friess, M.W. Büchler, A.D. Lander, and M. Korc. 1998. The cell surface heparan sulfate proteoglycan glypican-1 is an essential regulator of growth factor action in pancreatic carcinoma cells, and is overexpressed in human pancreatic cancer. *J. Clin. Invest.* 102:1662-1673.

36. Govindraj, P., West, L., Koob, T.J., Neame, P., Doege, K., and Hassell, J.R. 2002. Isolation and Identification of the Major Heparan Sulfate Proteoglycans in the Developing Bovine Rib Growth Plate. *J. Biol. Chem.* 277:19461-19469.

37. Battaglia, C., Aumailley, M., Mann, K., Mayer, U. Timpl, R. 1993. Structural basis of beta 1 integrin-mediated cell adhesion to a large heparan sulfate proteoglycan from basement membranes. *Eur. J. Cell Biol.* 61:92-99.

38. Iozzo, R. 1998. Matrix proteoglycans: from molecular design to cellular function. *Annu. Rev. Biochem.* 67:609-652.

39. Isemura, M., Sato, N., Yamaguchi, Y., Aikawa, J., Munakata, H., Hayashi, N. 1987. Isolation and characterization of fibronectin-binding proteoglycan carrying both heparan sulfate and dermatan sulfate chains from human placenta. *J. Biol. Chem.* 262:8926-8933.

40. Timpl, R., Brown, J.C. 1996. Supramolecular assembly of basement membranes. *BioEssays* 18:123-132.

41. Yang, W., Su, T., Yang, Y., Chang, S., Chen, C., Chen, C. 2005. Altered Perlecan Expression in Placental Development And Gestational Diabetes Melliuts. *Placenta* 26:780-788.

42. Denzer, A.J., Gesemann, M., Schumacher, B., and Ruegg, M.A. 1995. An amino-terminal extension is required for the secretion of chick agrin and its binding to extracellular matrix. *J. Cell Biol.* 131:1547-1560.

43. Hagen, S.G., Michael, A.F., and Butkowski, R.J. 1993. Immunochemical and biochemical evidence for distinct basement membrane heparan sulfate proteoglycans. *J. Biol. Chem.* 268:7261-7269.

44. Tsen, G., Halfter, W., Kröger, S., and Cole, G.J. 1995. Agrin Is a Heparan Sulfate Proteoglycan. *J. Biol. Chem.* 270:3392-3399.

45. Iozzo, R.V. 1998. MATRIX PROTEOGLYCANS: From Molecular Design to Cellular Function. *Annual Review of Biochemistry* 67:609-652.

46. Esko, J.D., and Lindahl, U. 2001. Molecular diversity of heparan sulfate. *J. Clin. Invest.* 108:169-173.

47. Gulberti, S., Lattard, V., Fondeur, M., Jacquinet, J.-C., Mulliert, G., Netter, P., Magdalou, J., Ouzzine, M., and Fournel-Gigleux, S. 2005. Modifications of the Glycosaminoglycan-Linkage Region of Proteoglycans: Phosphorylation and Sulfation Determine the Activity of the Human ß1,4-Galactosyltransferase 7 and ß1,3-Glucuronosyltransferase I. *The ScientificWorld Journal* 5:510.

48. Sugahara, K., and Kitagawa, H. 2002. Heparin and heparan sulfate biosynthesis. *IUBMB Life* 54:163-175.

49. Davies, G.J. 2001. Sweet secrets of synthesis. *Nat. Struct. Mol. Biol.* 8:98.

50. Sears, P., and Wong, C.-H. 1996. Intervention of carbohydrate recognition by proteins and nucleic acids. *PNAS* 93:12086-12093.

51. Bourdon, M.A., Oldberg, A., Pierschbacher, M. and Ruoslahti, E. 1985. *Proc. Natl. Acad. Sci. U.S.A* 82:1321-1325.

52. Bourdon, M.A., Krusius, T., Campbell, S., Schwartz, N., and Ruoslahti, E. 1987. Identification and synthesis of a recognition signal for the attachment of glycosaminoglycans. *Proc. Natl. Acad. Sci. U.S.A* 84:3194-3198.

53. Chopra, R.K., Pearson, C. H., Pringle, G. A., Fackre, D. S., and Scott, R. G. 1983. *Biochem. J.* 232:277-279.

54. Oldberg, A., Hayman, E. G., and Ruoslahti, E. 1981. *J. Biol. Chem.* 256:10847-10852.

55. Kearns, A.E., Vertel, B.M., and Schwartz, N.B. 1993. Topography of glycosylation and UDP-xylose production. *J. Biol. Chem.* 268:11097-11104.

56. Vertel, B.M., Walters, L.M., Flay, N., Kearns, A.E., and Schwartz, N.B. 1993. Xylosylation is an endoplasmic reticulum to Golgi event. *J. Biol. Chem.* 268:11105-11112.

57. Esko, J.D., Stewart, T.E., and Taylor, W.H. 1985. Animal cell mutants defective in glycosaminoglycan biosynthesis. *Proc. Natl. Acad. Sci.* 82:3197-3201.

58. Bai, X., Zhou, D., Brown, J.R., Crawford, B.E., Hennet, T., and Esko, J.D. 2001. Biosynthesis of the linkage region of glycosaminoglycans: cloning and activity of galactosyltransferase II, the sixth member of the β1,3-galactosyltransferase family (β3GalT6). *J. Biol. Chem.* 276:48189-48195.

59. Okajima, T., Yoshida, K., Kondo, T., and Furukawa, K. 1999. Human Homolog of Caenorhabditis elegans sqv-3 Gene Is Galactosyltransferase I Involved in the Biosynthesis of the Glycosaminoglycan-Protein Linkage Region of Proteoglycans. *J. Biol. Chem.* 274:22915-22918.

60. Lugemwa, F.N., Sarkar, A.K., and Esko, J.D. 1996. Unusual beta -D-Xylosides That Prime Glycosaminoglycans in Animal Cells. *J. Biol. Chem.* 271:19159-19165.

61. Almeida, R., Levery, S.B., Mandel, U., Kresse, H., Schwientek, T., Bennett, E.P., and Clausen, H. 1999. Cloning and Expression of a Proteoglycan UDP-Galactose:beta -Xylose beta 1,4-Galactosyltransferase I. A SEVENTH MEMBER OF THE HUMAN beta 4-GALACTOSYLTRANSFERASE GENE FAMILY. *J. Biol. Chem.* 274:26165-26171.

62. Okajima, T., Fukumoto, S., Furukawa, K., Urano, T., and Furukawa, K. 1999. Molecular Basis for the Progeroid Variant of Ehlers-Danlos Syndrome. IDENTIFICATION AND CHARACTERIZATION OF TWO MUTATIONS IN GALACTOSYLTRANSFERASE I GENE. *J. Biol. Chem.* 274:28841-28844.

63. Pedersen, L.C., Tsuchida, K., Kitagawa, H., Sugahara, K., Darden, T.A., and Negishi, M. 2000. Heparan/Chondroitin Sulfate Biosynthesis. STRUCTURE AND MECHANISM OF HUMAN GLUCURONYLTRANSFERASE I. *J. Biol. Chem.* 275:34580-34585.

64. Sven Inerot, D.H.S.-E.O.H.T.L.A. 1991. Proteoglycan alterations during developing experimental osteoarthritis in a novel hip joint model. *Journal of Orthopaedic Research* 9:658-673.

65. Gouze, J.N., Bordji, K., Gulberti, S., Terlain, B., Netter, P., Magdalou, J., Fournel-Gigleux, S., Ouzzine, M. 2001. Interleukin-1B down-regulates the expression of

glucuronosyltransferase I, a key enzyme priming glycosaminoglycan biosynthesis: Influence of glucosamine on interleukin-1?-mediated effects in rat chondrocytes. *Arthritis & Rheumatism* 44:351-360.

66. Seko, A., Dohmae, N., Takio, K., and Yamashita, K. 2003. ß1,4-Galactosyltransferase (beta 4GalT)-IV is specific for GlcNAc 6-O-sulfate. ß4GalT-IV acts on keratan sulfate-related glycans and a precursor glycan of 6-sulfosialyl-Lewis X. *J. Biol. Chem.* 278:9150-9158.

67. Sugahara, K., and Kitagawa, H. 2000. Recent advances in the study of the biosynthesis and functions of sulfated glycosaminoglycans. *Curr. Opin. Struct. Biol.* 10:518-527.

68. Kim, B.-T., Kitagawa, H., Tanaka, J., Tamura, J.-i., and Sugahara, K. 2003. In Vitro Heparan Sulfate Polymerization: CRUCIAL ROLES OF CORE PROTEIN MOIETIES OF PRIMER SUBSTRATES IN ADDITION TO THE EXT1-EXT2 INTERACTION. *J. Biol. Chem.* 278:41618-41623.

69. Lind, T., Tufaro, F., McCormick, C., Lindahl, U., and Lidholt, K. 1998. The putative tumor suppressors EXT1 and EXT2 are glycosyltransferases required for the biosynthesis of heparan sulfate. *J. Biol. Chem.* 273:26265-26268.

70. Fritz, T.A., Gabb, M.M., Wei, G., Esko, J.D. 1994. Two N-acetylglucosaminyltransferases catalyze teh biosynthesis of heparan sulfate. *J. Biol. Chem.* 269:28809-28814.

71. Kim, B.-T.K., H., Tamura, J., Saito, T., Kusche-Gullberg, M., Lindahl, U., and Sugahara, K. 2001. Human tumor suppressor EXT gene family members EXTI.1 and EXTL3 encode a1.4-N-acetylglucosaminyltransferases that likely are involved in heparan sulfate/heparin biosynthesis. *Proc. Natl. Acad. Sci. U.S.A* 98:7176-7181.

72. Lin, X., Wei, G., Shi, Z., Dryer, L., Esko, J.D., Wells, D.E., and Matzuk, M.M. 2000. Disruption of Gastrulation and Heparan Sulfate Biosynthesis in EXT1-Deficient Mice. *Developmental Biology* 224:299.

73. Wei, G., Bai, X., Baine, K. J., Koshy, T. I., Spear, P. G., and Esko, J. D. 2000. Location of the glucuronosyltransferase domain in the heparan sulfate copolymerase (EXT1) by analysis of Chinese hamster ovary cell mutants. *J. Biol. Chem.* 275:27733-27740.

74. Chapman, E., M.D., B., Hanson, S.R., and Wong, C.H. 2004. Sulfotransferases: Structure, mechanism, biological activity, inhibition, and synthetic utility. *Angew. Chem. Int. Ed.* 43:3526-3548.

75. Negishi, M., Pedersen, L.G., Petrotchenko, E., Shevtsov, S., Gorokhov, A., Kakuta, Y., and Pedersen, L.C. 2001. Structures and functions of sulfotransferases. *Arch. Biochem. Biophys.* 390:149-157.

76. Superti-Furga, A. 1994. *Am. J. Hum. Genet.* 55:1137-1145.

77. Aikawa, J.-i., Grobe, K., Tsujimoto, M., and Esko, J.D. 2001. Multiple isozymes of heparan sulfates/heparin GlcNAc N-deacetylase/GlcN N-sulfotransferase: Structure and activity of the fourth member, NDST4. *J. Biol. Chem.* 276:5876-5882.

78. Habuchi, H., Tanaka, M., Habuchi, O., Yoshida, K., Suzuki, H., Ban, K., and Kimata, K. 2000. The occurance of three isoforms of heparan sulfate 6-O-sulfotransferase having different specificities for hexuronic acid adjacent to the targeted N-sulfoglucosamine. *J. Biol. Chem.* 275:2859-2868.

79. Shworak, N., Liu, J., Petros, L., Zhang, L., Kobayashi, M., Copeland, N., Jenkins, N., and Rosenberg, R. 1999. Multiple isoforms of heparan sulfate D-glucosaminyl 3-O-sulfotransferase. Isolation, characterization, and expression of human cdnas and identification of distinct genomic loci. *J. Biol. Chem.* 274:5170-5184.

80. Xia, G., Chen, J., Tiwari, V., Ju, W., Li, J.-P., Malmström, A., Shukla, D., and Liu, J. 2002. Heparan sulfate 3-O-sulfotransferase isoform 5 generates both an antithrombin-binding site and an entry receptor for herpes simplex virus, type 1. *J. Biol. Chem.* 277:37912-37919.

81. Liu, J., Shworak, N.W., Sinaÿ, P., Schwartz, J.J., Zhang, L., Fritze, L.M.S., and Rosenberg, R.D. 1999. Expression of heparan sulfate D-glucosaminyl 3-*O*-sulfotransferase isoforms reveals novel substrate specificities. *J. Biol. Chem.* 274:5185-5192.

82. Perrimon, N., and Bernfield, M. 2000. Specificities of heparan sulfate proteoglcans in developmental processes. *Nature* 404:725-728.

83. Aikawa, J., and Esko, J.D. 1999. Molecular cloning and expression of a third member of the heparan sulfate/heparin GlcNAc N-deacetylase/N-sulfotransferase family. *J. Biol. Chem.* 274:2690-2695.

84. Grobe, K., Ledin, J., Ringvall, M., Holmborn, K., Forsberg, E., Esko, J.D., and Kjellen, L. 2002. Heparan sulfate and development: differential roles of the N-acetylglucosamine N-deacetylase/N-sulfotransferase isozymes. *Biochimica et Biophysica Acta (BBA) - General Subjects* 1573:209.

85. Duncan, M.B., Liu, M., Fox, C., and Liu, J. 2006. Characterization of the N-deacetylase domain from the heparan sulfate N-deacetylase/N-sulfotransferase 2. *Biochemical and Biophysical Research Communications* 339:1232.

86. Kusche-Gullberg, M., Eriksson, I., Pikas, D., and Kjellén, L. 1998. Identification and Expression in Mouse of Two Heparan Sulfate Glucosaminyl N-Deacetylase/N-Sulfotransferase Genes. *J. Biol. Chem.* 273:11902-11907.

87. Kakuta, Y., Sueyoshi, T., Negishi, M., and Pedersen, L.C. 1999. Crystal structure of the sulfotransferase domain of human heparan sulfate N-deacetylase/N-sulfotransferase 1. *J. Biol. Chem.* 274:10673-10676.

88. Kakuta, Y., Pedersen, L.G., Pedersen, L.C., and Negishi, M. 1998. Conserved structural motifs in the sulfotransferase family. *Trends in Biochemical Sciences* 23:129.

89. Sueyoshi, T., Kakuta, Y., Pedersen, L.C., Wall, F.E., Pedersen, L.G., and Negishi, M. 1998. A role of Lys^{614} in the sulfotransferase activity of human heparin sulfate *N*-deacetylase/*N*-sulfotransferase. *FEBS Lett.* 433:211-214.

90. Kakuta, Y., Petrotchenko, E.V., Pedersen, L.C., and Negishi, M. 1998. The sulfuryl transfer mechanism: crystal structures of a vanadate complex of estrogen sulfotransferase and mutational analysis. *J. Biol. Chem.* 273:27325-27330.

91. Kakuta, Y., Pedersen, L.G., Carter, C.W., Negishi, M., and Pedersen, L.C. 1997. Crystal structure of estrogen sulphotransferase. *Nat. Struct. Biol.* 4:904-908.

92. Kakuta, Y., Li, L., Pedersen, L.C., Pedersen, L.G., and Negishi, M. 2003. Heparan sulphate N-sulphotransferase activity: reaction mechanism and substrate recognition. *Biochem. Soc. Trans.* 31 (pt2):331-334.

93. Cheung, W.-F., Eriksson, I., Kusche-Gullberg, M., Lindahl, U., and Kjellen, L. 1996. Expression of the mouse mastocytoma glucosaminyl *N*-deacetylase/*N*-sulfotransferase in human kidney 293 Cells results in increased *N*-sulfation of heparan sulfate. *Biochemistry* 35:5250-5256.

94. Pikas, D.S., Eriksson, I., and Kjellen, L. 2000. Overexpression of Different Isoforms of Glucosaminyl N-Deacetylase/N-Sulfotransferase Results in Distinct Heparan Sulfate N-Sulfation Patterns. *Biochemistry* 39:4552-4558.

95. Forsberg, E., and Kjellen, L. 2001. Heparan sulfate: lessons from knockout mice. *J. Clin. Invest.* 108:175-180.

96. Forsberg E, P.G., Ringvall M, Lunderius C, Tomasini-Johansson B, Kusche-Gullberg M, Eriksson I, Ledin J, Hellman L, Kjellen L. 1999. Abnormal mast cells in mice deficient in a heparin-synthesizing enzyme. *Nature* 400.

97. Humphries DE, W.G., Friend DS, Gurish MF, Qiu WT, Huang C, Sharpe AH, Stevens RL. 1999. Heparin is essential for the storage of specific granule proteases in mast cells. *Nature* 400:769-772.

98. Ringvall, M., Ledin, J., Holmborn, K., van Kuppevelt, T., Ellin, F., Eriksson, I., Olofsson, A.-M., Kjellen, L., and Forsberg, E. 2000. Defective Heparan Sulfate Biosynthesis and Neonatal Lethality in Mice Lacking N-Deacetylase/N-Sulfotransferase-1. *J. Biol. Chem.* 275:25926-25930.

99. Crawford, B.E., Olson, S.K., Esko, J.D., and Pinhal, M.A.S. 2001. Cloning, Golgi Localization, and Enzyme Activity of the Full-length Heparin/Heparan Sulfate-Glucuronic Acid C5-epimerase. *J. Biol. Chem.* 276:21538-21543.

100. Hagner-McWhirter, A., Lindahl, U., Li, J. 2000. Biosynthesis of heparin/heparan sulphate: mechanism of epimerization of glucuronyl C-5. *Biochem. J.* 347:69-75.

101. Hagner-McWhirter, A., Hannesson, H.H., Campbell, P., Westley, J., Roden, L., Lindahl, U., and Li, J.-P. 2000. Biosynthesis of heparin/heparan sulfate: kinetic studies of the glucuronyl C5-epimerase with N-sulfated derivatives of the Escherichia coli K5 capsular polysaccharide as substrates. *Glycobiology* 10:159-171.

102. Hagner-McWhirter, A., Li, J.-P., Oscarson, S., and Lindahl, U. 2004. Irreversible Glucuronyl C5-epimerization in the Biosynthesis of Heparan Sulfate. *J. Biol. Chem.* 279:14631-14638.

103. Casu B, P.M., Provasoli M, Sinay P. 1988. Conformational flexibility: a new concept for explaining binding and biological properties of iduronic acid-containing glycosaminoglycans. *Trends Biochem. Sci.* 6:221-225.

104. Jacobsson, I., Lindahl, U., Jensen, J.W., Roden, L., Prihar, H., and Feingold, D.S. 1984. Biosynthesis of heparin. Substrate specificity of heparosan N-sulfate D-glucuronosyl 5-epimerase. *J. Biol. Chem.* 259:1056-1063.

105. Pinhal, M.A.S., Smith, B., Olson, S., Aikawa, J.-i., Kimata, K., and Esko, J.D. 2001. Enzyme interactions in heparan sulfate biosynthesis: Uronosyl 5-epimerase and 2-O-sulfotransferase interact in vivo. *PNAS* 98:12984-12989.

106. Turnbull J, D.K., Huang Z, Kinnunen T, Ford-Perriss M, Murphy M, Guimond S. 2003. Heparan sulphate sulphotransferase expression in mice and Caenorhabditis elegans. *Biochem. Soc. Trans.* 31:343-348.

107. Rong, J., Habuchi, H., Kimata, K., Lindahl, U., and Kusche-Gullberg, M. 2001. Substrate specificity of the heparan sulfate hexuronic acid 2-*O*-sulfotransferase. *Biochemistry* 40:5548-5555.

108. Rong J, H.H., Kimata K, Lindahl U, Kusche-Gullberg M. 2000. Expression of heparan sulphate L-iduronyl 2-O-sulphotransferase in human kidney 293 cells results in increased D-glucuronyl 2-O-sulphation. *Biochem. J.* 346:463-468.

109. Merry, C.L., Lyon, M., Deakin, J.A., Hopwood, J.J., and Gallagher, J.T. 1999. Highly sensitive sequencing of the sulfated domains of heparan sulfate. *J. Biol. Chem.* 274:18455-18462.

110. Merry, C.L.R., Bullock, S.L., Swan, D.C., Backen, A.C., Lyon, M., Beddington, R.S.P., Wilson, V.A., and Gallagher, J.T. 2001. The Molecular Phenotype of Heparan Sulfate in the Hs2st-/- Mutant Mouse. *J. Biol. Chem.* 276:35429-35434.

111. Fan, G., Xiao, L., Cheng, L., Wang, X., Sun, B., and Hu, G. 2000. Targeted disruption of NDST-1 gene leads to pulmonary hypoplasia and neonatal respiratory distress in mice. *FEBS Letters* 467:7.

112. Habuchi, H., Kobayashi, M., and Kimata, K. 1998. Molecular characterization and expression of heparan-sulfate 6-sulfotransferase: complete cDNA cloning in human and partial cloning in Chinese hamster ovary cells. *J. Biol. Chem.* 273:9208-9213.

113. Smeds, E., Habuchi, H., Do, A.-T., Hjertson, E., Grundberg, H., Kimata, K., Lindahl, U., and Kusche-Gullberg, M. 2003. Substrate specificities of mouse heparan sulphate glucosaminyl 6-O-sulfotransferases. *Biochem. J.* 372 (pt2):371-380.

114. Pye, D.A., Vives, R.R., Turnbull, J.E., Hyde, P., and Gallagher, J.T. 1998. Heparan sulfate oligosaccharides require 6-O-sulfation for promotion of basic fibroblast growth factor mitogenic activity. *J. Biol. Chem.* 273:22936-22942.

115. Liu, J.R., R. D. 2002. Heparan sulphate D-glucosaminyl 3-O-sulfotransferase-1, -2, -3, and -4. *Handbook of glycosyltransferases and their related genes.*:475–483.

116. Chen, J., Duncan, M.B., Carrick, K., Pope, M., and Liu, J. 2003. Biosynthesis of 3-O-sulfated heparan sulfate: unique substrate specificity of heparan sulfate 3-O-sulfotransferase isoform 5. *Glycobiology* 13:785-794.

117. Wu, Z.L., Lech, M., Beeler, D.L., and Rosenberg, R.D. 2004. Determining heparan sulfate structure in the vicinity of specific sulfotransferase recognition sites by mass spectrometry. *J. Biol. Chem.* 279:1861-1866.

118. Xu, D., Tiwari, V., Xia, G., Clement, C., Shukla, D., and Liu, J. 2004. Characterization of Heparan Sulfate 3-O-Sulfotransferase Isoform 6 and Its Role in Assisting the Entry of Herpes Simplex Virus, Type 1. *Biochem. J.*:in press.

119. Liu, J., and Rosenberg, R.D. 2002. Heparan sulfate D-glucosaminyl 3-*O*-sulfotransferase. In *Handbook of glycosyltransferases and their related genes*. N. Taniguchi, and M. Fukuda, editors. Tokyo: Springer-Verlag. 475-483.

120. Edavettal, S.C., Lee, K.A., Negishi, M., Linhardt, R.J., Liu, J., and Pedersen, L.C. 2004. Crystal structure and mutational analysis of heparan sulfate 3-O-sulfotransferase isoform 1. *J. Biol. Chem.* 279:25789-25797.

121. Moon, A., Edavettal, S.C., Krahn, J.X., Munoz, E.M., Negishi, M., Linhardt, R.J., Liu, J., and Pedersen, L.C. 2004. Structural analysis of the sulfotransferase (3-OST-3) involved in the biosynthesis of an entry receptor of herpes simplex virus 1. *J. Biol. Chem.* 279:45185-45193.

122. Edavettal, S.C., Carrick, K., Shah, R.R., Pedersen, L.C., Tropsha, A., Pope, R.M., and Liu, J. 2004. A conformational change in heparan sulfate 3-O-sulfotransferase-1 is induced by binding to heparan sulfate. *Biochemistry* 43:4680-4688.

123. Pedersen, L.C., Petrotchenko, E., Shevtsov, S., and Negishi, M. 2002. Crystal structure of the human estrogen sulfotransferase-PAPS complex: evidence for catalytic role of Ser^{137} in the sulfuryl transfer reaction. *J. Biol. Chem.* 277:17928-17932.

124. HajMohammadi, S., Enjyoji, K., Princivalle, M., Christi, P., Lech, M., Beeler, D.L., Rayburn, H., Schwartz, J.J., Barzegar, S., de Agostini, A.I., et al. 2003. Normal levels of anticoagulant heparan sulfate are not essential for normal hemostasis. *J. Clin. Invest.* 111:989-999.

125. Shworak, N., HajMohammadi, S., Agostini, A., Rosenberg, R. 2003. Mice deficient in heparan sulfate 3-O-sulfotransferase-1: Normal hemostasis with unexpected perinatal phenotypes. *Glycoconjugate Journal* 19:355-361.

126. Guo, Y.C., and Conrad, H.E. 1989. The disaccharide composition of heparins and heparan sulfates. *Anal. Biochem.* 176:96-104.

127. Koketsu, M., and Linhardt, R.J. 2000. Electrophoresis for the analysis of acidic oligosaccharides. *Anal. Biochem.* 283:136-145.

128. Lindahl, U., Backstrom, G., Thunberg, L., and Leder, I.G. 1980. Evidence for a 3-O-sulfated D-glucosamine residue in the antithrombin-binding sequence of heparin. *Proc. Natl. Acad. Sci.* 77:6551-6555.

129. Rosenberg, R.D., Oosta, G.M., Jordan, R.E., and Gardner, W.T. 1980. The interaction of heparin with thrombin and antithrombin. *Biochem. Biophys. Res. Commun.* 96:1200-1208.

130. Shukla, D., Liu, J., Blaiklock, P., Shworak, N.W., Bai, X., Esko, J.D., Cohen, G.H., Eisenberg, R.J., Rosenberg, R.D., and Spear, P.G. 1999. A novel role for 3-O-sulfated heparan sulfate in herpes simplex virus 1 entry. *Cell* 99:13-22.

131. Bame, K.J. 2001. Heparanases: endoglycosidases that degrade heparan sulfate proteoglycans. *Glycobiology* 11:91R-98.

132. Desai, U.R., Wang, H.M., and Linhardt, R.J. 1993. Substrate specificity of the heparin lyases from Flavobacterium heparinum. *Arch. Biochem. Biophys.* 306:461-468.

133. Shively, J.E., and Conrad, H.E. 1976. Formation of anhydrosugars in the chemical depolymerization of heparin. *Biochemistry* 15:3932-3942.

134. Liu, J., Desai, U.R., Han, X.-j., Toida, T., and Linhardt, R.J. 1995. Strategy for the sequence analysis of heparin. *Glycobiology* 5:765-774.

135. Rhomberg, A.J., Ernst, S., Sasisekharan, R., and Biemann, K. 1998. Mass spectrometric and capillary electrophoretic investigation of the enzymatic degradation of heparin-like glycosaminoglycans. *Proc. Natl. Acad. Sci. USA* 95:4176-4181.

136. Juhasz, P., and Biemann, K. 1994. Utility of non-covalent complex in the matrix-assisted laser desorption ionization mass spectrometry of heparin-derived oligosaccharides. *Carbohydr. Res.* 270:131-147.

137. Pope, M., Raska, C., Thorp, S.C., and Liu, J. 2001. Analysis of heparan sulfate oligosaccharides by nanoelectrospray ionization mass spectrometry. *Glycobiology* 11:505-513.

138. Venkataraman, G., Shriver, Z., Raman, R., and Sasisekharan, R. 1999. Sequencing complex polysaccharides. *Science* 286:537-542.

139. Huntington, J.A. 2003. Mechanisms of glycosaminoglycan activation of the serpins in hemostasis. *J. Thromb. Haemost.* 1:1535-1549.

140. Jones, M., Tussey, L., Athanasou, N., and Jackson, D.G. 2000. Heparan Sulfate Proteoglycan Isoforms of the CD44 Hyaluronan Receptor Induced in Human Inflammatory Macrophages Can Function as Paracrine Regulators of Fibroblast Growth Factor Action. *J. Biol. Chem.* 275:7964-7974.

141. Cardin, A.D., and Weintraub, H.J.R. 1989. Molecular modeling of protein-glycosaminoglycan interactions. *Arteriosclerosis* 9:21-32.

142. Capila, I., and Linhardt, R.J. 2002. Heparin-protein interactions. *Angew. Chem. Int. Ed. Engl.* 41:391-412.

143. Rabenstein, D.L. 2002. *Nat. Prod. Rep.* 19:312.

144. Mann, K.G., Butenas, S., and Brummel, K. 2003. The Dynamics of Thrombin Formation. *Arterioscler. Thromb. Vasc. Biol.* 23:17-25.

145. Ishiguro, K., Kojima, T., Kadomatsu, K., Nakayama, Y., Takagi, A., Suzuki, M., Takeda, N., Ito, M., Yamamoto, K., Matsushita, T., et al. 2000. Complete antithrombin deficiency in mice results in embryonic lethality. *J. Clin. Invest.* 106:873-878.

146. Egeberg, O. 1965. Inherited antithrombin III deficiency causing thrombophilia. *Thromb. Diath. Haemorrh.* 13:516-530.

147. Olson, S.T., Srinivasan, K.R., Bjork, I., and Shore, J.D. 1981. Binding of high affinity heparin to antithrombin III. Stopped flow kinetic studies of the binding interaction. *J. Biol. Chem.* 256:11073-11079.

148. Jin, L., Abrahams, P., Skinner, R., Petitou, M., Pike, R.N., and Carrell, R.W. 1997. The anticoagulant activation of antithrombin by heparin. *Proc. Natl. Acad. Sci.* 94:14683-14688.

149. Warkentin, T.E., Chong, B. H. & Greinacher, A. 1998. Heparin-induced thrombocytopenia: Towards consensus. *Thromb. Hemost.* 79:1-7.

150. Petitou, M., Casu, B., and Lindahl, U. 2003. 1976-1983, a critical period in the history of heparin: the discovery of the antithrombin binding site. *Biochimie.* 85:83-89.

151. Olson, S.T., Bjork, I., Sheffer, R., Craig, P.A., Shore, J.D., and Choay, J. 1992. Role of the antithrombin-binding pentasaccharide in heparin acceleration of antithrombin-proteinase reactions. Resolution of the antithrombin conformational change contribution to heparin rate enhancement. *J. Biol. Chem.* 267:12528-12538.

152. Desai, U.R., Petitou, M., Bjork, I., and Olson, S.T. 1998. Mechanism of Heparin Activation of Antithrombin: Evidence for an Induced-Fit Model of Allosteric Activation Involving Two Interaction Subsites. *Biochemistry* 37:13033-13041.

153. Monien, B.H., Krishnasamy, C., Olson, S.T., and Desai, U.R. 2005. Importance of Tryptophan 49 of Antithrombin in Heparin Binding and Conformational Activation. *Biochemistry* 44:11660-11668.

154. Faham, S., Hileman, R.E., Fromm, J.R., Linhardt, R.J., and Rees, D.C. 1996. Heparin structure and interactions with basic fibroblast growth factor. *Science* 271:1116-1120.

155. Noti, C., and Seeberger, P.H. 2005. Chemical Approaches to Define the Structure-Activity Relationship of Heparin-like Glycosaminoglycans. *Chemistry & Biology* 12:731.

156. Kwan, C.-P., Venkataraman, G., Shriver, Z., Raman, R., Liu, D., Qi, Y., Varticovski, L., and Sasisekharan, R. 2001. Probing Fibroblast Growth Factor Dimerization and Role of Heparin-like Glycosaminoglycans in Modulating Dimerization and Signaling. *J. Biol. Chem.* 276:23421-23429.

157. Digabriele, A.D., Lax, I., Chen, D.I., Svahn, C.M., Jaye, M., Schlessinger, J., and Hendrickson, W.A. 1998. Structure of a heparin-linked biologically active dimer of fibroblast growth factor. *Nature* 393:812.

158. Pellegrini, L., Burke, D.F., Von Delf, F., Mulloy, B., and Blundell, T.L. 2000. Crystal structure of fibroblast growth factor receptor ectodomain bound to ligand and heparin. *Nature* 407:1029.

159. Schlessinger, J., Plotnikov, A.N., Ibrahimi, O.A., Eliseenkova, A.V., Yeh, B.K., Yayon, A., Linhardt, R.J., and Mohammadi, M. 2000. Crystal structure of a ternary FGF-FGFR-heparin complex reveals a dual role for heparin in FGFR binding and dimerization. *Mol. Cell* 6:743-750.

160. Guerrini, M., Agulles, T., Bisio, A., Hricovini, M., Lay, L., Naggi, A., Poletti, L., Sturiale, L., Torri, G., and Casu, B. 2002. Minimal heparin/heparan sulfate sequences for binding to fibroblast growth factor-1. *Biochem. and Biophys. Res. Comm.* 292:222.

161. Ashikari-Hada, S., Habuchi, H., Kariya, Y., Itoh, N., Reddi, A.H., and Kimata, K. 2004. Characterization of Growth Factor-binding Structures in Heparin/Heparan Sulfate Using an Octasaccharide Library. *J. Biol. Chem.* 279:12346-12354.

162. Ianelli, C.J., DeLellis, R., and Thorley-Lawson, D.A. 1998. CD48 binds to heparan sulfate on the surface of epithelial cells. *J. Biol. Chem.* 273:23367-23375.

163. Garson, J.A., Lubach, D., Passas, J., Whitby, K., and Grant, P.R. 1999. Suramin blocks hepatitis C binding to human hepatoma cells in vitro. *J. Med. Virol.* 57:238-242.

164. Tyagi, M., Rusnati, M., Presta, M., and Giacca, M. 2001. Internalization of HIV-1 Tat requires cell surface heparan sulfate proteoglycans. *J. Biol. Chem.* 276:3254-3261.

165. WuDunn, D., and Spear, P.G. 1989. Initial interaction of herpes simplex virus with cells is binding to heparan sulfate. *J. Virol.* 63:52-58.

166. Spear, P.G., and Longnecker, R. 2003. Herpesvirus Entry: an Update. *J. Virol.* 77:10179-10185.

167. Corey, L., and Spear, P.G. 1986. Infections with herpes simplex viruses. *N. Engl. J. Med.* 314:686-691 and 749-757.

168. Gupta, R., and Wald, A. 2006. Genital herpes: antiviral therapy for symptom relief and prevention of transmission. *Expert Opinion on Pharmacotherapy* 7:665-675.

169. Montgomery, R.I., Warner, M.S., Lum, B.J., and Spear, P.G. 1996. Herpes simplex virus-1 entry into cells mediated by a novel member of the TNF/NGF receptor family. *Cell* 87:427-436.

170. Spear, P.G., Eisenberg, R.J., and Cohen, G.H. 2000. Three classes of cell surface receptors for alphaherpesvirus entry. *Virology* 275:1-8.

171. Shukla, D., and Spear, P.G. 2001. Herpesviruses and heparan sulfate: an intimate relationship in aid of viral entry. *J. Clin. Invest.* 108:503-510.

172. Gruenheid, S., Gatzke, L., Meadows, H., and Tufaro, F. 1993. Herpes simplex virus virus infection and propagation in a mouse L cell mutant lacking heparan sulfate proteoglycans. *J. Virol.* 67:93-100.

173. Shieh, M.-T., WuDunn, D., Montgomery, R.I., Esko, J.D., and Spear, P.G. 1992. Cell surface receptors for herpes simplex virus are heparan sulfate proteoglycans. *J. Cell Biol.* 116:1273-1281.

174. Herold, B.C., Visalli, R.J., Sumarski, N., Brandt, C.R., and Spear, P.G. 1994. Glycoprotein C-independent binding of herpes simplex virus to cells requires cell surface heparan sulfate and glycoprotein B. *J. Gen. Virol.* 75:1121-1222.

175. Feyzi, E., Trybala, E., Bergstrom, T., Lindahl, U., and Spillmann, D. 1997. Structural requirement of heparan sulfate for interaction with herpes simplex virus type 1 virons and isolated glycoprotein C. *J. Biol. Chem.* 272:24850-24857.

176. Spear, P.G. 1993. Membrane fusion induced by herpes simplex virus. In *viral fusion mechanisms*. J. Bentz, editor. Boca Raton, FL: CRC Press, Inc., pp. 201-232.

177. Long, D., Wilcox, W.C., Abrams, W.R., Cohen, G.H., and Eisenberg, R.J. 1992. Disulfide bond structure of glycoprotein D of herpes simplex virus types 1 and 2. *J. Virol.* 66:6668-6685.

178. Carfi, A., Willis, S.H., Whitbeck, J.C., Krummenacher, C., Cohen, G.H., Eisenberg, R.J., and Wiley, D.C. 2001. Herpes simplex virus glycoprotein D bound to the human receptor HveA. *Mol. Cell* 8:169-179.

179. Milne, R.S.B., Hanna, S.L., Rux, A.H., Willis, S.H., Cohen, G.H., and Eisenberg, R.J. 2003. Function of herpes simplex virus type 1 gD mutants with different receptor-binding affinities in virus entry and fusion. *J. Virol.* 77:8962-8972.

180. Geraghty, R.J., Krummenacher, C., Cohen, G.H., Eisenberg, R.J., and Spear, P.G. 1998. Entry of alphaherpesviruses mediated by poliovirus receptor-related protein 1 and poliovirus receptor. *Science* 280:1618-1620.

181. Liu, J., Shriver, Z., Pope, R.M., Thorp, S.C., Duncan, M.B., Copeland, R.J., Raska, C.S., Yoshida, K., Eisenberg, R.J., Cohen, G., et al. 2002. Characterization of a heparan sulfate octasaccharide that binds to herpes simplex viral type 1 glycoprotein D. *J. Biol. Chem.* 277:33456-33467.

182. Yoon, M., Zago, A., Shukla, D., and Spear, P.G. 2003. Mutations in the N-termini of herpes simplex virus type 1 and 2 gDs alter functional interactions with the entry/fusion receptors HVEM, Nectin-2, and 3-O-sulfated heparan sulfate but not with Nectin-1. *J. Virol.* 77:9221-9231.

183. Manoj, S., Jogger, C.R., Myscofski, D., Yoon, M., and Spear, P.G. 2004. Mutations in herpes simplex virus glycoprotein D that prevent cell entry via nectin and alter celll tropism. *Proc. Natl. Acad. Sci.* 101:12414-12421.

184. Lohman, G.J.S., and Seeberger, P.H. 2004. A stereochemical surprise at the late stage of the synthesis of fully N-differentiated heparin oligosaccharides containing amin, acetamido, and N-sulfonate groups. *J. Org. Chem.* 69:4081-4093.

185. Kondo, K., Seno, N., and Anno, K. 1971. Mucopolysaccharides from chicken skin of three age groups. *Biochim. Biophys. Acta.* 244:513-522.

186. Bjornsson, S. 1993. Simultaneous preparation and quantitation of proteoglycans by precipitation with alcian blue. *Anal. Biochem.* 210:282-291.

187. Lee, M.K., and Lander, A.D. 1991. Analysis affinity and strutural selectivity in the binding of proteins to glycosamineglycans: Development of a sensitive electrophoretc approach. *Proc. Natl. Acad. Sci. USA* 88:2768-2772.

188. Zhang, L., Yoshida, K., Liu, J., and Rosenberg, R.D. 1999. Anticoagulant heparan sulfate precursor structures in F9 embryonic carcinoma cells. *J. Biol. Chem.* 274:5681-5691.

189. Bigge, J.C., Patel, T. P., Bruce, J. A., Goulding, P. N., Charles, S. M., and Parekh, R. B. 1995. Non-selective and efficient fluorescent labeling of glycans using 2-aminobenzamide and anthranilic acid. *Anal. Biochem.* 230:229-238.

190. Kinoshita, A., and Sugahara, K. 1999. Microanalysis of glycosaminoglycan-derived oligosaccharides labeled with a fluorophore 2-aminobenzamide by high-performance liquid chromatography: application to disaccharide composition analysis and exosequencing of oligosaccharides. *Anal. Biochem.* 269:367-378.

191. Burkart, M.D., Izumi, M., Chapman, E., Lin, C., and Wong, C. 2000. Regeneration of PAPS for the enzymatic synthesis of sulfated oligosaccharides. *J. Org. Chem.* 65:5565-5574.

192. Hartl, F.U., and Hayer-Hartl, M. 2002. Molecular Chaperones in the Cytosol: from Nascent Chain to Folded Protein. *Science* 295:1852-1858.

193. Cohen, G.H., Long, D., Matthews, J.T., May, M., and Eisenberg, R. 1983. Glycopeptides of the Type-Common Glycoprotein gD of Herpes Simplex Virus Types 1 and 2. *J. Virol.* 46:679-689.

194. Pervin, A., Gallo, C., Jandik, K., Han, X., and Linhardt, R.J. 1995. Preparation and structural characterization of large heparin-derived oligosaccharides. *Glycobiology* 5:83-95.

195. Liu, J., Shriver, Z., Blaiklock, P., Yoshida, K., Sasisekharan, R., and Rosenberg, R.D. 1999. Heparan sulfate D-glucosaminyl 3-O-sulfotransferase-3A sulfates N-unsubstituted glucosamine residues. *J. Biol. Chem.* 274:38155-38162.

196. Herndon, M.E., Stipp, C.S., and Lander, A.D. 1999. Interactions of neural glycosaminoglycans and proteoglycans with protein ligands: assessment of selectivity, heterogeneity and the participation of core proteins in binding. *Glycobiology* 9:143-155.

197. McLean, M.W., Bruce, J.S., Long, W.F., and Williamson, F.B. 1984. *Flavobacterium heparinum* 2-*O*-sulfatase for 2-*O*-sulfato-$\Delta_{4,5}$-glycuronate terminated oligosaccharides from heparin. *Eur. J. Biochem.* 145:607-615.

198. Anumula, K.R. 2006. Advances in fluorescence derivatization methods for high-performance liquid chromatographic analysis of glycoprotein carbohydrates. *Anal. Biochem.* 350:1.

199. C.-H. Lin, G.-J.S., E. Garcia-Junceda, C.-H. Wong. 1995. *J. Am. Chem. Soc.* 117:8031.

200. Duffel, M.W., and Jakoby, W.B. 1981. On the mechanism of aryl sulfotransferase. *J. Biol. Chem.* 256:11123-11127.

201. Herold, B., Gerber, S.I., Belval, B.J., Siston, A.M., and Shulman, N. 1996. Differences in the susceptibility of herpes simplex virus types 1 and 2 to modified heparin compounds suggest serotype differences in viral entry. *J. Virol.* 70:3461-3469.